UNIVERSIDAD AUTÓNOMA DE MADRID

Programa de Doctorado en Biociencias Moleculares

Unraveling the molecular mechanisms behind the regulation of mesenchymal cell proliferation during cardiac valve remodeling

Vera Lúcia Ferreira Oliveira

MADRID, 2020

UNIVERSIDAD AUTÓNOMA DE MADRID

FACULTAD DE MEDICINA

DEPARTAMENTO DE BIOQUÍMICA

Unraveling the molecular mechanisms behind the regulation of mesenchymal cell proliferation during cardiac valve remodeling

Vera Lúcia Ferreira Oliveira

Directores: José Luis de la Pompa, Donal MacGrogan

Centro Nacional de Investigaciones Cardiovasculares Carlos III (CNIC)

This work was performed in Dr. José Luis de la Pompa laboratory at the Centro Nacional de Investigaciones Cardiovasculares Carlos III (CNIC) in Madrid. This work was supported by the Ministerio de Ciencia, Innovación y Universidades from Spain (MCIU, grants SAF2016-78370-R, CB16/11/00399, CIBER CV, and RD16/0011/0021, TERCEL) and the Fundación BBVA (grant BIO14_298) and Fundación La Marató TV3 (grant 20153431) to J.L.dlP

Dr. José Luis de la Pompa Mínguez, head of the Intercellular Signalling in Cardiovascular Development & Disease Lab, Centro Nacional de Investigaciones Cardiovasculares Carlos III (CNIC),

CERTIFIES:

That Ms. Vera Lúcia Ferreira Oliveira, graduate in Biochemistry by the University of Porto, Portugal, has completed her Doctoral Thesis entitled "*Unraveling the molecular mechanisms behind the regulation of mesenchymal cell proliferation during cardiac valve remodeling*" under my supervision and meets the necessary requirements to obtain the PhD degree in Molecular Biosciences. To this purpose, she will defend her doctoral thesis at the Universidad Autónoma de Madrid.

I hereby authorize its defense in front of the appropriate Thesis evaluation tribunal.

I issue this certificate in Madrid on November, 5th of 2020.

Dr. José Luis de la Pompa Mínguez
Thesis Director

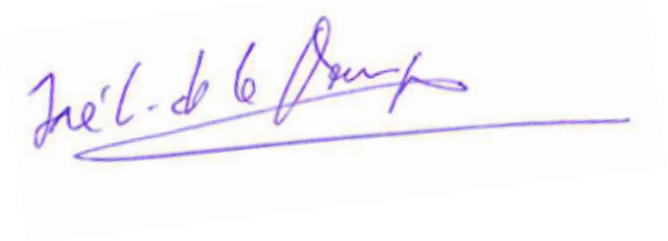

ACKNOWLEDGEMENTS

First, I would like to thank my group leader and thesis director, José Luis de la Pompa. Thank you for your scientific guidance and support throughout the years. I would also like to thank my co-director, Donal MacGrogan. Without your vast experience in the valve field, this thesis would have not been possible.

I would like to thank everyone at CNIC, from the animal facility workers to the maintenance crew, for making the center run smoothly and efficiently. Special thanks to the Pluripotent Cell Technology Unit, the Histology Unit and the Microscopy Unit for their contribution to this project.

I owe many thanks to my lab mates, current and former, who were always there for me. You helped when I needed help, you made me laugh when I needed a break, and you listened to my complaints and complained with me. Ha sido un placer trabajar a vuestro lado estos años y soy muy afortunada de teneros como amigos.

Muchas gracias a Esme y a Bea, por mantenerme sana estos años, con nuestros viajes y aventuras compartidas.

Mil gracias a David, que me ha apoyado como nadie más en la recta final, que siempre es la más dura. Sin ti, este año habría sido imposible.

E, por último, obrigada à minha família. Obrigada paizotes, por nunca duvidarem de mim e pelo vosso amor inquestionável e incondicional. Obrigada Diana e Tiago, pelos conselhos, sugestões, paciência e comida grátis ao longo destes anos. Um apoio como o vosso faz com que tudo pareça possível e alcançável. E obrigada pequena Sofi, por me fazeres tão feliz só por existires.

RESUMEN/ABSTRACT

La importancia de las válvulas cardiacas es evidente cuando uno considera la frecuencia con la que abren y cierran cada minuto. La frecuente presencia de defectos valvulares en varias formas de enfermedad cardiaca congénita enfatiza la complejidad de su formación. A pesar de que muchos de estos defectos son sutiles, muy habitualmente terminan causando enfermedad y mayor tasa de mortalidad en edades más avanzadas. Por lo tanto, entender los mecanismos implicados en la valvulogénesis es extremadamente importante desde el punto de vista clínico.

El receptor quimioquino CXCR4 y su ligando CXCL12 son conocidos como importantes actores en la movilidad y comportamiento celular en múltiples contextos. Se ha demostrado que la deleción genética de *Cxcr4* en el endotelio resulta en el engrosamiento de las válvulas cardiacas, siendo que sus valvas no llegan a realizar un proceso de remodelado. El factor de crecimiento HBEGF es sintetizado como un propéptido transmembranar que, bajo escisión, es liberado para activar receptores cercanos, como el EGFR. Tanto el HBEGF soluble (sHBEGF) como otros miembros de su ruta metabólica han sido establecidos como importantes actores en la formación de las válvulas. Varios estudios han demostrado que la disrupción de miembros de la ruta metabólica HBEGF-EGFR resultan en fenotipos similares a aquellos obtenidos con la deleción de *Cxcr4.*

Nuestra comprensión acerca de los mecanismos moleculares que hay detrás de la maduración de las válvulas primitivas hasta su estado final sigue siendo limitada. Aunque muchas de las proteínas implicadas han comenzado a salir a la luz en la última década, queda mucho por descifrar con respecto a cómo operan y se relacionan entre sí. Utilizando modelos genéticos novedosos, nuestro objetivo ha sido obtener nuevos conocimientos sobre las funciones que desempeña el eje de señalización CXCR4-CXCL12 y la vía HBEGF-EGFR en el proceso de remodelado de las valvas y maduración de las válvulas en el corazón. Teniendo en cuenta esta información, hemos comenzado por corroborar cómo la pérdida endocárdica de *Cxcr4* resulta en el fenotipo de valvas engrosadas previamente encontrado en otros estudios, con un aumento asociado en la proliferación de las células mesenquimales. Esta observación *in vivo* quedó además confirmada con el sistema *ex vivo* de explantes de tracto de salida del corazón. El tratamiento de explantes control con el antagonista de CXCR4 AMD3100 ha confirmado el aumento de la proliferación de las células mesenquimales.

Otra herramienta genética que hemos empleado es un modelo de ratón que sobreexpresa específicamente *sHBEGF* en células endoteliales, que hemos generado utilizando técnicas clonaje de restricción. Sorprendentemente, hemos descubierto que la liberación adicional de sHBEGF también causa válvulas agrandadas, con una mayor proliferación de las células mesenquimales de la valva. El tratamiento de explantes control con sHBEGF genera igualmente un aumento pronunciado en la proliferación. La activación de diferentes receptores o dímeros de receptores por sHBEGF podría explicar las discrepancias entre estas observaciones y estudios previos.

Estos resultados preliminares apuntan hacia un nuevo papel para CXCR4 durante la remodelado de las válvulas. Además, destacan la importancia de la regulación precisa de los niveles de sHBEGF durante este proceso. Un análisis más detallado de ambas vías podría ayudar a descubrir cómo falla el proceso de valvulogénesis en las muchas formas de valvulopatía congénita.

The importance of the cardiac valves is apparent when one considers how often they are required to open and shut on a minute-to-minute basis. The complexity of their formation is underlined by the frequent involvement of valvular defects in several forms of congenital heart disease. Even though many of these defects are subtle, they often lead to disease and significant mortality later in life. Therefore, a comprehensive understanding of the mechanisms underlying valvulogenesis is of critical clinical importance.

The chemokine receptor CXCR4 and its ligand CXCL12 are known to play important roles in cell mobility and behavior in various contexts. Targeted deletion of *Cxcr4* using an endothelial driver has been shown to hamper the remodeling of the cardiac valves, which develop thickened leaflets. Nonetheless, the precise mechanism through which these chemotactic cytokines act during cardiac valvulogenesis remains unclear.

The growth factor HBEGF is synthesized as a membrane bound proprotein that, upon cleavage, is released in order to activate nearby receptors, such as EGFR. Both soluble HBEGF (sHBEGF) itself and members of its pathway have been established as important players in valve formation. Several studies have demonstrated that disruption of members of the HBEGF-EGFR pathway results in valvular phenotypes similar to the ones observed upon *Cxcr4* deletion.

Our understanding of the molecular mechanisms underlying valve maturation is still limited. Even though many of the proteins and pathways involved have been studied in the last two decades, there is still much to be determined regarding the role they play and how they interact. Using novel mouse models, our aim was to obtain new knowledge about the CXCL12-CXCR4 and the HBEGF-EGFR signaling pathways during the remodeling phase of valvulogenesis.

With that in mind, we began by corroborating how endocardial loss of *Cxcr4* recapitulated the thickened leaflets phenotype previously found in other studies, with an associated increase in the proliferation of mesenchymal cells. This *in vivo* observation was further confirmed with the *ex vivo* system of outflow tract (OFT) heart explants. Treatment of control OFT explants with the CXCR4 antagonist AMD3100 confirmed the increase in mesenchymal cell proliferation.

Another genetic tool we have employed is a mouse model that specifically overexpresses *sHBEGF* in endothelial cells, which we have generated using restriction cloning techniques. Surprisingly, we have found that the extra release of sHBEGF also led enlarged valves, accompanied by increased valve mesenchymal cell proliferation. Control OFT explants treated with recombinant sHBEGF also resulted in a pronounced increase in mesenchymal proliferation. Activation of different receptors or receptor dimers might explain the discrepancies between these observations and previous studies.

These preliminary results point towards a novel role for CXCR4 during valve remodeling. Furthermore, they highlight the importance of the precise regulation of sHBEGF levels during this process. Further analysis of both of these pathways could help uncover how the process of valvulogenesis goes awry in the many different forms of congenital valve disease.

Index

ACKNOWLEDGEMENTS 7

RESUMEN/ABSTRACT 9

ABBREVIATIONS 15

Abbreviation Meaning 16

INTRODUCTION 17

Early heart development 18

Early valvulogenesis 19
1. Endothelial to Mesenchymal Transition (EMT) 19
2. Origins of cardiac mesenchyme 21

Valve elongation and remodeling 24
1. Structure of the mature valves 24
2. Remodeling of the ECM and reduction of mesenchymal proliferation 25

Congenital valve disease and BAV 29

The CXCL12 and CXCR4 signaling axis 31

HBEGF 34

Role(s) of HBEGF-EGFR signaling in valve development 36

OBJECTIVES 39

Our Hypothesis 40

Our Objectives 40

MATERIALS AND METHODS 41

Mouse model generation 42

Collection and processing of mouse samples 43

In situ hybridization 44

Hematoxylin and eosin and DAB stainings 44

Immunofluorescence 44

OFT explant assay 45

Proliferation analysis and quantification 46

RNA extraction and quantitative real-time PCR 46

X-gal staining 47

Imaging 47

Quantification of valve mesenchymal area and cell number 48

Quantification of pSmad area 48

Statistical analysis 49

RESULTS 51

Cxcr4 and *Cxcl12* are both expressed in cardiac valve regions during embryonic development 52

Generation of mice lacking *Cxcr4* in endocardium 52

Endocardial *Cxcr4* deletion results in hypercellular and dysmorphic valves, including bicuspid aortic valve 54

Cartilaginous metaplasia and ventricular septal defects in *Cxcr4^{flox}; Nfatc1-Cre* mice 58

Increased mesenchyme cell proliferation underlies valve hypercellularity in *Cxcr4^{flox}; Nfatc1-Cre* embryos 61

Endocardial *Cxcr4* mutant valve enlargement is not due to decreased apoptosis or reduced macrophage recruitment 63

Canonical BMP signaling is not affected in *Cxcr4^{flox}; Nfatc1-Cre* valves 66

Pharmacological inhibition of CXCR4 results in increased mesenchymal cell proliferation in explanted OFT 68

Generation of a soluble HBEGF (sHBEGF) gain-of-function transgenic mouse model 70

Endocardial/endothelial overexpression of *sHBEGF* leads to valve defects that persist and worsen post-natally 73

Excessive EMT does not contribute to the enlarged valve phenotype in *R26-sHBEGF$^{tg/+}$; Tie2-Cre* transgenic mice 76

Increased post-EMT mesenchymal cell proliferation in *R26-sHBEGF$^{tg/+}$; Tie2-Cre* mice 78

Mesenchymal cell proliferation is increased in explanted *R26-sHBEGF$^{tg/+}$; Tie2-Cre* OFT tissue 80

Supplementing explanted OFT tissue with sHBEGF increases mesenchymal cell proliferation and migration 82

Supplementing OFT explants with a pan-ErbB inhibitor decreases mesenchymal cell proliferation, migration and invasion 84

sHBEGF overexpression using the *Nfatc1-valveCre* driver does not recapitulate the *Tie2-Cre* driver phenotype 86

DISCUSSION 89

Insights from previous *Cxcl12*, *Cxcr4* and *Cxcr7* knockout models 90

BMP-Smad1/5/8 is not a CXCR4 effector pathway 93

Nuanced effects of AMD3100 on CXCR4 and CXCR7 94

Insights from *Hbegf* knockout models 95

Parallels between *sHBEGF* overexpression and *Shp2* overactivation models 96

The complex relationship between HBEGF and the ErbB family of receptors 97

Insights from the perturbation of the HBEGF-ErbB signaling axis ex vivo 98

Limitations of the *sHBEGF* gain-of-function model 99

Final considerations 100

CONCLUSIONES/CONCLUSIONS 103

BIBLIOGRAPHY 107

ABBREVIATIONS

Abbreviation Meaning

AAA, aortic arch arteries
ADAM, a disintegrin and metalloprotease
ANOVA, analysis of variance
Aov, aortic valve
AV, atrioventricular
AVV, atrioventricular valves
AVC, atrioventricular canal
BAV, bicuspid aortic valve
BMP, bone morphogenetic protein
BrdU, 5-bromo-2'-deoxyuridine
cDNA, complementary DNA
cTNT, cardiac troponin T
E, embryonic day
ECM, extracellular matrix
EdU, 5-ethynyl-2'-deoxyuridine
EGFR, epidermal growth factor receptor
EMT, endothelial to mesenchymal transition
FHF, first heart field
GPCR, G protein-coupled receptor
H&E, hematoxylin and eosin
HBEGF, heparin-binding epidermal growth factor-like growth factor
IB4, isolectin B4
ISH, *in situ* hybridization
La, left atrium
Lv, left ventricle
MAP, mitogen-activated protein
Mv, mitral valve
NCC, neural crest cell
Ns, non-significance
OFT, outflow tract
ON, overnight
PFA, paraformaldehyde
Pv, pulmonary valve
PCR, polymerase chain reaction
qPCR, quantitative real-time PCR
Ra, right atrium
RT, room temperature
RTK, receptor tyrosine kinase
Rv, right ventricle
SMA, smooth muscle actin
sHBEGF, soluble HBEGF
SHF, second heart field
SL, semilunar
SLV, semilunar valves
TGF, transforming growth factor
Tv, tricuspid valve
VE-cadherin, vascular endothelial cadherin
VSD, ventricular septal defects
WT, wild type

INTRODUCTION

Early heart development

The heart is the first organ to be formed during vertebrate embryogenesis (Figure 1). Heart development begins during gastrulation around embryonic day 7 (E7), when cardiac progenitor cells migrate to the lateral region underlying the head folds to form the cardiac crescent (Abu-Issa & Kirby, 2007; Vincent & Buckingham, 2010). These progenitors express transcription factors crucial for proliferation and differentiation. They originate from mesodermal cells located in the lateral plate of the primitive streak (Lawson et al., 1991; Tam & Behringer, 1997) and express Mesp1/2 (Bondue & Blanpain, 2010; Saga et al., 2000). The cardiac crescent contains the first heart field (FHF) (Fig. 1A), which is characterized by the early expression of Nkx2.5 and GATA4 (Buckingham et al., 2005). There is a second source of cardiac progenitors, called the second heart field (SHF) (Fig. 1A), which is later incorporated into the heart tube (Dyer & Kirby, 2009) and is characterized by expression of Isl1 and Foxh1 (Buckingham et al., 2005). The SHF is characterized by a proliferation and differentiation delay with respect to the FHF (Van Den Berg & Moorman, 2009). Thus, the FHF differentiates at the cardiac crescent stage, whereas differentiation of the SHF is relatively delayed, occurring as the second lineage migrates in to join the differentiated cells of the first lineage (Srivastava, 2006). Both lineages are regulated by complex signaling networks involving members of the bone morphogenetic protein (BMP) family, sonic hedgehog, fibroblast growth factor, Wnt, and Notch proteins (Srivastava, 2006). Whereas the FHF contributes to the atria, left ventricle, and part of the ventricular septum, the SHF contributes to the outflow tract (OFT) and right ventricle (Cai et al., 2003; Srivastava, 2006; Zaffran et al., 2004).

As the embryo grows, the crescent of the FHF fuses in the ventral midline, forming a structure that closes dorsally to form the primitive heart tube (Fig. 1B). This linear tube is suspended from the body wall by dorsal mesocardium and is composed of an inner endocardial layer separated from surrounding myocardium by an acellular gelatinous extracellular matrix (ECM) named cardiac jelly (Fig. 1B). The cardiac jelly is produced first by endocardial and myocardial progenitors and incorporates ECM synthetized by lateral mesodermal cells (Aleksandrova et al., 2012; Srivastava, 2006; Suzuki et al., 1995). The heart tube elongates on both the arterial and venous poles by addition of SHF-derived progenitor cells (Buckingham et al., 2005; Cai et al., 2003; Kelly et al., 2001; Mjaatvedt et al., 2001) and the proliferation of cells already present (de Boer et al., 2012). Concurrently, the dorsal mesocardium dissolves except at the poles, liberating the majority of the heart tube and allowing it to undergo rightward looping (Fig. 1C) (Lin et al., 2012). While looping occurs, the heart becomes regionalized into the atrial and ventricular

segments from the OFT and the atrioventricular canal (AVC) (Fig. 1D) and express different patterning genes (Lin et al., 2012).

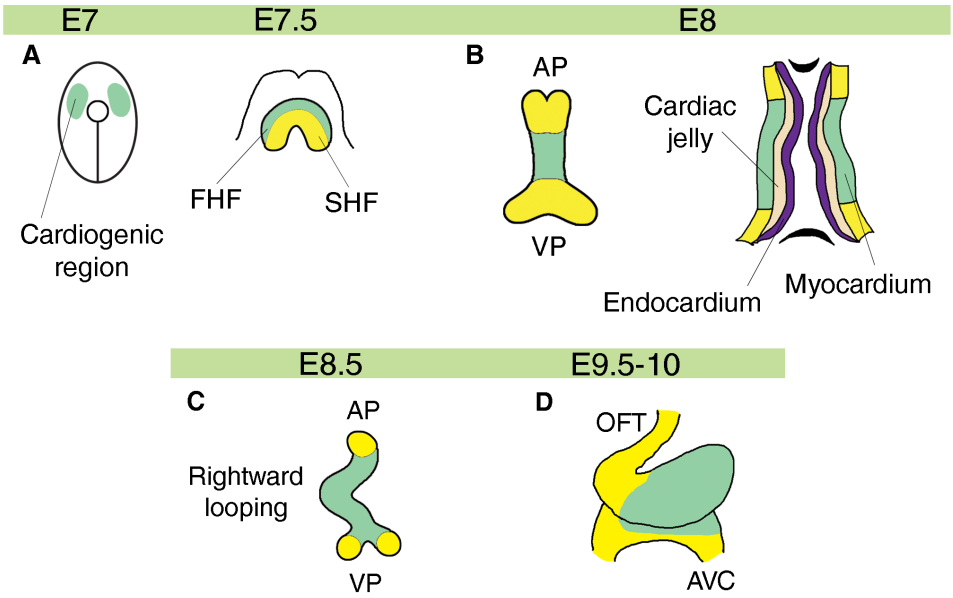

Figure 1. Summary of the main events during early heart development in mice. Structures derived from the FHF and the SHF are shown in green and yellow, respectively. **A**: Cardiac progenitors migrate antero-laterally in the embryo after emerging from the primitive streak at approximately E7. Cardiogenic regions of the lateral plate mesoderm fuse at the embryo ventral midline and form the cardiac crescent at E7.5, containing FHF and SHF progenitors. **B**: The primitive heart tube extends by addition of SHF progenitors to the arterial and venous poles. The tube is a linear structure composed of myocardium lined by endocardium, separated by cardiac jelly. **C**: As the heart tube elongates, it undergoes rightward looping (E8.5). **D**: At E9.5, formation of the AVC and the OFT separates the developing atria and ventricles. (modified from D'Amato et al., 2015; Luxán et al., 2013; MacGrogan et al., 2016). FHF, first heart field; SHF, second heart field; AP, arterial pole; VP, venous pole; OFT, outflow tract; AVC, atrioventricular canal.

Early valvulogenesis

1. Endothelial to Mesenchymal Transition (EMT)

The first evidence of endocardial cushion formation is the appearance of localized swellings in the AVC and OFT regions of the heart at E9.5 (Fig. 2A) (Fishman & Chien, 1997; Martinsen, 2005; A. Moorman et al., 2003). The myocardium of the AVC and the OFT secretes ECM, adding to the cardiac

jelly between the myocardium and endocardium (Moorman & Christoffels, 2003). This causes the region to swell into the lumen of the heart, thereby forming the endocardial cushions (Camenisch et al., 2000; Henderson & Copp, 1998; Markwald et al., 1977). These swellings work as rudimentary valves at this stage, as they are able to act as physical barriers that prevent the backflow of blood through the primitive heart tube. The cellularization of the endocardial cushions is a complex process, wherein a subset of endocardial cells undergoes endothelial to mesenchymal transition (EMT) (Eisenberg & Markwald, 1995; Person et al., 2005). Cells undergoing EMT delaminate from neighboring cells and invade the cardiac jelly, where they differentiate into mesenchymal cells and subsequently proliferate. In the mouse, EMT occurs around 9.5 in the AVC, whereas in the OFT it takes place around E10.5 (Markwald et al., 1977). Endocardial cushion formation is induced by signaling molecules emanating from the OFT and AVC myocardium (Fig. 2B) (Chang et al., 2004; Harrelson et al., 2004; Moorman & Christoffels, 2003; Plageman & Yutzey, 2005; Rivera-Feliciano & Tabin, 2006). In parallel, a sheath of progenitor cells originating from the proepicardial organ grows over the myocardium, forming the epicardium, the outermost layer of the heart, via epithelial to mesenchymal transition (von Gise et al., 2011).

Crucial EMT drivers in the AVC and OFT myocardium are BMPs, members of the Transforming Growth Factor Beta (TGFβ) superfamily, which act as the major myocardium-derived signals for the initiation of EMT (Combs & Yutzey, 2009). Bmp2 activates a regulatory cascade in both the myocardium and the neighboring endocardium (Combs & Yutzey, 2009; Rivera-Feliciano & Tabin, 2006). Expression of Bmp2 is essential for conferring non-chamber identity to the AVC and OFT myocardium. Mice lacking myocardial *Bmp2* fail to express Tbx2 in AVC myocardium, which is necessary for the suppression of chamber-specific genes (Harrelson et al., 2004; L. Ma et al., 2005; Rivera-Feliciano & Tabin, 2006). Furthermore, Bmp2 expression is sufficient to induce EMT in monolayer cultures of mouse endothelium (Sugi et al., 2004) and ventricular explants (Luna-Zurita et al., 2010). On the other hand, conditional ablation of *Bmp4* in the myocardium results in atrioventricular septal defects, suggesting that it regulates septation of the cardiac chambers after the cushions are formed (Jiao et al., 2003). Myocardial TGFβ signaling is also crucial. It has been shown to induce expression of the transcription factor Snail2 in the chicken heart, which represses epithelial genes (Romano & Runyan, 1999, 2000). Another key player is Notch1, which is expressed throughout the endocardium of the heart tube, with elevated levels in the AVC and OFT regions. Endocardial Notch1, via its effector RBPJK, directly activates the expression of Snail1, a critical EMT driver that represses vascular endothelial cadherin (VE-cadherin),

thereby allowing activated mesenchymal cells to break contact with neighboring cells and migrate into the cardiac jelly (Fig. 2B) (Timmerman et al., 2004). On the other hand, the subset of endocardial cells that do not undergo EMT have high levels of the transcription factor Nfatc1 (Zhou et al., 2005). Nfatc1 is known to inhibit Snail1 and Snail2, therefore preserving VE-cadherin expression and allowing the cells to retain their adhesiveness. Nfatc1-high cells are consequently able to remain in the endocardium as a proliferative population that later supports valve leaflet extension (Wu et al., 2011; Zhou et al., 2005).

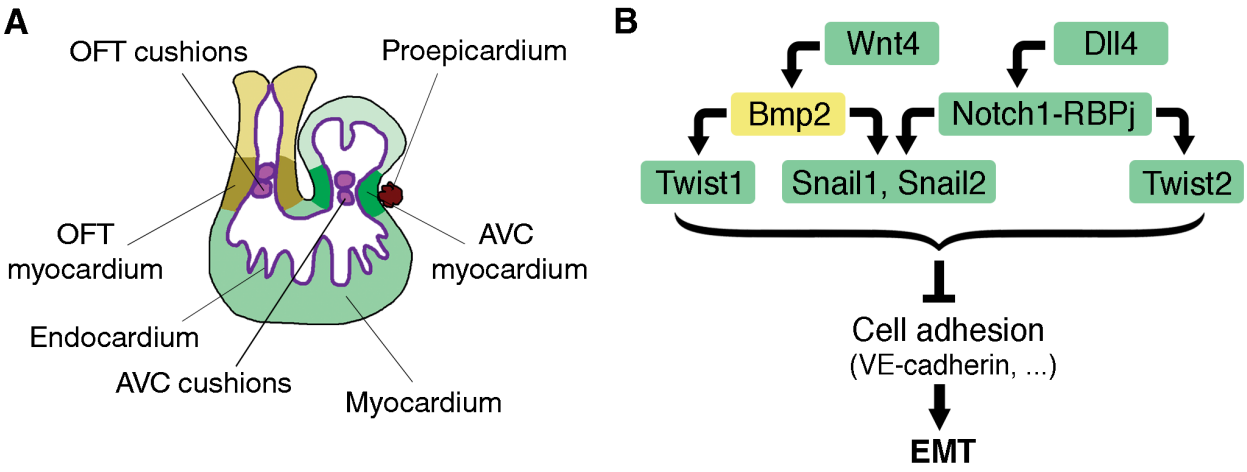

Figure 2. The early four chamber heart and regulation of valve primordia formation via EMT. A: Formation of the endocardial cushions occurs at E9.5 in the AVC and E10.5 in the OFT, together with ventricular chamber development that begins with trabeculae formation in the myocardium and epicardial formation from the proepicardium. **B**: Key signaling molecules intervening in EMT. Myocardium-derived signals are shaded in yellow and molecules secreted by the endocardium are shaded in green. Myocardial Bmp2 is required for Snail1, Snail2, and Twist1 expression. Endocardial Notch1 signaling also leads to Snail1/2 activation, which in turn repress VE-cadherin so that EMT can occur. Wnt4 expression promotes myocardial Bmp2 expression. (modified from MacGrogan et al., 2018). OFT, outflow tract; AVC, atrioventricular canal; EMT, endothelial to mesenchymal proliferation.

2. Origins of cardiac mesenchyme

Cell lineage analysis of neonatal *Rosa26*; *Tie2-Cre* mice demonstrate that most cells throughout the final leaflets of mature valves derive from the endothelium/endocardium (Lincoln et al., 2004). However, other extra-cardiac cell types invade and mix with endocardium-derived mesenchymal cells, adding complexity to the valve morphogenic process (Figure 3) (Poelmann et al., 2002).

After the rearrangement of the cardiac jelly and before OFT septation, four ridge-like cushions surround the OFT lumen. There are two larger and elongated cushions, most commonly referred to as the septal and parietal ridges, and, between them, two smaller ones, known as the intercalated ridges (Pérez-Pomares et al., 2003; Ya et al., 1998). The major ridges are formed by proximal and distal components (Fig. 3A). From E10.5 onward, the OFT is remodeled from a single OFT vessel, which circulates blood into the three main aortic arch arteries (AAA) to join two dorsal aortae that distribute the blood throughout the embryo (Luxán et al., 2016) (Fig. 3B). The proximal OFT (also referred to as the conal cushions) fuses and creates separate outlets connecting the left and right ventricles to the aortic and pulmonary valve, respectively (Snarr et al., 2008). Remodeling of the distal OFT (also known as the truncal cushions) results in the formation of the aortic and pulmonary semilunar valves (Lin et al., 2012; Snarr et al., 2008). In addition, the fusion of the distal OFT results in the formation of the aortopulmonary septum, which divides the aorta and pulmonary trunk (Jiang et al., 2000; Lin et al., 2012; Snarr et al., 2008). This enables the separation of the arterial and venous circulation. Interestingly, mesenchymal cells derived from the endocardium via EMT are found solely at the proximal region of the OFT cushions (Fig. 3A) (Snarr et al., 2008). At least two additional cell types contribute to the formation of SL valve leaflets and to aortopulmonary septation: the cardiac neural crest cells (NCCs) and SHF-derived cells (Snarr et al., 2008).

A population of NCCs derived from the hindbrain migrates into the distal OFT, in a process concurrent with EMT (Fig. 3A, B) (Jiang et al., 2000; Kirby, 1999; Kirby et al., 1983). NCCs invade the AAA to reach the distal OFT and differentiate into smooth muscle cells covering the AAA endothelium (Fig. 3B) (Luxán et al., 2016). Intermingled with these NCCs, mesenchymal cells derived from the SHF are also found. SHF-derived cells contribute not only to the formation of the leaflets of the semilunar valves, but also to the outflow tract walls (Snarr et al., 2008). SHF-derived smooth muscle cells from the OFT wall and the myocardium enter the emerging aortopulmonary septum to complete the septation process through myocardialization (Van Den Hoff et al., 1999).

In the AVC, the mesenchyme of the superior and inferior cushions fuses, dividing the canal into mitral and tricuspid orifices that form ventricular inlets (Lin et al., 2012). Meanwhile, the primary atrial septum grows from the atrial roof towards the AVC, with a mesenchymal cap at its leading edge (Lin et al., 2012) (Fig. 3A). This muscular outgrowth partially septates the atrial chamber but leaves an opening (the ostium primum) between the mesenchymal cap and the AVC, which is later sealed off (Mommersteeg et al., 2006; A. Wessels et al., 1996; Andy Wessels & Sedmera, 2004) (Fig. 3A).

SHF progenitors give rise to the dorsal mesenchymal protrusion, a mesenchymal tissue that protrudes into the atrial chamber through the dorsal mesocardium and merges with AV cushions to become part of the atrial septum (Goddeeris et al., 2008; Lin et al., 2012; Snarr et al., 2008) (Fig. 3A). Another cellular type that contributes to the developing AV septum is epicardium-derived cells (Gittenberger-de Groot et al., 1998; Pérez-Pomares et al., 2003; Pérez-Pomares & Muñoz-Chápuli, 2002). These cells contribute not only to the annulus, but also to the mural mitral and tricuspid leaflets (Gittenberger-de Groot et al., 1998; Andy Wessels et al., 2012; Zhou et al., 2010).

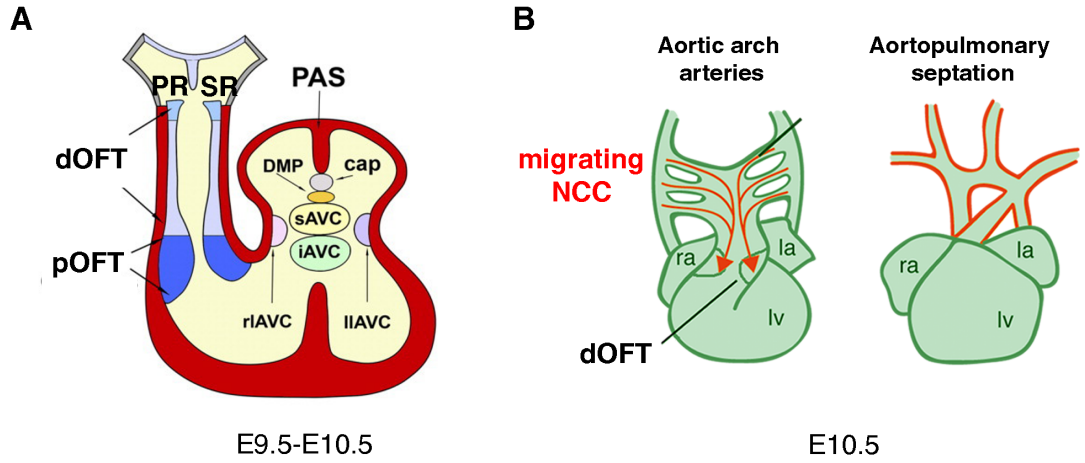

Figure 3. Components of the OFT and AVC cushions and NCC-dependent AAA remodeling and aortopulmonary septum formation. **A**: The OFT cushions are composed of a septal and parietal ridge, which are further divided into distal and proximal components. The AVC cushions are composed of four cushions: two major cushions, the superior and inferior, and the lateral cushions, which form after the major ones. Proper AV septation also requires the contribution of two additional mesenchymal structures; the mesenchymal cap on the leading edge of the primary atrial septum and the dorsal mesenchymal protrusion. **B**: The OFT region of the heart initially exists as a single outflow vessel, which circulates blood into three major pairs of AAA to join the two dorsal aortae that distribute the blood throughout the embryo. NCCs migrate from the neural tube to the OFT, where they remodel to form the mature aortic arch, with NCC–derived vascular smooth muscle cells contributing to most of the aortic arch and its major branches. (modified from Snarr et al., 2008 and Luxán et al., 2016). PR, parietal ridge; SR, septal ridge; dOFT, distal outflow tract; pOFT, proximal outflow tract; PAS, primary atrial septum; DMP, dorsal mesenchymal protrusion; sAVC, superior AV cushion; iAVC, inferior AV cushion; llAVC, left lateral AV cushion; rlAVC, right lateral AV cushion; NCC, neural crest cell; ra, right atrium; la, left atrium; lv, left ventricle.

Valve elongation and remodeling

After EMT and cushion formation, the primitive valves continue to grow via high proliferation of the mesenchymal cells and continued ECM synthesis (Armstrong & Bischoff, 2004; Hinton et al., 2006). Unlike the highly stratified layers of the mature valves, the ECM of the endocardial cushions is initially composed primarily of hyaluronan and a loosely organized collagen network, that allows for cell migration (Schroeder et al., 2003). There is elongation of the mesenchymal core, which becomes thickened and stratified over time (de la Cruz & Markwald, 1998).

1. Structure of the mature valves

The cardiac valves ensure unidirectional blood flow through the heart to the rest of the body. A mature valve is formed by leaflets, composed of lamellae of extracellular matrix and connective tissue, and the annulus, which runs circumferentially around the valve and anchors the leaflet at its base (Icardo & Colvee, 1995). The connective tissue includes fibroblasts, myofibroblasts and smooth muscle cells, that are collectively referred to as valve interstitial cells (Butcher & Markwald, 2007; Mulholland & Gotlieb, 1996). The mitral and tricuspid atrioventricular (AV) valves separate the atria from the ventricles (Fig. 4A). They close during the start of ventricular contraction (systole). Mature AV valves are characterized by leaflets hinged together with ring-shaped annuli and tethered to the ventricles by the tendinous cords and papillary muscles (Fig. 4B). The tendinous supporting apparatus governs tension and movements of the leaflets during the cardiac cycle (Camenisch et al., 2010). The mitral valve is composed of two leaflets, whereas the tricuspid valve is composed of three. The aortic and pulmonary semilunar (SL) valves separate the ventricles from the great arteries (Fig. 4A). They close at the beginning of ventricular relaxation (diastole). The aortic root is made up of the fibrous valve annulus region and the arterial tissue within the aortic sinuses (Hinton & Yutzey, 2011). The pulmonary valve is separated from the other valves by a muscular sleeve and has a poorly defined annulus structure. Unlike the AV valves, the SL valve leaflets are anchored directly to the arterial roots. Both pulmonary and aortic valves are composed of three leaflets.

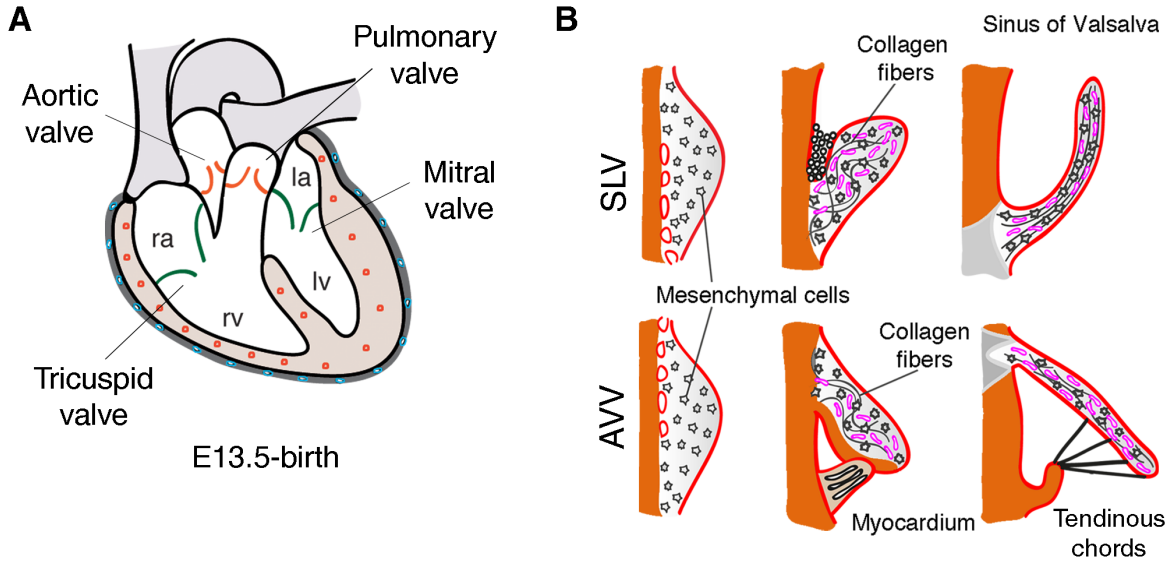

Figure 4. Final location of the valves in the mid-gestation heart and AV and SL valve morphogenesis. A: From E13.5 onwards, the valves ensure unidirectional blood flow through the heart to the rest of the body. The mitral and tricuspid AV valves separate the atria from the ventricles, while the aortic and pulmonary SL valves separate the ventricles from the great arteries. The myocardium is depicted in brown, the epicardium in gray, and the coronary vessels in red and blue. **B**: Leaflet remodeling in SL (top) and AV (bottom) valves. The SL cusps undergo excavation and eventually give rise to the sinus of Valsalva. The mural leaflets of both AV valves are supported by AV myocardium at their ventricular side. As the primordial leaflets distend into the lumen, thin strands of elongated muscle remain attached to the valve leaflet. Eventually, apoptosis yields a mobile leaflet plus remnants that contribute to the tendinous cords and papillary muscles. The myocardium is depicted in orange, proteoglycans in pink, and mesenchyme in gray. (modified from Luxán et al., 2016). la, left atrium; lv, left ventricle; ra, right atrial; rv, right ventricle; SLV, semilunar valves; AVV, atrioventricular valves.

2. Remodeling of the ECM and reduction of mesenchymal proliferation

The window of time during which the undifferentiated mesenchymal cushions stop proliferating and remodel their local environment into mature leaflets and supporting valve apparatus is known as the remodeling phase. Valve remodeling is a poorly understood multi-step process that continues into postnatal life (Camenisch et al., 2010; Hinton et al., 2006). Remodeling events depend on the downregulation of the earlier mesenchymal cell proliferation (Aikawa et al., 2006; Hinton et al., 2006), as well as apoptosis at the base of the leaflets (Hurle et al., 1980; Watanabe et al., 2001). From E12.5 to E15.5, proteoglycans are diffusely expressed throughout developing valves, and no stratification is observed (Fig. 4B) (Hinton et al., 2006). Remodeling also implies stratification of the ECM into organized layers rich in

collagens, elastins and proteoglycans, which are secreted in large amounts by cushion mesenchymal cells (Hinton et al., 2006; Lincoln et al., 2004; Lincoln & Yutzey, 2011; Peacock et al., 2008). This is accompanied by upregulation of other ECM remodeling enzymes, such as metalloproteases, cathepsins and hyaluronidases (Combs & Yutzey, 2009; McGuire & Orkin, 1992; Person et al., 2005).. ECM stratification is a central feature of mouse valvulogenesis and begins during late development (starting at around E18.5) (Hinton et al., 2006). Nevertheless, a fully mature valve structure is not appreciated until postnatal life (Hinton et al., 2006; Rabkin-Aikawa et al., 2004).

It is crucial that mesenchymal proliferation is well-timed, as failure in doing so leads to hyperplastic cardiac valves. To help highlight and understand the complexity of valve remodeling, a summary of the valvuloseptal phenotypes found in several mouse models is shown on Table 1. Table 1 illustrates the diversity of signals involved in the regulation of mesenchymal proliferation, considering that disruption of a wide array of pathways results in leaflet hyperplasia. Interestingly, several of the mutations leading to valve hyperplasia affect the endothelium/endocardium specifically, which is consistent with the endocardium being the tissue coordinating many developmental processes in the heart (José Luis de la Pompa & Epstein, 2012; Luxán et al., 2016; MacGrogan et al., 2018). In fact, many of the pathways implicated are known to interact in the endocardium, including Notch, EGFR and Wnt. Deletion of genes encoding several classes of proteins, including transcription factors, receptors, ligands, all lead to defects in valve and septum morphogenesis. Furthermore, many of the targeted genes listed in Table 1 are found mutated in human patients with congenital valve disease, emphasizing the clinical relevance of studying the remodeling phase of valvulogenesis.

Genotype	Target tissue	Cardiac Phenotype	CV Disease	Reference
Notch				
Mib1flox; Nkx2.5-Cre	EC, myo	SLV and AVV hyperplasia; BAV; VSD	BAV; LVNC	MacGrogan et al., 2016
Mib1flox; Tnt-Cre-Cre	Myo	BAV	BAV	Captur et al., 2016
Jag1flox; VE-Cad-Cre	End	SLV and AVV hyperplasia; Ventricular hypertrophy; OA; CAD; VSD	Alagile syndrome	Hofmann et al., 2012
Jag1flox; Nkx2.5-Cre	EC, myo	SLV and AVV hyperplasia; BAV; VSD; DORV	BAV	MacGrogan et al., 2016
Jag1flox; Nfatc1-valveCre	Valve EC	SLV and AVV hyperplasia; BAV; VSD; DORV	BAV	MacGrogan et al., 2016
Jag1flox;Jag2flox; TnT-Cre	Myo	VNC; BAV	LVNC; BAV	Eley et al., 2018
Notch1flox; Nfatc1-valveCre	Valve EC	SLV and AVV hyperplasia; BAV; VSD	HLHS; BAV; CAVVD	MacGrogan et al., 2016
Notch1flox; Cdh5-CreERT2	End	SLV and AVV hyperplasia; BAV; VSD	HLHS; BAV; CAVVD	MacGrogan et al., 2016
RbpJflox; Nfat1-valveCre	Valve EC	SLV and AVV hyperplasia; BAV; VSD	BAV	MacGrogan et al., 2016
BMP				
Alk2flox/flox; Gata5-Cre	Epi	BAV; VSD	BAV	Thomas et al., 2012
Smad6-/-		SLV and AVV hyperplasia; Cartilaginous metaplasia	CAVVD	Galvin et al., 2000
Tgfb				
Tgfb2-/-		SLV and AVV hyperplasia	Loeys-Dietz	Azhar et al., 2011
EGFR				
Hbegf-/-		SLV and AVV hyperplasia		Jackson et al., 2003; Iwamoto et al., 2003
Hbegfflox; SM22α-Cre	SM	SLV and AVV hyperplasia		Nanba et al., 2006
Hbegfflox; Tie2-Cre	End	SLV and AVV hyperplasia		Nanba et al., 2006
Hbegfuc/uc		SLV and AVV hyperplasia		Yamazaki et al., 2003
HbegfΔTM		Ventricular Hypertrophy		Yamazaki et al., 2003
HbegfΔhb		SLV and AVV hyperplasia		Iwamoto et al., 2010
Egfrwa2/wa2		SLV hyperplasia		Chen et al., 2000
Egfrwa2/wa2,Ptpn11+/–		SLV hyperplasia		Chen et al., 2000
Egfr-/-		SLV and AVV hyperplasia		Jackson et al., 2003
Adam17-/-		SLV and AVV hyperplasia		Jackson et al., 2003
Adam17ΔEx5/ΔEx5		SLV and AVV hyperplasia		Jackson et al., 2003
Adam17flox/ΔEx5 ; Tie2-Cre	End	SLV hyperplasia		Wilson et al., 2013
Adam19-/-		SLV and AVV hyperplasia; VSD; OA		Zhou et al, 2004; Kurohara et al., 2004
Adam17-/-;Adam19-/-		SLV and AVV hyperplasia; VSD; OA		Horiuchi et al., 2005
Intracellular transducers				
D61G-Shp2		SLV and AVV hyperplasia; DORV; VSD; VNC	Noonan syndrome	Araki et al., 2004
Q79R-Shp2; Tie2-Cre		SLV and AVV hyperplasia; DORV; VSD; VNC	Noonan syndrome	Krenz et al., 2008
caMEK1; Tie2-Cre		SLV and AVV hyperplasia		Krenz et al., 2008
NF1Fcr		Cushion hyperplasia; VSD	NF-1	Brannan et al., 1994
PLCeΔX/ΔX		SLV hyperplasia		Tadano et al, 2005

Wnt/b-catenin				
Axin2-/-		SLV and AVV hyperplasia; MVD	MVP	Hulin et al., 2016
GPCR				
Cxcl12-/-		SLV hyperplasia; CAD; DORV; OA; VSD		Ivins et al., 2015
Cxcr4-/-		SLV hyperplasia; CAD; BAV	BAV	Ivins et al., 2015
Cxcr4flox/-; Tie2-Cre	End	SLV hyperplasia; CAD; BAV; VSD; OA	BAV	Ivins et al., 2015
Cxcr7-/-		SLV hyperplasia; BAV; VSD; OA	BAV	Sierro et al., 2007; Yu et al., 2010
Cxcr7flox/-; Tie2-Cre	End	SLV hyperplasia; Hypertrophy		Yu et al., 2010
Ephrin				
Ephrinb2rev		Hyperplasia		Cowan et al., 2003
Robo/SLVit				
Robo1-/-;Robo2-/-		SLV and AVV hyperplasia; BAV; VSD	BAV	Mommersteeg et al., 2015
Robo4tm1Lex/tm1Lex		AoV hyperplasia; BAV	BAV; AscAA	Gould et al., 2018
Gata				
Gata5+/-		BAV	BAV	Laforest et al., 2011
Gata5flox; Tie2-Cre	End	BAV	BAV	Azhar et al., 2011
Gata6+/-		AoV hyperplasia; BAV	BAV	Gharibeh et al., 2018
Gata6flox; ISLV1-Cre	Myo	AoV hyperplasia; BAV	BAV	Gharibeh et al., 2018
Other Transcription Factors				
Nkx2.5+/-		BAV	BAV	Biben et al., 2000
Krox20-/-		BAV	BAV	Odelin et al., 2014; Odelin et al., 2017
ECM				
Matr3+/-		BAV; VSD; CoA; PDA; DORV	LVOTO; BAV	Quintero-Rivera et al., 2015
Nos3+/-		BAV	BAV	Lee et al., 2000
Adamts5-/-		SLV hyperplasia		Dupuis et al., 2013
Adamts5-/-;Smad2+/-		BAV, BPV	BAV	Dupuis et al., 2013
Adamts19-/-		SLV and AVV hyperplasia	familial HVD	Wunnemann et al., 2020
Cilia				
Ift88flox/flox; Nfatc1-Cre	End	BAV; VSD	BAV	Toomer et al., 2017
Exoc5flox/flox; Nfatc1-Cre	End	BAV; VSD	BAV	Fulmer et al., 2019
Modifying Enzymes				
GalNt1-/-		SLV and AVV hyperplasia		Tian et al., 2015

Table 1. Valvuloseptal phenotypes in mouse models. Summary of the major valve and septal phenotypes found upon disruption of genes involved in several signaling pathways, and their association to congenital valve disease. SLV, semilunar valves; AVV, atrioventricular valves; BAV, bicuspid aortic valve; LVNC, left ventricular non-compaction; VSD, ventricular septal defects; OA, overriding aorta; DORV, double outlet right ventricle; CoA, coarctation of the aorta; CAVD, calcified aortic valve disease; NF-1, neurofibromatosis type 1; MVP, mitral valve prolapse; LVOTO, left ventricular outflow tract obstruction; HVD, heart valve disease; AscAA, ascending aortic aneurysm; HLHS, hypoplastic left heart syndrome; PDA, patent

ductus arteriosus; EC, endocardium; End, endothelium; Myo, myocardium; Epi, epithelium; SM, smooth muscle.

Congenital valve disease and BAV

The mature mammalian heart has four valves and four chambers, which separate systemic from pulmonary circulation and ensure unidirectional blood flow (Fig. 4A). The formation of these structures is a complex process that requires integration of a wide range of signals coming from multiple cell types. These processes often go awry in the developing human fetus, leading to heart malformations affecting from 0.4% to 5% of live births (Hoffman & Kaplan, 2002). Defective development of the heart valves occurs in 20–30% of all congenital cardiovascular malformations (Pierpont et al., 2007). Developmental defects in valve structure and function occur in several genetic disorders, including Down, Noonan, Marfan and Williams syndrome (Weismann & Gelb, 2007). With age, the incidence of heart valve disease increases significantly. Degenerative abnormalities associated with severe aortic stenosis and mitral and tricuspid regurgitation are found in no less than 10% of the population aged 75 years or older (Rostagno, 2019). Hence, congenital valve disease represents a major cause of morbidity and mortality later in life (Brickner et al., 2000), and constitutes a substantial medical issue challenging our society today.

The morphogenesis of the OFT is a complex process due to the contribution of different cell types, which are regulated by the spatio-temporal coordination of many signaling pathways. In fact, anomalies in OFT development underlie 30% of all human congenital heart defects (Srivastava & Olson, 2000). Misaligned or incomplete OFT septation leads to a spectrum of malformations such as double outlet right ventricle, overriding aorta, tetralogy of Fallot, transposition of great arteries, among others (Brickner et al., 2000; Neeb et al., 2013).

Bicuspid aortic valve (BAV) is the most common form of congenital heart defect, with a prevalence estimated at 0.5-2% (Hinton & Yutzey, 2011; Sillesen et al., 2018). Although usually asymptomatic at birth, BAV predisposes individuals to several valvular dysfunctions, such as valve insufficiency, early calcification and progressive ossification of the leaflets and aortic stenosis, which may eventually require treatment and/or replacement (Fedak et al., 2002; Garg, 2006; Otto, 2002).

Anatomically, BAVs display two aortic cusps, instead of the normal three (Fig. 5A). BAVs have either two cusps of unequal size (where the larger of the two represents a fusion) or incomplete separation of two cusps (Ladich et al., 2016). Fusion of adjacent leaflets in fetal life, resulting in the presence

of a raphe, is presumed to cause many cases of BAV (Fig. 5B) (Eley et al., 2018; Ladich et al., 2016; Sievers & Schmidtke, 2007). When no raphe is present, the valve is called strictly bicuspid (Fig. 5C). BAVs induce an abnormal, turbulent flow pattern and higher tissue stresses (Ladich et al., 2016). Loss of SHF progenitors, either because of a failure of their formation or their premature differentiation, may be a common mechanism underlying the formation of strictly bicuspid BAV (Eley et al., 2018).

There are three main BAV morphologies: type 1, when there is fusion of the right and left coronary cusps; type 2, when there is fusion of the right and non-coronary cusps; and the more rare type 3, when the left and non-coronary cusps are fused (Fig. 5B, C) (Schaefer et al., 2008). These types can be further divided based on the presence or absence of raphe (Fig. 5B, C) (Sievers & Schmidtke, 2007). In humans, the most common BAV subtype is type 1, with fusion of right and left coronary leaflets (R-L), accounting for 50-60% of all cases, with type 2 coming in second (Friedman et al., 2008; Koenraadt et al., 2018).

The genetic causes of BAV represent a complex model involving different interacting pathways. As illustrated in Table 1, disruption of a wide range of genes has been shown to cause BAV, such as Notch1 (Garg et al., 2005; Theis et al., 2015), its ligand Jag1 (MacGrogan et al., 2016), eNOS (T. C. Lee et al., 2000), GATA5 and 6 (Bonachea et al., 2014; Gharibeh et al., 2018), among many others.

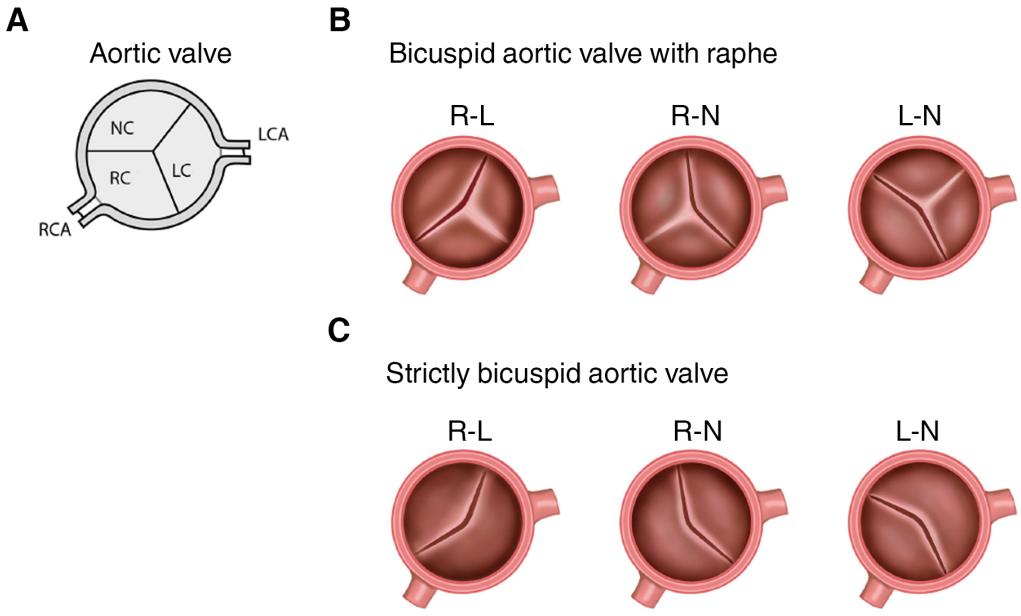

Figure 5. Schematic overview of the different types of bicuspid aortic valve (BAV). A: Normal aortic valve, composed by right, left and non-coronary cusps. **B**: Depiction of BAV with raphe, showing type 1 fusion (right and left coronary cusps; R-L), type 2 (right and non-coronary cusps; R-N) and type 3 (left and non-coronary cusps; L-N). **C**: Depiction of strictly BAV (no raphe) showing type 1 fusion (R-L), type 2 (R-N) and type 3 (L-N). (modified from Koenraadt et al., 2018). RCA, right coronary artery; LCA, left coronary artery; Nc, non-coronary cusp; LC, left coronary cusp; RC, right coronary cusp.

The CXCL12 and CXCR4 signaling axis

Chemokines are the largest family of cytokines. They are known to mediate cell chemotaxis along a concentration gradient, by binding to their respective receptors on the cell surface (Baggiolini, 1998; Blanchet et al., 2012). Chemokine receptors are classified into two groups, G protein-coupled receptors (GPCRs) and atypical chemokine receptors. While GPCRs typically mediate intracellular signaling by activation of G-proteins, atypical chemokine receptors are thought to serve as decoys independently of G-protein signaling (Bachelerie et al., 2015). GPCRs are classically thought to signal through heterotrimeric G proteins and be desensitized by β-arrestins. Heterotrimeric G-proteins are composed of Gα, Gβ, and Gγ subunits (Figure 6). CXCL12 binding triggers conformational changes in CXCR4, inducing the dissociation of the G-protein (Allen & Roth, 2011; Blanchet et al., 2012). The Gα subunit inhibits adenylyl cyclase activity and activates mitogen-activated protein (MAP) kinase and the PI3K pathway, while the Gβγ heterodimer triggers intracellular calcium mobilization through the activation of phospholipase C gamma (PLCγ) (Figure 6) (Teicher & Fricker, 2010). Both PI3K signaling and the MAP kinase pathway are involved in cell mobilization (Jiménez et al., 2000) (Figure 6). The phosphorylated residues in the C-terminal of CXCR4 also recruit cytosolic β-arrestin. β-arrestins uncouple receptors from G-protein subunits and, thus, desensitize G-protein-mediated signaling and mediate endocytosis (Figure 6) (Orsini et al., 1999; Rajagopal & Shenoy, 2018).

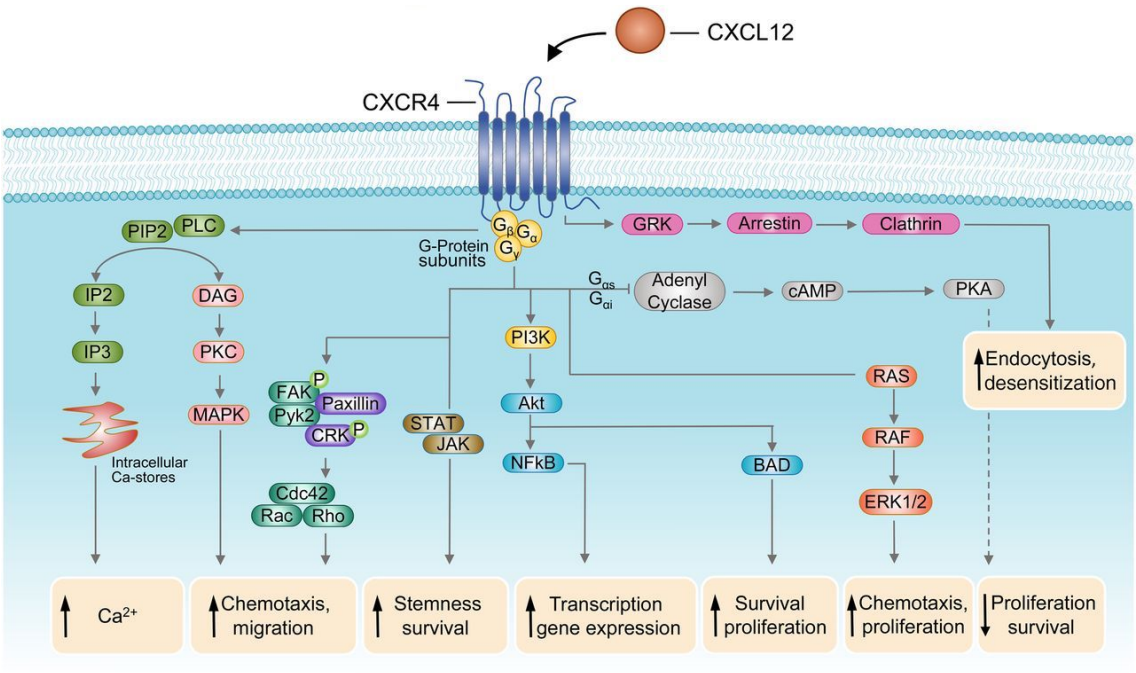

Figure 6. Key signaling cascades thought to be involved in CXCR4-CXCL12 pathway. Activation of CXCR4 induces β-arrestin–mediated endocytosis and G protein signaling via different routes, leading to several cellular outcomes, such as chemotaxis, cell survival and proliferation. (modified from Walenkamp et al., 2017).

The chemokine receptor CXCR4 belongs to the family of seven-span transmembrane GPCRs, also known as seven-transmembrane receptors (7TMRs). These receptors are the most common class of receptors in the genome and the most common target for medical therapeutics (Ma et al., 2002). CXCR4 is a ubiquitously expressed and highly conserved protein (Döring et al., 2014). It was first discovered and called leukocyte-derived seven-transmembrane domain receptor (LESTR) (Federsppiel et al., 1993), but did not receive much attention until its isolation as a coreceptor for HIV-1 (Feng et al., 1996). CXCL12, initially named SDF-1, was identified as a ligand for CXCR4 in 1996 (Bleul et al., 1996; Oberlin et al., 1996). CXCL12 is evolutionary conserved as well, and its two isoforms (α and β) are ubiquitously expressed (Shirozu et al., 1995).

The CXCL12/CXCR4 axis is known for its crucial function in the homing of hematopoietic stem and progenitor cells (HSPC). The trafficking of HSPC between tissues is intimately connected with the establishment and maintenance of hematopoiesis in different organs, which starts early in embryonic development and continues after birth (Mazo et al., 2011). Because these cells are constantly circulating from the bone marrow to the blood and back, CXCL12 binding to $CXCR4^{+}$ HSPC is essential in guiding cells for colonization and retaining them in bone marrow hematopoietic niches (Mazo et al., 2011).

CXCL12 binds an additional receptor, CXCR7, which has long been thought to function as a decoy receptor, sequestering CXCL12 from the extracellular space and thus modulating signaling through CXCR4 (Boldajipour et al., 2008; Dambly-Chaudière et al., 2007; Luker et al., 2010; Naumann et al., 2010). CXCR4-CXCR7 heterodimers have been described in the context of overexpression in transfected cells (Levoye et al., 2009; Sierro et al., 2007). Thus, it has been suggested that CXCR7 is implicated in modulating CXCR4 function by forming co-receptors (Sierro et al., 2007).

Loss of both *Cxcl12* and *Cxcr4* causes embryonic lethality in mice. *Cxcr4*- and *Cxcl12*-null mice die *in utero* or perinatally, and present hematopoietic and nervous system defects as well as VSD (Table 1) (Q. Ma et al., 1998; Nagasawa et al., 1996; Zou et al., 1998). Interestingly, more recent studies have demonstrated that CXCR4-CXCL12 signaling also plays a role during cardiac valve development. Abnormally enlarged SL valves have been described in *Cxcr4*-, *Cxcr4^{flox}; Tie2-Cre* and *Cxcl12*-null mutant mice (Table 1), in addition to extensive coronary artery defects (Ivins et al., 2015). Similarly, genetic ablation of *Cxcr7*, whether ubiquitous or endothelial, results in SL valve thickening, often accompanied by VSD and BAV (Table 1) (Sierro et al., 2007; Yu et al., 2011). Endocardial inactivation of the Notch pathway via deletion of its ligand *Jag1* leads to valve hyperplasia, similar to the phenotype seen in endothelial *Cxcr4* mutants (Table 1) (MacGrogan et al., 2016). Interestingly, RNA sequencing of *Jag1* mutant SL valves revealed that *Cxcr4* and *Cxcl12* expression was mis-regulated (MacGrogan et al., 2016), suggesting that the two pathways may interact functionally. Together, these studies point towards a novel, essential function for the CXCR4/CXCR7-CXCL12 signaling axis during valvulogenesis, that remains poorly understood.

HBEGF

Heparin-binding epidermal growth factor-like growth factor (HBEGF) was first described by Higashiyama in 1991 and 1992, as a ubiquitously expressed epidermal growth factor family member (Higashiyama et al., 1992; Higashiyama et al., 1991). HBEGF is synthesized as a transmembrane precursor protein of 208 amino acids composed of signal peptide, heparin-binding, EGF-like, juxtamembrane, transmembrane, and cytoplasmic domains (Figure 7) (Higashiyama et al., 1992). As indicated by its name, HBEGF has a high affinity for heparin and heparan sulfate, and its association with the latter on the cell surface upregulates its concentration and activity (Higashiyama et al., 1993; Raab & Klagsbrun, 1997). Proteolytic cleavage on the cell surface yields a soluble growth factor (sHBEGF) and the remaining transmembrane and cytoplasmic part (HBEGF-C) (Figure 7) (Blobel, 2005; Goishi et al., 1995). This type of proteolytic processing, known as ectodomain shedding, is mediated by metalloproteases, which cleave proHBEGF at the juxtamembrane domain (Figure 7) (Blobel, 2005). Thus, regulation of sHBEGF levels is achieved not only by gene expression, but also by controlling its proteolytic release.

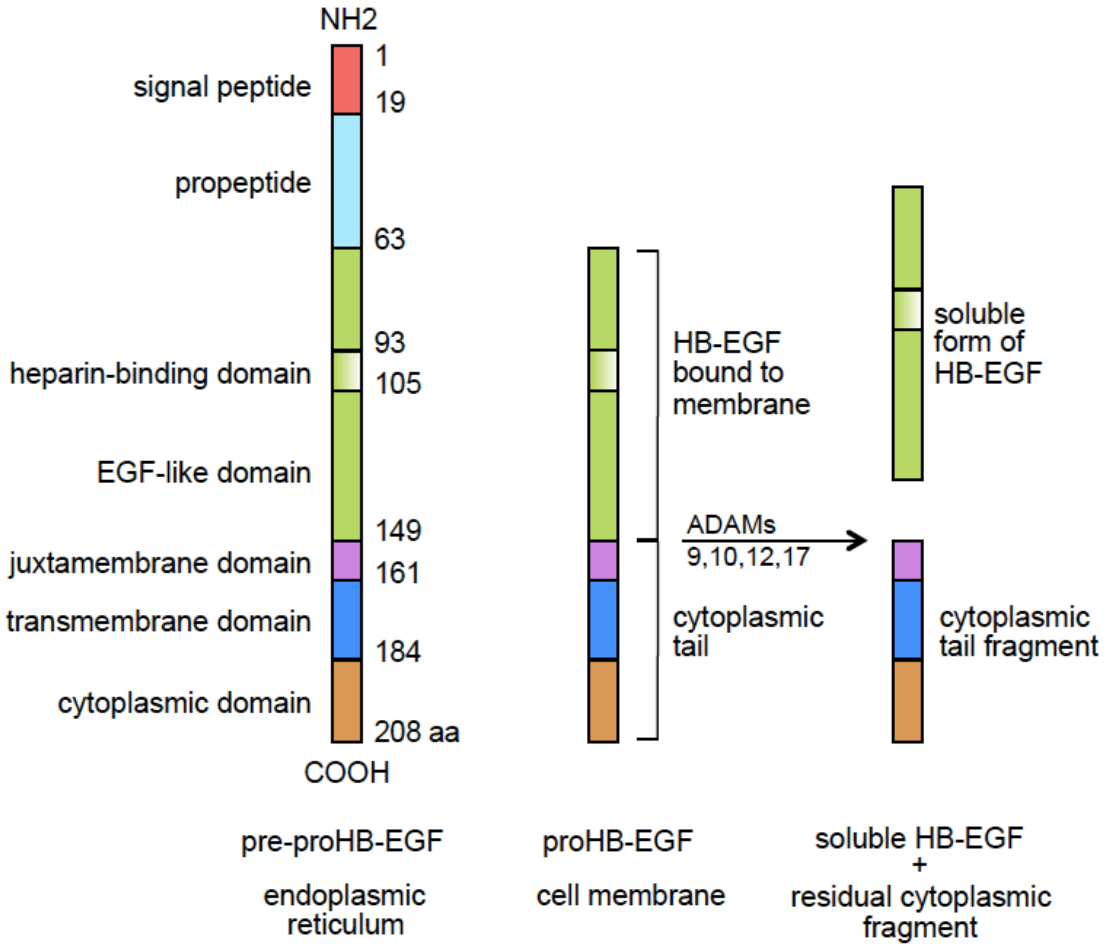

Figure 7. Basic structure, functional domains, and processing of HBEGF. HBEGF is synthesized a transmembrane proprotein that requires cleavage by A Disintegrin And Metalloproteases (ADAMs) at the juxtamembrane domain, in order to be released into the extracellular space (from Vinante & Rigo, 2013).

HBEGF has been associated with a plethora of physiologic and pathologic processes, including heart development and function (Iwamoto et al., 2003; Jackson et al., 2003), eyelid closure (Mine et al., 2005), skin wound healing (Shirakata et al., 2005; Tokumaru et al., 2000) and cardiac hypertrophy (Asakura et al., 2002), among others.

sHBEGF is a ligand for the ErbB family of receptor tyrosine kinases (RTKs). It binds and activates the epidermal growth factor receptor (EGFR, also known as ErbB1) and ErbB4 directly (Elenius et al., 1997; S. Higashiyama et al., 1992; Shigeki Higashiyama et al., 1991), and ErbB2 and ErbB3 indirectly by heterodimerization (Mekada & Iwamoto, 2008). Ligand binding induces the formation of homo- and/or heterodimers, which trigger the autophosphorylation of cytoplasmic tyrosine residues. These residues work as docking sites for a variety of signal transducers, which can be adaptor proteins or enzymes (Prenzel et al., 1999; Riese & Stern, 1998). Enzymes such as PLCγ trigger calcium signaling pathways, whereas kinases such as c-src link EGFR activation to MAP kinase signaling cascades (Belsches et al., 1997; Prenzel et al., 1999). The MAP kinase pathway is currently the best understood downstream effector of EGFR activation, and several distinct MAP kinases, such as Erk1/2 and Jnks, have been identified as signal transducers (Prenzel et al., 1999).

EGFR signaling also induces the transcription of EGFR ligands (Hashimoto et al., 1994), resulting in a positive feedback loop of ligand shedding and EGFR activation. Shedding of sHBEGF leads to paracrine activation of EGFR and ErbB4 in neighbor cells, resulting in pro-mitogenic and chemotactic effects on many cell types, such as monocytes/macrophages (Higashiyama et al., 1991), fibroblasts (Blotnick et al., 1994), smooth muscle cells (Higashiyama et al., 1993) endothelial cells (Abramovitch et al., 1998) and epithelial cells (Hashimoto et al., 1994).

Most of HBEGF's biological activities are carried out by the soluble component of the protein. Metalloproteases of the A Disintegrin And Metalloprotease (ADAM) family are thought to mediate the secretion proHBEGF. ADAM9, 10, 12 and 17 have all been shown to be involved the release of sHBEGF from its membrane-bound precursor (Asakura et al., 2002; Izumi et al., 1998; Lemjabbar & Basbaum, 2002; Sunnarborg et al., 2002; Yan et al., 2002). Several types of stimuli can trigger ectodomain

cleavage by ADAMs (Raab & Klagsbrun, 1997). One of the major ways through which sHBEGF shedding is triggered is via GPCR signaling (Figure 8). Several GPCR ligands have been shown to stimulate EGFR tyrosine phosphorylation, in a process called transactivation (Eguchi et al., 1998; George et al., 2013; Prenzel et al., 1999). Transactivation of EGFR occurs when GPCR signaling induces ectodomain shedding of its ligands by ADAMs (Figure 8), with HBEGF being often the preferred ligand for this process (Prenzel et al., 1999). Activation of EGFR in this manner is a general function of GPCR signaling and is crucial for the mitogenic activity of many GPCR ligands (Shah & Catt, 2003).

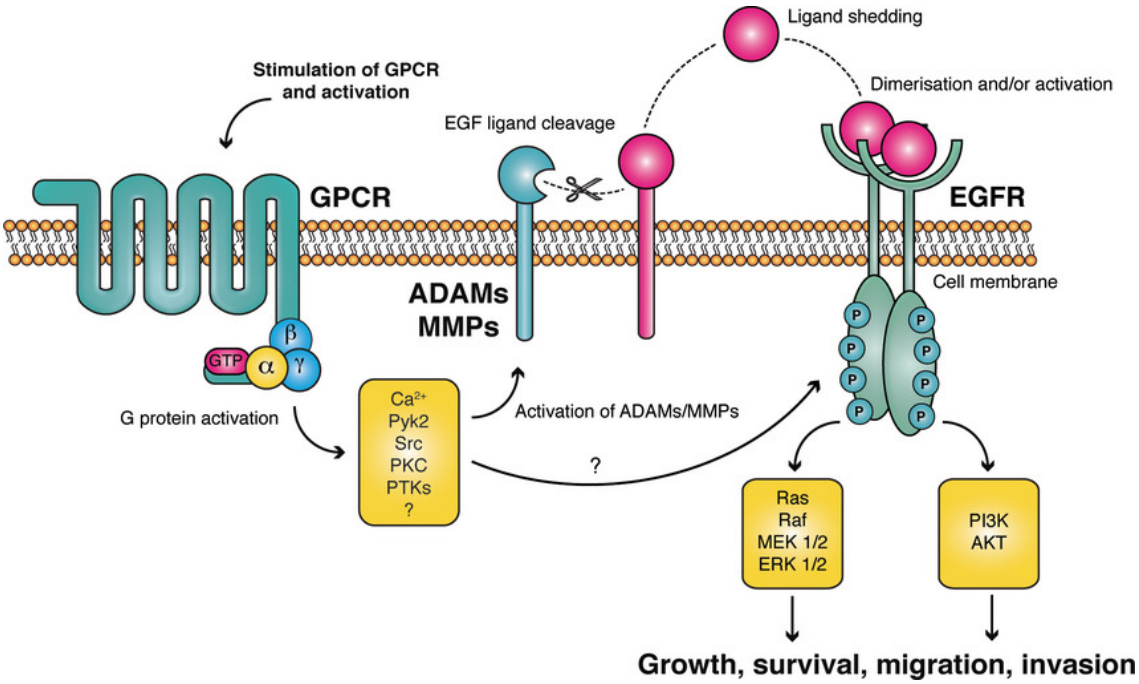

Figure 8. GPCR-induced EGFR transactivation. GPCR-induced and metalloprotease-mediated proteolytic cleavage of ligand precursors leads to transactivation of the EGFR. This mechanistic signaling model for ligand-dependent interreceptor communication couples receptor activation to the Ras/MAP kinase pathway (from George et al., 2013).

Role(s) of HBEGF-EGFR signaling in valve development

Despite the pro-mitogenic effect of sHBEGF on several cell types, numerous studies have described an inhibitory role for the HBEGF-EGFR signaling pathway during valve cushion remodeling. HBEGF is expressed in the endocardium of the developing cardiac valves of mouse embryos (Iwamoto et al., 2003; Iwamoto & Mekada, 2006; MacGrogan et al., 2016) and

in adult cardiomyocytes (Iwamoto et al., 2003). More than half of *Hbgef*-null mice die after birth, and the survivors develop grossly enlarged SL and AV valves, with hyperplastic mesenchymal cells (Table 1) (Iwamoto et al., 2003; Iwamoto & Mekada, 2006; Jackson et al., 2003). The same thickened leaflet phenotype is obtained when *Hbegf* is specifically deleted with the *Tie2-Cre* driver (Table 1) (Nanba et al., 2006), suggesting that the origin of the defects is endothelial. Deletion of *Adam17* also leads to hyperplastic SL and AV valves (Table 1) (Wilson et al., 2013). Moreover, mice expressing uncleavable proHBEGF displayed similar cardiac valve enlargement, indicating the increase in mesenchymal cell proliferation is mediated by the soluble growth factor (Table 1) (Yamazaki et al., 2003). Interestingly, knockin mice expressing the sHBEGF form exhibit severe skin hyperplasia and heart hypertrophy, with most animals dying in the neonatal stage (Table 1) (Yamazaki et al., 2003). All of these studies strongly indicate that sHBEGF release must be precisely controlled by ectodomain shedding *in vivo* during heart development.

Deletion of *Egfr* or reduction of its activity in mice leads to severe defects in brain, skin, eye, lung, and other organs, which ultimately cause embryonic or perinatal death, depending on strain background (Luetteke et al., 1994; Miettinen et al., 1995; Sibilia et al., 1998; Sibilia & Wagner, 1995; Threadgill et al., 1995). Moreover, mice homozygous for the allele $Egfr^{waved\text{-}2}$ (which encodes a mutant protein with 10–20% of the normal kinase activity) develop severe SL valve enlargement (Table 1) (Chen et al., 2000). In another study, surviving *Egfr*-null mice display both SL and AV valve thickening, resulting from an overabundance of mesenchymal cells (Table 1) (Jackson et al., 2003).

The aberrantly thickened valves in mice lacking either *Hbegf* or *Egfr* suggest that these proteins are involved in the control of mesenchymal cell proliferation. Hence, the current view is that, during valve remodeling, sHBEGF is shed from proHBEGF by ADAMs and secreted from the endocardium. sHBEGF then diffuses into the ECM and activates EGFR in nearby mesenchymal cells, resulting in the reduction of mesenchymal cell proliferation (Iwamoto & Mekada, 2006).

OBJECTIVES

Our Hypothesis

The regulation of mesenchymal cell proliferation during valve remodeling is a complex process, involving many different signaling pathways. Inactivation of the GPCR CXCR4 or its ligand CXCL12 results in cardiac valves with enlarged leaflets (Table 1) (Ivins et al., 2015). Similar valvular phenotypes are obtained upon disruption of members of the HBEGF-EGFR pathway (Table 1). (Chen et al., 2000; Iwamoto et al., 2003; Jackson et al., 2003; Nanba et al., 2006; Yamazaki et al., 2003).

Considering that transactivation of EGFR can occur via GPCR-mediated induction of ectodomain shedding of its ligands (Prenzel et al., 1999) and the similarities between the *Cxcl12/Cxcr4* and *Hbegf/Egfr* loss-of-function mutants, we hypothesize that CXCR4 is an GPCR functioning upstream of EGFR during valve remodeling. In this context, CXCR4 activates EGFR signaling by promoting the release of its ligand, sHBEGF, via activation of ADAM metalloproteases.

Our Objectives

The main objective of this thesis was to contribute to the study of the molecular mechanisms governing mesenchymal cell proliferation during valvulogenesis. With that goal in mind, we set the following objectives:

1. Characterization of the valvular phenotype of mice lacking endocardial *Cxcr4* (*Cxcr4^{flox}; Nfatc1-Cre*);

2. Generation of a sHBEGF gain-of-function mouse model and characterization of its valvular phenotype (*R26-sHBEGF$^{tg/+}$; Tie2-Cre*);

3. Rescue of the phenotype derived from *Cxcr4* deletion (*Cxcr4^{flox}; Nfatc1-Cre*) by crossbreeding with transgenic mice overexpressing sHBEGF (*R26-sHBEGF$^{tg/+}$; Tie2-Cre*);

4. *Ex vivo* study of the roles played by CXCR4 and sHBEGF during valve remodeling.

MATERIALS AND METHODS

Mouse model generation

The *Cxcr4*$^{flox/flox}$ (referred to as *Cxcr4*^{flox} in this text) transgenic model was generated by Nie et al. This mouse line has two loxP sites along with a neomycin cassette into the *Cxcr4* locus flanking exon 2 (Nie et al., 2004). To delete *Cxcr4* from the endocardium, we crossed *Cxcr4*^{flox} mice with *Nfatc1-Cre* (Wu et al., 2012; Zhou et al., 2002) and *Tie2-Cre* (Kisanuki et al., 2001) transgenic mice to allow Cre-mediated recombination. In both cases, we began by generating double heterozygous, *Cxcr4*$^{flox/+}$*; Nfatc1-Cre* and *Cxcr4*$^{flox/+}$*; Tie2-Cre*, which were then crossed with *Cxcr4*^{flox} homozygous mice, thus generating *Cxcr4*^{flox}*; Nfatc1-Cre* or *Cxcr4*$^{flox/+}$*; Tie2-Cre. Cxcr4* loss-of-function mutants were genotyped by polymerase chain reaction (PCR) of tail genomic DNA samples using primers that specifically detect the *Cxcr4* wild type (WT) allele and *Cxcr4* null allele. Primer sequences and reaction conditions are listed below in Table 2.

We generated the *sHBEGF* gain-of-function line in collaboration with the Pluripotent cell technology unit of the CNIC, via traditional restriction cloning methods and ES targeting/selection. The complementary DNA (cDNA) encoding the soluble component of the HBEGF protein (sHBEGF) was obtained from Addgene (plasmid #11601). We designed primers for PCR amplification, which added a NheI cutting site and a myc-tag to the cDNA. Amplification was carried out with the Phusion® High-Fidelity DNA Polymerase (#M0530S, New England BioLabs) (Table 2). Purification of PCR products and digestion fragments was performed using the DNA Clean & Concentrator-5 kit (#D4013, Zymo Reasearch). Previously in the laboratory, we had generated a p-BigT plasmid that, in addition to the PGK-neo cassette and tpA transcriptional stop sequence flanked by loxP sites, contained an IRES-eGFP. This was achieved by cloning a SalI-IRESeGFP fragment into the XhoI cutting site of pBigT. The PCR amplification product was digested with NheI and cloned into this altered pBigT plasmid, using NheI and AflII cutting sites. Afterwards, the fragment containing the loxP-PGK-neo-STOP-loxP-sHBEGF-myc-IRES-eGFP was cut out using PacI and AscI sites and ligated into the pROSA26PA plasmid (Soriano, 1999). The final construct was linearized with PvuI and electroporated into G4 mouse embryonic stem cells derived from a cross of 129S6/SvEvTac and C57BL/6Ncr mice (Vintersten, Testa and Stewart, 2004). After G418 (200 µg/ml) selection for 7 days, 8 clones were picked and identified by Southern blot of EcoRV-digested DNA, hybridized with 5' and 3' probes. Correctly targeted clone #1 was injected into C57/BL6C blastocysts to generate chimaeras that transmitted the transgene to their offspring. The resulting founders were genotyped by PCR of tail genomic DNA using primers in the R26 locus before and after the cloning site and in the polyA signal of the transgene (Table 2).

To overexpress *sHBEGF* in the endocardium, we employed the *Tie2-Cre* and the *Nfatc1-valveCre* (Wu et al., 2011; Zhou et al., 2005) drivers and generated heterozygous *R26-sHBEGF$^{tg/+}$; Tie2-Cre* and *R26-sHBEGF$^{tg/+}$; Nfatc1-valveCre* mice.

Gene		Genotyping primers	Annealing T (ºC)	Product (bp)
Nfatc1-Cre	Fwd	GAAGCAACTCATCGATTGATTTACG	58	1000
	Rv	AACCCTGGACGCCTGGGACAC		
Tie2-Cre	Fwd	GGGAAGTCGCAAAGTTGTGAGTT	60	500
	Rv	CTAGAGCCTGTTTTGCACGTTC		
Nfatc1-valveCre	Fwd	GCCTGCATTACCGGTCGATGCAACGA	67	700
	Rv	GTG GCA GAT GGC GCG GCA ACA CCA TT		
Cxcr4flox	Fwd	CACTACGCATGACTCGAAATG	60	330 (WT), 430 (flox)
	Rv	GTGTGCGGTGGTATCCAGC		
R26-sHBEGFtg/+	Fwd	AAAGTCGCTCTGAGTTGTTAT	62	585 (WT); 853 (tg)
	Fwd	TGCCCGACAACCACTACCTGAG		
	Rv	GGAGCGGGAGAAATGGATATG		
Gene		**Amplification primers**	**Annealing T (ºC)**	**Product (bp)**
sHBEGF-myc-NheI	Fwd	CCCTCGACCTGCAGCCCAAGCTAGCCGAG CTCGGATCCATGAA	61	453
	Rv	ACCAAGCTTAAGTTTAAACGCTAGGTATGCA TATTCAGATCCT		

Table 2. Primer sequences and reaction conditions. Fwd, forward; Rv, reverse; T, temperature; bp, base pairs.

Collection and processing of mouse samples

Adult mice were euthanized by cervical dislocation, in accordance with the appropriate mouse handling guidelines.

Embryo collection was done by removing the litter from the uterus of the sacrificed pregnant female and immediately transferring it to cold PBS. Either the yolk sac or a small piece of tail was removed and saved in order to genotype each embryo. DNA was extracted by incubating with a solution of Proteinase K (3ul, 03115801001, Roche) and lysis buffer, at 500 revolutions per minute (rpm) overnight (ON) at 55ºC. PCR reactions were performed using 200nM of each primer, 1µL of extracted DNA and DreamTaq Green PCR Master Mix (K1081, Thermo Scientific). Primers and reaction conditions can be found below in Table 2.

Samples destined for histological procedures were fixed in a solution of 4% paraformaldehyde (PFA) in PBS, ON and at 4ºC. In the case of E12.5 or earlier embryos, the whole embryo was fixed. To improve the penetrance of the fixative agent, bigger embryos (E13.5 onwards) were first beheaded and

its lower limbs removed before incubating the torsos in 4% PFA. Embryonic hearts destined for RNA extraction were dissected out and directly placed in pre-cooled tubes, which were stored at -80ºC until processing. Following cervical dislocation, collection of adult hearts started by opening the mouse thorax and, with the heart still beating, perfusing with 1mL of PBS immediately followed by 1mL of 4% PFA. The heart was then removed and incubated for 2 days in 4% PFA at room temperature (RT). After fixation, samples were rinsed extensively in PBS at RT and then washed in a series of increasingly concentrated ethanol solutions, ending with a wash in xylene before being embedded in paraffin.

In situ hybridization

In situ hybridization (ISH) in sections was performed as previously described (J L de la Pompa et al., 1998; Kanzler et al., 1998). ISH riboprobes were synthesized using Dig RNA labelling mix (11277073910, Roche) and purified with Illustra AutoSeq G-50 columns (27534001, GE Life Sciences).

Hematoxylin and eosin and DAB stainings

Hematoxylin and eosin (H&E) and 3,3'-diaminobenzidine (DAB) stainings were performed according to standard protocols by the Histopathology Unit at CNIC.

Immunofluorescence

Eight µm-thick sections were deparaffinized and boiled for 15' in 10mM citrate buffer (pH=6) for antigen retrieval. When an HRP-conjugated antibody was to be used, we pre-treated the sections with 3% hydrogen peroxide in methanol for 40' at RT, to reduce non-specific endogenous peroxidase activity. Permeabilization of membranes was done by incubating with 3% Triton X-100 in PBS for 20' at RT. To prevent non-specific binding, a final blocking step with 3% BSA was carried out for 1 hour at RT followed by incubation with primary antibodies, ON at 4ºC. The following day, we incubated the slides with a secondary antibody conjugated to a fluorescent-dye. When extra amplification was necessary, we used the tyramide signal

amplification (TSA) Plus Fluorescein System (NEL701A001KT, Perkin Elmer). All the information regarding the antibodies used is listed in Table 3.

Primary antibody	Host	Dilution	Amplification	Reference	Company
BrdU	mouse	1/100	yes	347580	BD Biosciences
Caspase-3	rabbit	1/200	no	559565	BD Biosciences
pSmad1/5/8	rabbit	1/100	yes	13820S	Cell Signaling
αSMA-Cy3	mouse	1/200	no	C6198	Sigma Aldrich
cTNT	mouse	1/100	no	CT3	Developmental Studies Hybridoma Bank
IB4-AlexaFluor647		1/100	no	I32450	Invitrogen
DAPI		1/500	no	D9542	Sigma Aldrich
Secondary antibody	**Host**	**Dilution**	**Amplification**	**Reference**	**Company**
anti mouse-biotinilated	goat	1/200	-	115-066-071	Jackson ImmunoResearch
anti rabbit-biotinilated	goat	1/200	-	111-066-003	Jackson ImmunoResearch
anti mouse-AlexaFluor488	goat	1/200	-	A-11029	Thermo Fisher Scientific

Table 3. Primary and secondary antibodies used for immunofluorescence.

OFT explant assay

Collagen gels were prepared by pouring a solution of 1.5mg/ml rat-tail collagen type I (BD Biosciences), NaOH and DMEM into 4-well microculture dishes (500µl per well). The gels were allowed to solidify inside a 37°C, 5% CO2 incubator for 20' before being washed 3 times for 30' with explant medium: a solution containing Dulbecco's Modified Eagle Medium (DMEM, Thermo Fischer), GlutaMAX™-I CTS™ (#A12860-01, Gibco, ThermoFischer Scientific) 10% FBS, 1% insulin-transferrin-selenium (#51500056, Gibco, ThermoFischer Scientific), Pen/Strep and fungizone. When a drug was to be applied to the explants, we performed the washes using explant medium containing the respective molecule, in order to pre-soak the gel. OFTs were dissected from E11.5 embryos in fresh medium. The OFTs were then opened, placed with the endocardium side lying face down in the dry gel and allowed to attach for 24 hours at 37°C, 5%CO2. The following day, we added 500µl of explant medium containing the specific drugs to the wells and left them in culture for 3 days. The AMD3100 drug was purchased from Selleckchem (#S8030), mouse recombinant sHBEGF from Prospec (#cyt-068), CP380736 from Sigma-Aldrich (#PZ0129) and PD158780 from TOCRIS (#2615).

Proliferation analysis and quantification

Valve mesenchymal cell proliferation was analyzed via a 5-bromo-2'-deoxyuridine (BrdU) incorporation assay. Pregnant females received an intraperitoneal injection of 300µl of 10 mg/ml BrdU, 1 hour prior to the removal of the litter. After that, the embryos were processed as usual for immunofluorescence. The percentage of BrdU incorporation was calculated as the number of $BrdU^+$ cells over the total number of mesenchymal cells. Mesenchymal cells in the valve leaflets were determined by DAPI staining but lack of cTNT or IB4 staining. Using Fiji image software analysis, three non-consecutive sections of 3-5 control and 3-5 transgenic mice were counted and averaged.

Explant proliferation was determined by using the Click-iT® EdU Alexa Fluor647 Imaging Kit (#C10337, Thermo Fischer). Explants were incubated in explant medium containing 10µM 5-ethynyl-2'-deoxyuridine (EdU) for 6 hours and then fixed with 4% PFS for 30' at RT. Permeabilization of membranes was done by incubation with 1% Triton X-100 in PBS for 30' at RT. After blocking with X% BSA for 3h at RT, we stained with αSMA-Cy3, ON at 4ºC, to detect invading mesenchymal cells. EdU was detected by using the Click-iT® reaction cocktail provided by the kit. The percentage of EdU incorporation was calculated as the number of EdU^+, SMA^+, $DAPI^+$ cells over the total number of mesenchymal cells (SMA^+, $DAPI^+$).

RNA extraction and quantitative real-time PCR

Whole hearts were collected and pooled into groups of 4-5 according to genotype. Samples were disrupted by homogenizing the hearts with steel beads for 2' at 50Hz in a TissueLyser LT (Cat No: 85600, Qiagen). RNA was extracted using the RNeasy Mini Kit (74014, Qiagen).

cDNA synthesis was done using the High Capacity cDNA Reverse Transcription Kit (4368814, Applied Biosystems). Quantitative real-time PCR (qPCR) reactions were performed using Power SYBR Green PCR Mastermix (4367659, Applied Biosystems) in a 7900HT Fast Real-Time PCR system (4329001, Applied BioSystems). Relative expression analysis relative to □-actin was calculated applying the 2-ΔΔCt method to the Ct values. qPCR primers are listed in Table 4.

Gene		qPCR primers
sHBEGF	Fwd	TGAAGCTGCTGCCGTCGGT
	Rv	AGGCTCAGCCCATGACACCT
eGFP	Fwd	ACGTAAACGGCCACAAGTTC
	Rv	ACGTAGCCTTCGGGCATG
Snail1	Fwd	GACACATTAGAACTCACACTG
	Rv	GACATTCTGGAGAAGGTTTTG
Snail2	Fwd	GACACATTAGAACTCACACTG
	Rv	GACATTCTGGAGAAGGTTTTG
Twist1	Fwd	GAGACGTAGATGTCATTGTTTC
	Rv	GAATTTGGTCTCTGCTCTTC

Table 4. List of qPCR primers.

X-gal staining

Whole-mount X-gal staining of embryos began by fixing the embryos for 30 minutes at RT in a solution containing 25% glutareldahyde, 3% formaldehyde, 5mM EGTA, 2mM $MgCl_2$ and 0,1M phosphate buffer. To prepare the phosphate buffer, we mixed monobasic sodium phosphate and dibasic sodium phosphate in a 3 to 7 ratio and adjusted the pH to 7.3. The samples were then rinsed several times in wash buffer, composed of 2mM $MgCl_2$ and 0,1M phosphate buffer. Next, the embryos were stained ON at RT in a solution of 1mg/ml X-gal, 5mM potassium ferrocyanide and 5mM potassium ferricyanide in wash buffer. The following day, the embryos were washed in PBS and fixed in 4% PFA ON at 4ºC. After fixation, samples were rinsed extensively in PBS at RT and then washed in a series of increasingly concentrated ethanol solutions, ending with a wash in xylene before being embedded in paraffin.

Imaging

Confocal imaging of immunofluorescence was performed using Nikon Air and the NIS-Elements software, and Leica SP5 or Leica SP8 Navigator using the LAS X software. Bright field images of H&E and ISH sections were taken using an Olympus BX51 Microscope and Olympus CellSense software. Image processing and analysis was done using FIJI.

Quantification of valve mesenchymal area and cell number

Consecutive H&E sections containing a full view of the valve leaflets were selected. We used 5 or more sections from at least 4 different animals of each genotype (mutant or control). Bright field photos were obtained and opened with FIJI. We manually selected the region of interest (ROI), the valve mesenchyme, applied an automatic threshold and measured the area. As for the cell number, we designed a macro that counted cell number autonomously. Each image was automatically thresholded. The previous ROI was selected using the shortcut “select previous selection” and the number of cells for the thresholded region was measured. The script of the macro used is the following:

```
run("8-bit")
run("Set Scale...", "distance=134.0037 known=[60.2 ] unit=microns");
setAutoThreshold("MaxEntropy");
setOption("BlackBackground", true);
run("Convert to Mask", "method=MaxEntropy background=Light calculate black");
run("Watershed");
waitForUser("Draw ROI, then hit OK");
run("Find Maxima...", "noise=10 output=Count");
```

Quantification of pSmad area

Three non-consecutive sections containing a full view of the valve leaflets were selected for each animal. 3 animals of each genotype (mutant or control) were used. Confocal photos were obtained and opened with FIJI. For each photo, valve mesenchyme (ROI) was manually selected. Then the photo was split into the different channels and the DAPI channel was selected and automatically thresholded. The area covered by DAPI staining was measured. Next, the pSmad1/5/8 channel was selected and an automatic threshold was applied. Using the image calculator “AND” function, a new image was created containing the pixels where both DAPI and pSMAD1/5/8 signal overlapped. A threshold was applied to this image and its area was measured. The percentage of pSmad1/5/8-covered area was calculated as the ratio between the area where DAPI and pSmad1/5/8 signal overlap over the total area covered by DAPI. The script for the macro used is the following:

```
rename("FOTO");
run("Z Project...", "projection=[Max Intensity]");
run("Make Composite");
```

```
waitForUser("define ROI");
run("Clear Outside");
run("Split Channels");
selectWindow("C1-MAX_FOTO");
run("8-bit");
setAutoThreshold("Moments dark");
//run("Threshold...");
//setThreshold(128, 255);
setOption("BlackBackground", true);
run("Convert to Mask");
run("Measure");
selectWindow("C3-MAX_FOTO");
run("8-bit");
setAutoThreshold("Moments dark");
//run("Threshold...");
//setThreshold(128, 255);
setOption("BlackBackground", true);
run("Convert to Mask");
imageCalculator("AND create", "C1-MAX_FOTO","C3-MAX_FOTO");
selectWindow("Result of C1-MAX_FOTO");
setAutoThreshold("Moments dark");
//run("Threshold...");
//setThreshold(128, 255);
setOption("BlackBackground", true);
run("Convert to Mask");
run("Measure");
```

Statistical analysis

All statistical analyses were performed in GraphPadPrism Version 7. When comparing controls with transgenic samples, at least 3 animals per genotype were used and statistical significance was calculated using the two-tailed Student's *t* test. For immunofluorescence quantifications, at least 3 sections per animal were quantified. To compare multiple groups submitted to different treatments, we performed ordinary one-way Analysis of Variance test (ANOVA), together with Dunnett's multiple comparisons test. Differences were considered statistically significant at $P \leq 0.05$.

RESULTS

Cxcr4 and *Cxcl12* are both expressed in cardiac valve regions during embryonic development

We examined the expression patterns of *Cxcr4* and *Cxcl12* in the developing WT mouse heart by *in situ* hybridization (ISH) (Figure 9). *Cxcr4* mRNA is expressed in the endocardium and underlying valve leaflet mesenchyme of both SL (Fig. 9A-B') and AV valves, at E14.5 (Fig. 9C, C'). *Cxcr4* is also highly expressed in the endothelial cells of the coronary vessels, but not in chamber endocardium (Fig. 9D, E). *Cxcl12* is expressed in the smooth muscle of the ascending aorta and aortic root of the SL valves (Fig. 9F-G'). In addition, high levels of *Cxcl12* are visible in the tendinous cords and papillary muscles tethering the AV leaflets to the ventricle chambers (Fig. 9H, H'). *Cxcl12* mRNA is also present in the myocardium of the left ventricle and, at a lower level, the right ventricle (Fig. 9I, J).

Therefore, the location of *Cxcr4* and *Cxcl12* mRNA at E14.5 suggests a role for CXCL12/CXCR4 signaling during cardiac valve remodeling.

Generation of mice lacking *Cxcr4* in endocardium

To determine the function of CXCR4 during valvulogenesis, we used the *Nfatc1-Cre* pan-endocardial driver line, which is expressed in endocardium lining the valves and chambers from E8.5 onwards (Zhou et al., 2005). We crossed this driver with mice bearing floxed *Cxcr4* alleles (*Cxcr4*^{flox}, Nie et al., 2004), to obtain *Cxcr4*^{flox}*; Nfatc1-Cre* mice. These mice survive till birth and are born at expected Mendelian ratios. To confirm efficient endocardial *Cxcr4* deletion, we performed ISH on heart sections from *Cxcr4* mutant animals and control WT littermates. As expected, mutant hearts display almost complete loss of *Cxcr4* mRNA expression in both the leaflets of the valves and intra-myocardial vessels, when compared to controls (Fig. 9K-L').

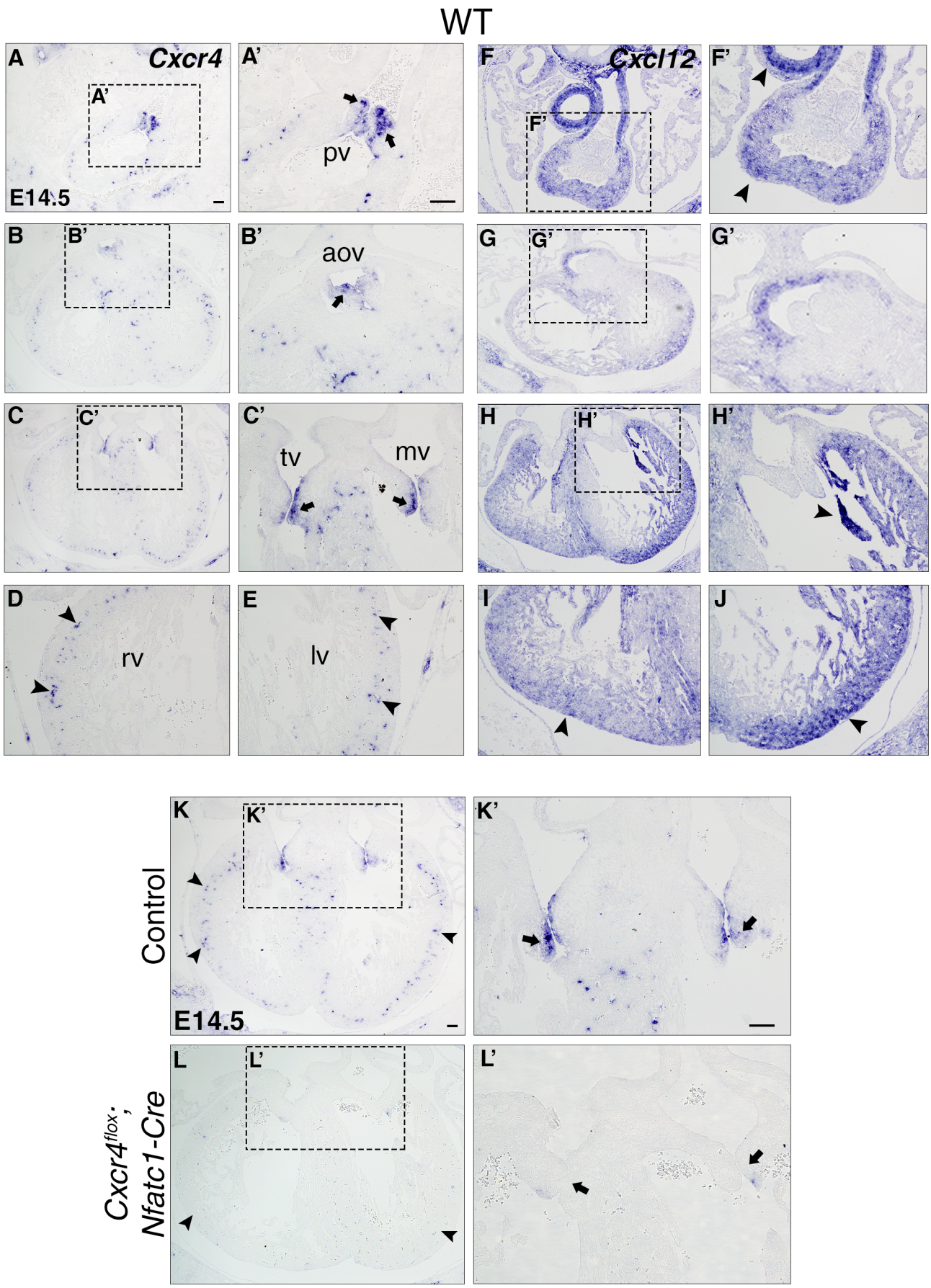
WT
A
Cxcr4
A'
E14.5
pv
F
Cxcl12
F'
B
B'
aov
G
G'
C
C'
tv
mv
H
H'
D
rv
E
lv
I
J
Control
K
K'
E14.5
L
L'
Cxcr4flox;
Nfatc1-Cre

Figure 9. Expression of *Cxcr4* and *Cxcl12* in WT hearts at E14.5 and loss of *Cxcr4* mRNA in *Cxcr4^{flox}; Nfatc1-Cre* mutants. **A-J:** ISH of *Cxcr4* and *Cxcl12* on WT 14.5 heart sections. *Cxcr4* is expressed in the endocardium and mesenchyme of the valve leaflets of the (**A, A'**) pulmonary, (**B, B'**) aortic and (**C, C'**) tricuspid and mitral valves (arrows). *Cxcr4* expression is also found in intra-myocardial vessels (arrowheads in **D**, **E**). *Cxcl12* expression is present in the smooth muscle surrounding the SL valves (arrowheads in **F'**, **G')**, tendinous cords (arrowhead in **H'**) and ventricular myocardium (arrowheads in **I**, **J**). **K-L':** ISH of *Cxcr4* on E14.5 control and *Cxcr4^{flox}; Nfatc1-Cre* heart sections. Loss of *Cxcr4* expression is visible in myocardial vessels (arrowheads) and valve leaflets (arrows). Scale bar: 100µm. pv, pulmonary valve; aov, aortic valve; tv, tricuspid valve; mv, mitral valve; rv, right ventricle; lv, left ventricle.

Endocardial *Cxcr4* deletion results in hypercellular and dysmorphic valves, including bicuspid aortic valve

The effect of deleting endocardial *Cxcr4* was examined in *Cxcr4^{flox}; Nfatc1-Cre* mice at different stages of embryonic development (Figure 10). H&E staining of transverse sections of E14.5 hearts revealed a spectrum of phenotypes. *Cxcr4^{flox}; Nfatc1-Cre* mutant hearts displayed larger valve leaflets to a varying degree (Fig. 10B, D, F). At E16.5, *Cxcr4^{flox}; Nfatc1-Cre* cardiac valves cusps were clearly enlarged and appeared dysmorphic compared to control littermates (Fig. 10G-N), suggesting that endocardial *Cxcr4* deletion affects post-EMT cardiac valve remodeling. Valve leaflet area and number of populating cells were measured at E16.5. There were significant increases in both leaflet area and number of populating cells in the mutants compared to controls (Fig. 10W-Z). Given that *Cxcr4* is also expressed in coronaries and required for their development (Ivins et al., 2015), we might have expected morphological differences in the ventricular myocardial wall. However, we did not observe any obvious difference in number or caliber of coronaries nor in ventricular wall thickness between mutants and controls (Fig. 10O-R).

The dysmorphia and enlargement observed in *Cxcr4^{flox}; Nfatc1-Cre* SL valves (Fig. 10H, J) appeared to be more severe than in the AV valves (Fig. 10L, N). This suggests that SL valve development is more sensitive to variations of *Cxcr4* expression than that of the AV valves. Moreover, a high percentage of *Cxcr4^{flox}; Nfatc1-Cre* mutants displayed a bicuspid aortic valve (BAV) (Table 5; Fig. 10T, V). Out of the 10 E16.5 mutant embryos analyzed by H&E staining, 4 (40%) presented aortic valves with an apparent L-NC morphology, likely caused by fusion of the left cusp and the non-coronary cusp (Fig. 10T, V). Furthermore, mutant leaflet enlargement was ubiquitous at this stage, and never seen in controls (Table 5).

To confirm the valve phenotype seen upon endocardial *Cxcr4* deletion, we crossed *Cxcr4^{flox}* mice with the *Tie2-Cre* driver line (Kisanuki et al., 2001), which is active in the endocardium and endothelium from E7.5 onwards. *Cxcr4^{flox}; Tie2-Cre* mutant mice also displayed leaflet thickening to a variable degree at E14.5 and clear valve enlargement and dysmorphia at E16.5 (Figure 11). Furthermore, BAV was seen at E16.5 (Figure 11). These data indicate that endothelial/endocardial deletion of *Cxcr4* with *Tie2-Cre* recapitulates the phenotype obtained with *Nfatc1-Cre.*

Together, these data demonstrate that CXCR4 function in the endocardium is essential for post-EMT control of valve leaflet size, cellularity and morphology.

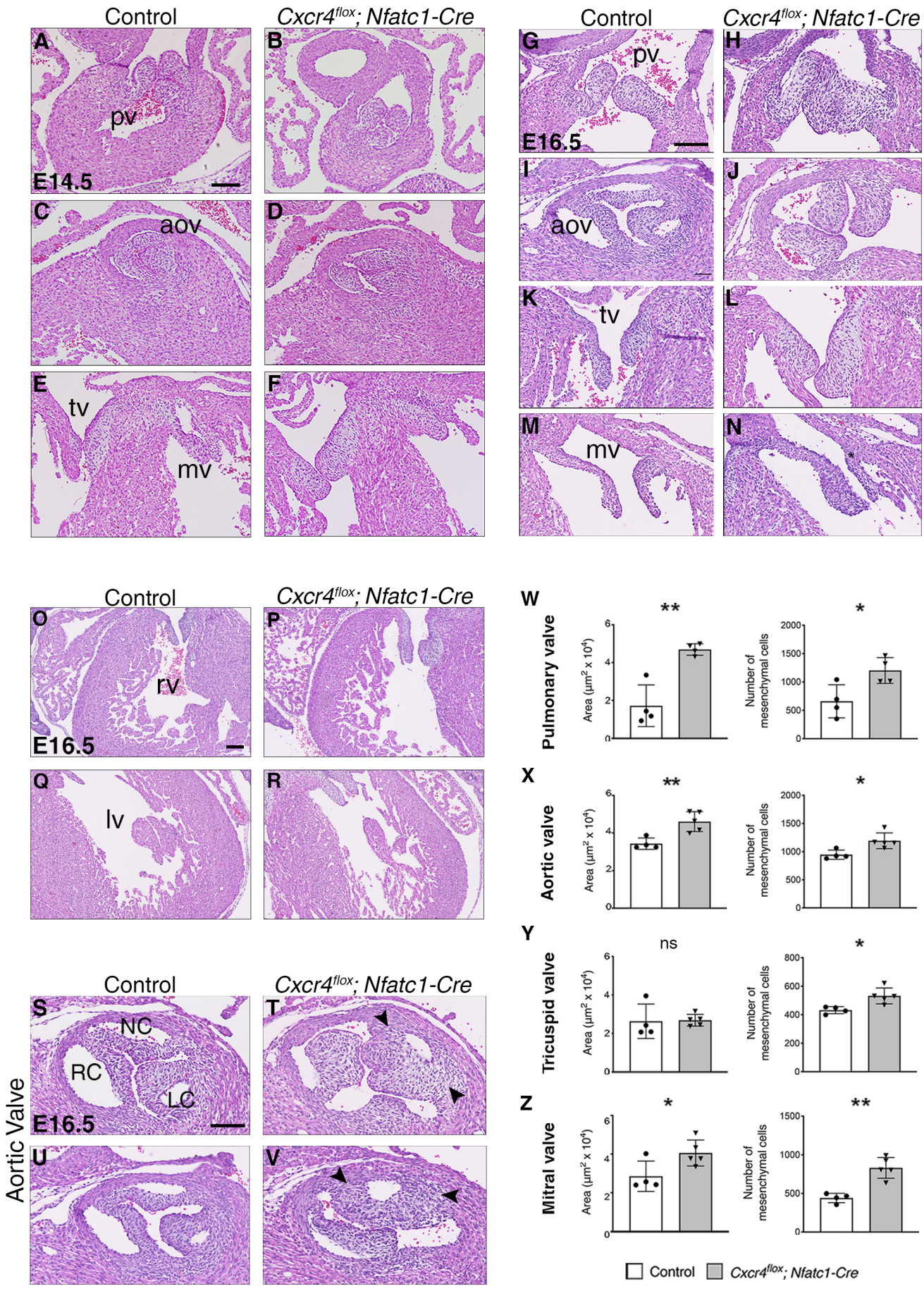
Control
Cxcr4flox; Nfatc1-Cre
A
B
pv
E14.5
C
D
aov
E
F
tv
mv
G
H
pv
E16.5
I
J
aov
K
L
tv
M
N
mv
O
P
rv
E16.5
Q
R
lv
Aortic Valve
S
T
NC
RC
LC
E16.5
U
V
W
Pulmonary valve
X
Aortic valve
Y
Tricuspid valve
Z
Mitral valve
Area (μm2 x 10⁴)
Number of mesenchymal cells
**
*
ns
Control
Cxcr4flox; Nfatc1-Cre

Figure 10. *Cxcr4^{flox}; Nfatc1-Cre* mutants display SL and AV valve enlargement, accompanied by frequent BAV. A-N: H&E staining of control WT and *Cxcr4^{flox}; Nfatc1-Cre* mutant heart sections at E14.5 (**A-F)** and 16.5 (**G-N**). At E14.5, the phenotype is heterogeneous, but by E16.5 there is clear leaflet enlargement of both the SL (**H, J**) and AV (**L, N**) valves, compared to control littermates (**G, I, K, M**). **O-R**: H&E staining of both control (**O**, **Q**) and mutant (**P**, **R**) ventricles reveals normal thickness and the presence of coronary vessels. **S-V:** H&E staining of control and mutant aortic valves at 16.5. Control valves display three well-defined cusps **(S, U),** whereas *Cxcr4^{flox}; Nfatc1-Cre* mutant exhibit BAV, with the left and the noncoronary cusp fused together **(**arrows in **T, V**). **W-Z**: Quantifications of valve leaflet area and cell number of pulmonary (**W**), aortic (**X**), tricuspid (**Y**) and mitral (**Z**) valves at E16.5. Scale bar: 100µm. pv, pulmonary valve; aov, aortic valve; tv, tricuspid valve; mv, mitral valve; rv, right ventricle; lv, left ventricle; NC, noncoronary cusp; RC, right cusp; LC, left cusp. Data are means±SD. **P≤0.01, *P≤0.05, ns indicates non-significance by Student's *t* test (n=4 for controls, n=5 for *Cxcr4^{flox}; Nfatc1-Cre* mutants).

Aortic Valve (E16.5)	Control	%	*Cxcr4flox; Nfatc1-Cre*	%
Normal	8	100	0	0
Enlarged	0	0	6	60
BAV	0	0	4	40

Table 5. Bicuspid aortic valve (BAV) occurs frequently in *Cxcr4^{flox}; Nfatc1-Cre* mutant mice.

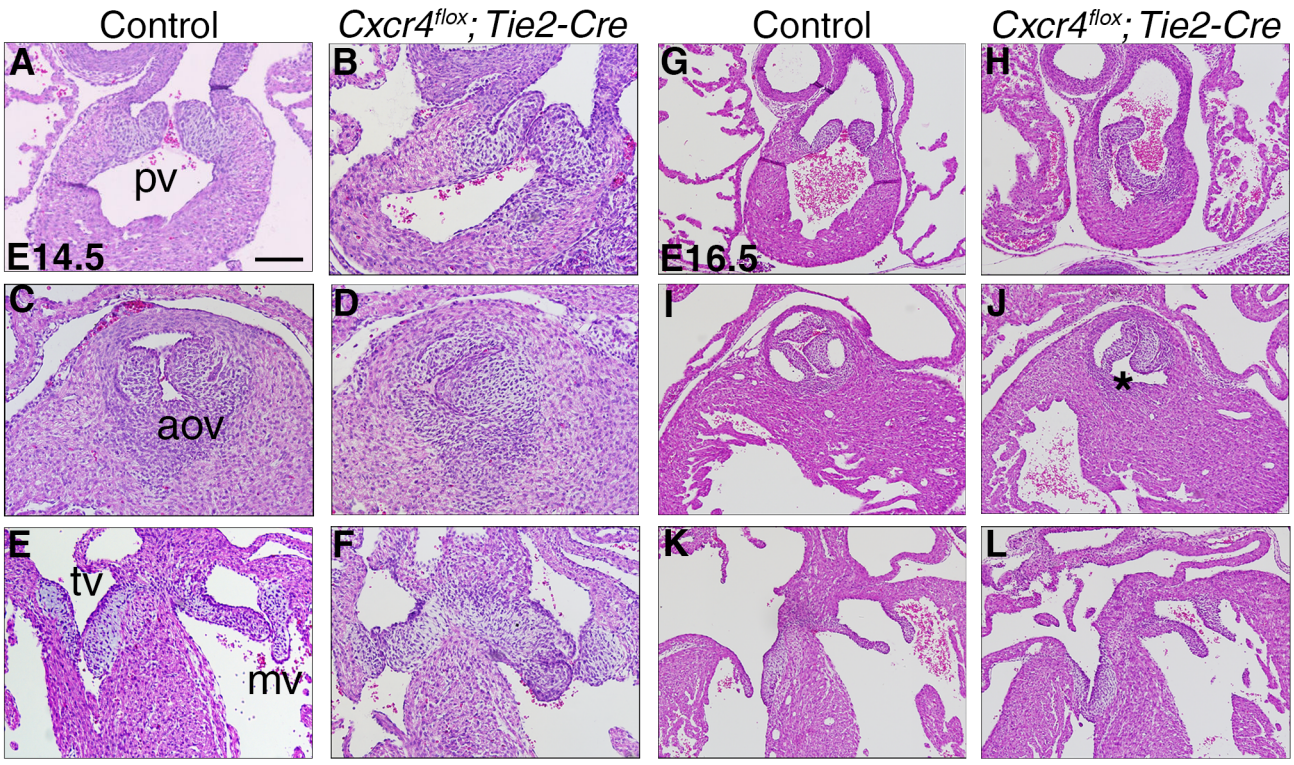

Figure 11. *Cxcr4^{flox}; Tie2-Cre* mutants recapitulate the *Cxcr4^{flox}; Nfatc1-Cre* phenotype. H&E staining of control and *Cxcr4^{flox}; Tie2-Cre* heart sections at E14.5 (**A-F**) and 16.5 (**G-L**). At E14.5, mutants display variable thickening in both SL (**B, D**) and AV valve leaflets (**F**). At E16.5, there is severe leaflet enlargement of SL (**H, J**) and AV (**L**) valves, compared to control littermates (**G, I, K**). The asterisk indicates the presence of bicuspid aortic valve in the mutant. Scale bar: 100µm. pv, pulmonary valve; aov, aortic valve; tv, tricuspid valve; mv, mitral valve.

Cartilaginous metaplasia and ventricular septal defects in *Cxcr4^{flox}; Nfatc1-Cre* mice

From E18.5 into adulthood, cardiac valves continue to mature and undergo further elongation and thinning (Hinton et al., 2006). Given that all *Cxcr4^{flox}; Nfatc1-Cre* mice survived birth, we assessed if the valve developmental defects were resolved or became more severe with time. Thus, histological examination of one-month-old (P30) *Cxcr4^{flox}; Nfatc1-Cre* mutants revealed severe thickening of the cusps compared to the hearts of control littermates (Figure 12). Both SL and AV valve cusps were considerably enlarged in the mutants compared to control littermates (Fig. 12A-F''). Furthermore, one of the three *Cxcr4^{flox}; Nfatc1-Cre* mutants displayed cartilaginous metaplasia formation in the fibrosa tissue surrounding the aortic valve (Fig. 12G, G'). Cartilage formation is part of the process of endochondral ossification, which has been reported in humans as a clinically

significant feature of valve calcification and stenosis (Fernández Gonzalez et al., 1997; Mohler et al., 2001; Torre et al., 2016).

In addition to the cartilaginous metaplastic tissue, P30 *Cxcr4^{flox}; Nfatc1-Cre* hearts also seemed larger than control ones, with thicker ventricular walls, especially in the left ventricle region (Fig. 12B, F). We interpret this as a morphological process of remodeling of the myocardial wall, in an effort to adapt to defective valve function. In one of the mutants, we also detected fibrosis and necrosis in the septum, which was thinner than those of the controls and structurally compromised (Fig. 12H-H'').

These results show that *Cxcr4* deletion from the endocardium during development elicits severe valve defects in the embryo that worsen and extend to the myocardium in juvenile mice.

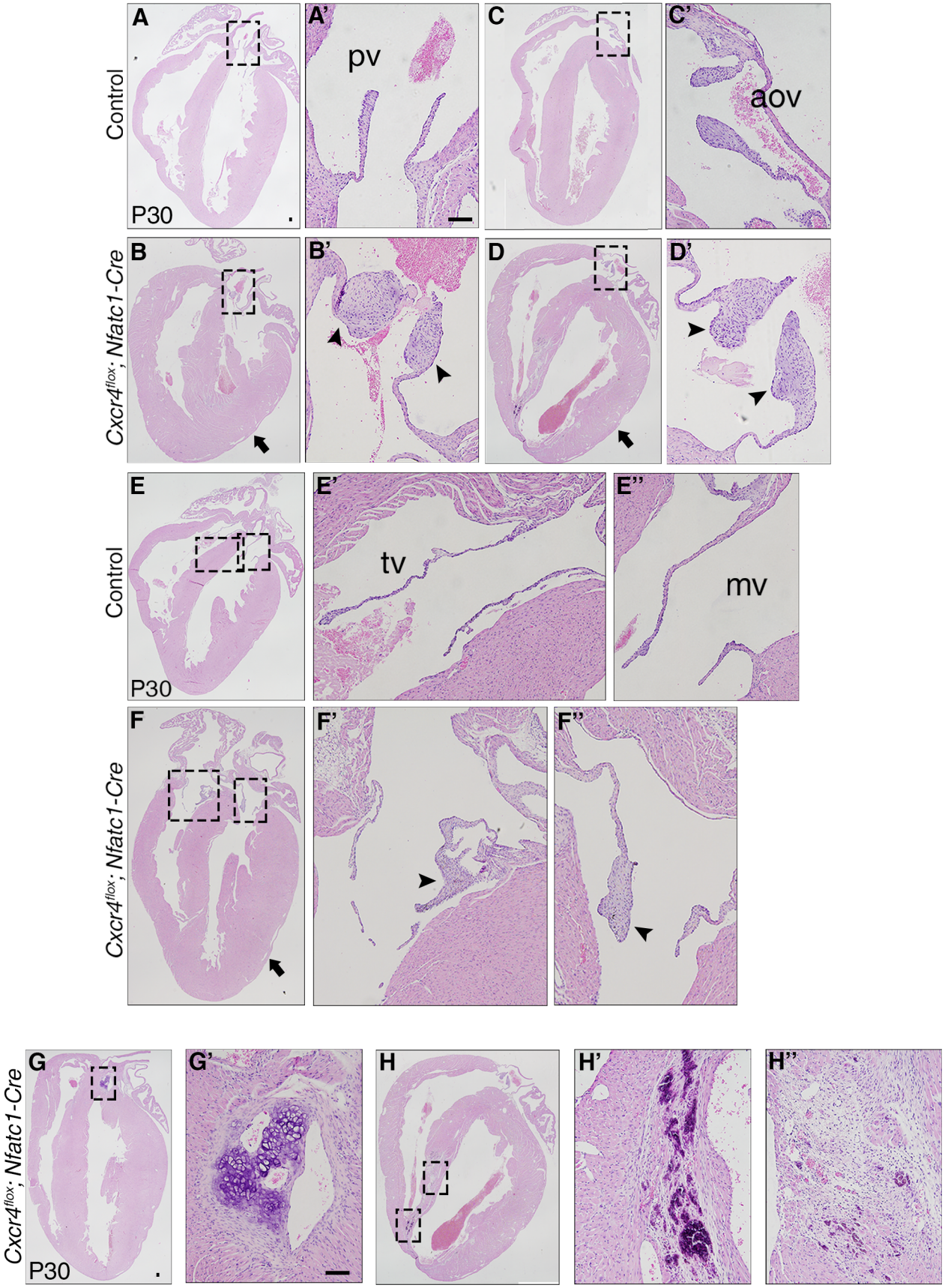
Control
Cxcr4flox; Nfatc1-Cre
A
A'
pv
C
C'
aov
P30
B
B'
D
D'
E
E'
tv
E''
mv
F
F'
F''
G
G'
H
H'
H''

Figure 12. Enlarged valves, cartilaginous metaplasia and ventricular chamber septal defects in juvenile *Cxcr4^{flox}; Nfatc1-Cre* mice. H&E staining of control (**A-C'**, **E-E''**) and *Cxcr4^{flox}; Nfatc1-Cre* (**B-B'**, **D-D', F-F'', G-H''**) heart sections at P30. There is severe enlargement of SL (**B-B'**, **D-D'**) and AV (**F-F''**) mutant valve leaflets. Black arrowheads denote thickened valve cusps. Left ventricular wall thickening is also visible (black arrows in **B** and **F**). Cartilaginous formation suggestive of endochondral ossification is visible in the aortic valve of an endocardial *Cxcr4* mutant (**G-G'**). An aberrant septal structure indicative of necrosis and evidence of fibrosis are present in the septum of a mutant animal (**H-H''**). Scale bar: 100µm. pv, pulmonary valve; aov, aortic valve; tv, tricuspid valve; mv, mitral valve.

Increased mesenchyme cell proliferation underlies valve hypercellularity in *Cxcr4^{flox}; Nfatc1-Cre* embryos

To understand the mechanism underlying valve enlargement in endocardial *Cxcr4* mutants, we examined the rate of proliferation in valve leaflets. The incorporation of 5-bromodeoxyuridine (BrdU), during the S-phase of the cell cycle, provides an estimate of cell cycle rate. We measured BrdU incorporation in valve leaflets at E12.5 and E14.5 (Figure 13), since mesenchymal cell proliferation is high at early post-EMT stages and declines as development advances (Hinton et al., 2006). To distinguish valve mesenchyme from surrounding tissues, we counterstained with isolectin B4 (IB4), to exclude the endothelium/endocardium, and cardiac troponin T (cTNT), to exclude the myocardium. At E12.5, the proportion of BrdU-positive valve mesenchymal cells was similar between *Cxcr4^{flox}; Nfatc1-Cre* mutants and control littermates (Fig. 13A-F, M), consistent with mutant valves being morphologically indistinguishable at this developmental stage. However, by E14.5, there was a significant increase in the rate of mesenchymal proliferation in *Cxcr4^{flox}; Nfatc1-Cre* mutant SL valves compared to controls (Fig. 13G-L, N). Although AV valves displayed a trend towards increased mesenchymal cell proliferation (Student's *t* test p= 0.16651), the difference was not significant, again suggesting that SL valve development is more sensitive to endocardial *Cxcr4* deletion than that of the AV valves.

Thus, we conclude that the increase in size and cellularity observed in the valve leaflets of E14.5 *Cxcr4^{flox}; Nfatc1-Cre* mice is likely due to increased proliferation of mesenchymal cells.

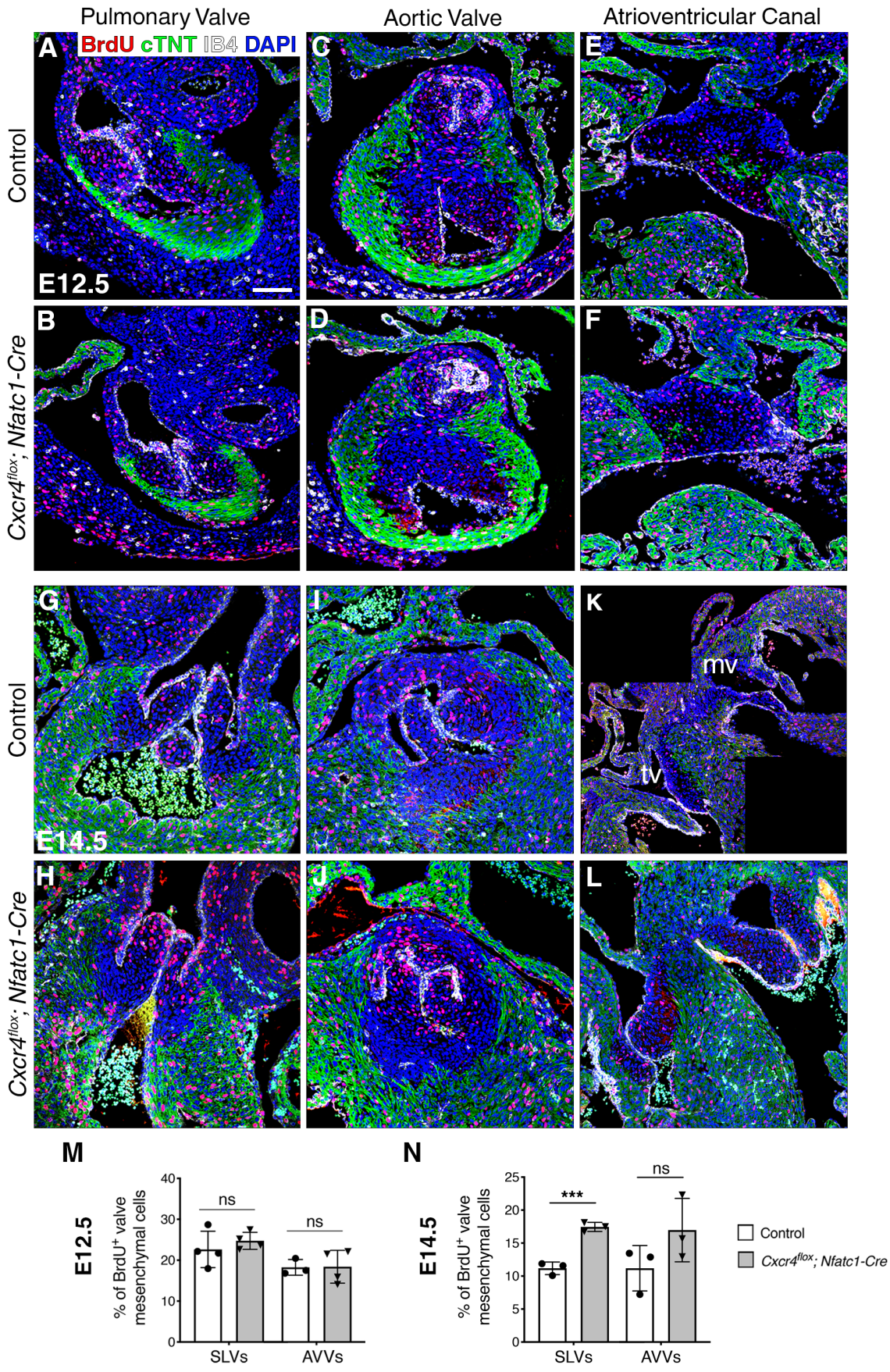
Pulmonary Valve
Aortic Valve
Atrioventricular Canal
A
BrdU cTNT IB4 DAPI
C
E
Control
E12.5
B
D
F
Cxcr4flox; Nfatc1-Cre
G
I
K
mv
tv
Control
E14.5
H
J
L
Cxcr4flox; Nfatc1-Cre
M
E12.5
% of BrdU+ valve mesenchymal cells
ns
ns
SLVs
AVVs
N
E14.5
% of BrdU+ valve mesenchymal cells
***
ns
SLVs
AVVs
Control
Cxcr4flox; Nfatc1-Cre

Figure 13. Increased mesenchymal cell proliferation in the SL valves of *Cxcr4^{flox}; Nfatc1-Cre* mutant mice at E14.5. 5-Bromodeoxyuridine (BrdU) immunostaining (in red) of heart sections of WT controls and *Cxcr4^{flox}; Nfatc1-Cre* mutant littermates at E12.5 (**A**-**F**) and E14.5 (**G**-**L**). Valve mesenchymal cells were identified by DAPI staining and the lack of cTNT and IB4 expression. **A, C, E**: BrdU staining of sections of control mice, showing the precursors of SL (**A, C**) and AV valves (**E**). **B, D, F**: BrdU staining of sections of *Cxcr4^{flox}; Nfatc1-Cre* mutants, showing the precursors of the SL (**B**, **D**) and the AV valves (**F**). **G, I, K**: BrdU staining of sections of control SL (**G**, **I**) and AV valves (**K**). **H, J, L**: BrdU staining of sections of *Cxcr4^{flox}; Nfatc1-Cre* mutant SL (**H, J**) and AV valves (**L**). Quantification of proliferation, defined as the percentage of BrdU-positive nuclei in both control and mutant embryos, at E12.5 (**M**) and E14.5 (**N**). Scale bar: 100µm. tv, tricuspid valve; mv, mitral valve; SLVs, semilunar valves; AVVs, atrioventricular valves. Data are means±SD. ***P≤0.001, ns indicates non-significance by Student's *t* test (n=3-4 for controls, n=3-4 for *Cxcr4^{flox}; Nfatc1-Cre* mutants).

Endocardial *Cxcr4* mutant valve enlargement is not due to decreased apoptosis or reduced macrophage recruitment

Since the proliferative increase was relatively mild compared to what might be expected given the morphological changes, we wondered whether additional mechanisms might contribute to the *Cxcr4^{flox}; Nfatc1-Cre* mutant phenotype. Recently, a population of macrophage-like cells derived from the endocardium was reported to be essential for proper valvular remodeling (Shigeta et al., 2019). Endocardial-specific deletion of *Csf1r*, a receptor essential for macrophage development, resulted in severe valve thickening in adult mice, with excess mesenchymal cells. Given that *Cxcr4* is expressed by macrophages and is principally known for mediating immune cell chemotaxis (Ganju et al., 1998), we wondered whether macrophage-mediated clearance of apoptotic cells was defective in *Cxcr4^{flox}; Nfatc1-Cre* mutant valves (Figure 14).

To detect cells undergoing apoptosis in the valve mesenchyme, we stained for caspase-3, a critical mediator of programmed cell death (Jänicke et al., 1998). Both *Cxcr4^{flox}; Nfatc1-Cre* and control mice presented very few mesenchymal cells positive for caspase-3 at E14.5 (Fig. 14 A-H). In fact, most sections of the heart did not present any staining whatsoever (<1%). Moreover, we did not detect any differences between the number of caspase-positive cells in the mutants compared to control WT mice. Therefore, decreased apoptosis cannot account for the enlargement seen in the valves of *Cxcr4* mutants.

Next, we determined whether there were changes in macrophage recruitment, using F4/80, a well-known murine macrophage marker antibody.

F4/80 immunostaining revealed the presence of macrophages populating the valve leaflets (Fig. 14I-P), but there were no significant differences between C*xcr4*^{flox}*; Nfatc1-Cre* mutants and control animals (Fig. 14Q).
Together, these data suggest that neither defects in apoptosis nor the decreased presence of macrophages linked to the removal of apoptotic cells can account for the hyperplastic valve phenotype of C*xcr4*^{flox}*; Nfatc1-Cre* mice.

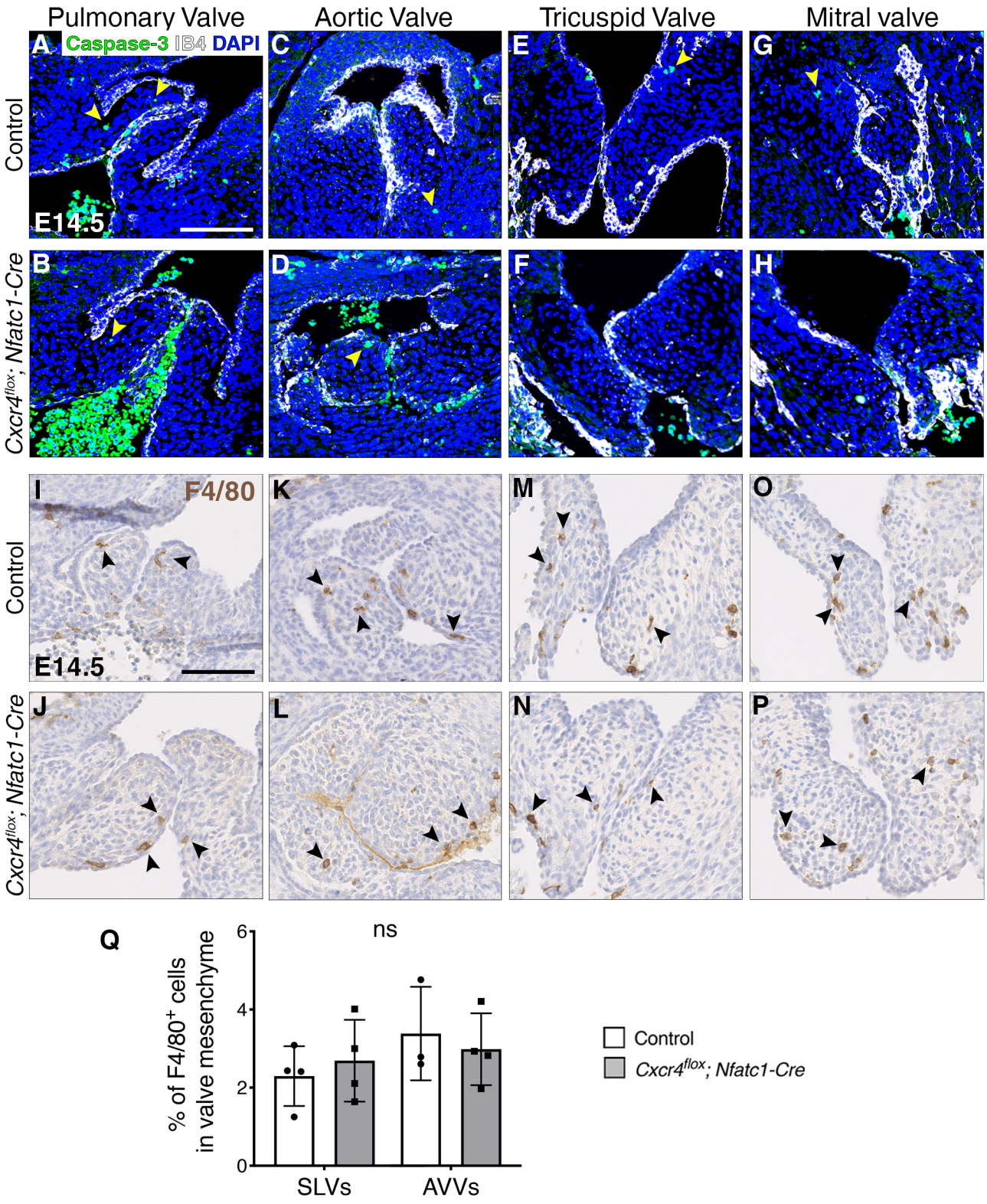

Figure 14. No defective apoptosis or lack of macrophage recruitment in *Cxcr4^{flox}; Nfatc1-Cre* mutant mice. A-H: Caspase-3 immunostaining of heart sections at E14.5, showing control SL (**A**, **C**) and AV valves (**E, G**), and mutant SL (**B, D**) and AV valves (**F**, **H**). Yellow arrowheads mark cells undergoing apoptosis. **I-P**: F4/80 immunostaining of heart sections at E14.5, showing control SL (**I**, **K**) and AV valves (**M, O**), and mutant SL (**J, L**) and AV valves (**N**, **P**). Black arrowheads indicate

the location of macrophages in the mesenchymal region. **Q**: Quantification of macrophage recruitment at E14.5, defined as the number of F4/80^{+} positive cells over total number of valve mesenchymal cells. Scale bar: 100µm. SLVs, semilunar valves; AVVs, atrioventricular valves. Data are means±SD. ns indicates non-significance by Student's *t* test (n=3-4 for controls, n=4 for *Cxcr4^{flox}; Nfatc1-Cre* mutants).

Canonical BMP signaling is not affected in *Cxcr4^{flox}; Nfatc1-Cre* valves

BMPs transduce signals by binding serine/threonine kinase receptors, that activate canonical signaling via receptor Smads 1, 5 and 8 (Massagué et al., 2005). Several models of valve hyperplasia have been linked to enhanced BMP signaling via the canonical downstream effector, Smad1/5/8 (Iwamoto et al., 2003; Jackson et al., 2003; MacGrogan et al., 2016; Tadano et al., 2005). Notably, *Cxcr7*-null mice display increased valve cell proliferation associated with increased pSmad1/5/8 (Sierro et al., 2007; Yu et al., 2011).

To determine if the BMP/Smad pathway was altered in *Cxcr4^{flox}; Nfatc1-Cre* valves, we performed immunofluorescence against the active (nuclear) phosphorylated form of Smad1/5/8 (Figure 15). The pattern of pSmad1/5 immunostaining revealed higher levels of pSmad1/5/8 at the base of the valve cusps and lower levels at the tips of the cusps (Fig. 15 A-F). Additionally, there were different levels of staining, with some nuclei more intensely labeled than others. However, the total area of overlapping nuclear pSmad staining with DAPI staining in endocardial *Cxcr4* mutant valves did not significantly differ from control littermates (Fig. 15G).

This suggests that, unlike other valve hyperplasia models, the increase in proliferation seen in valve mesenchymal cells of endocardial *Cxcr4* mutants is not due to dysregulated BMP/Smad1/5/8 signaling.

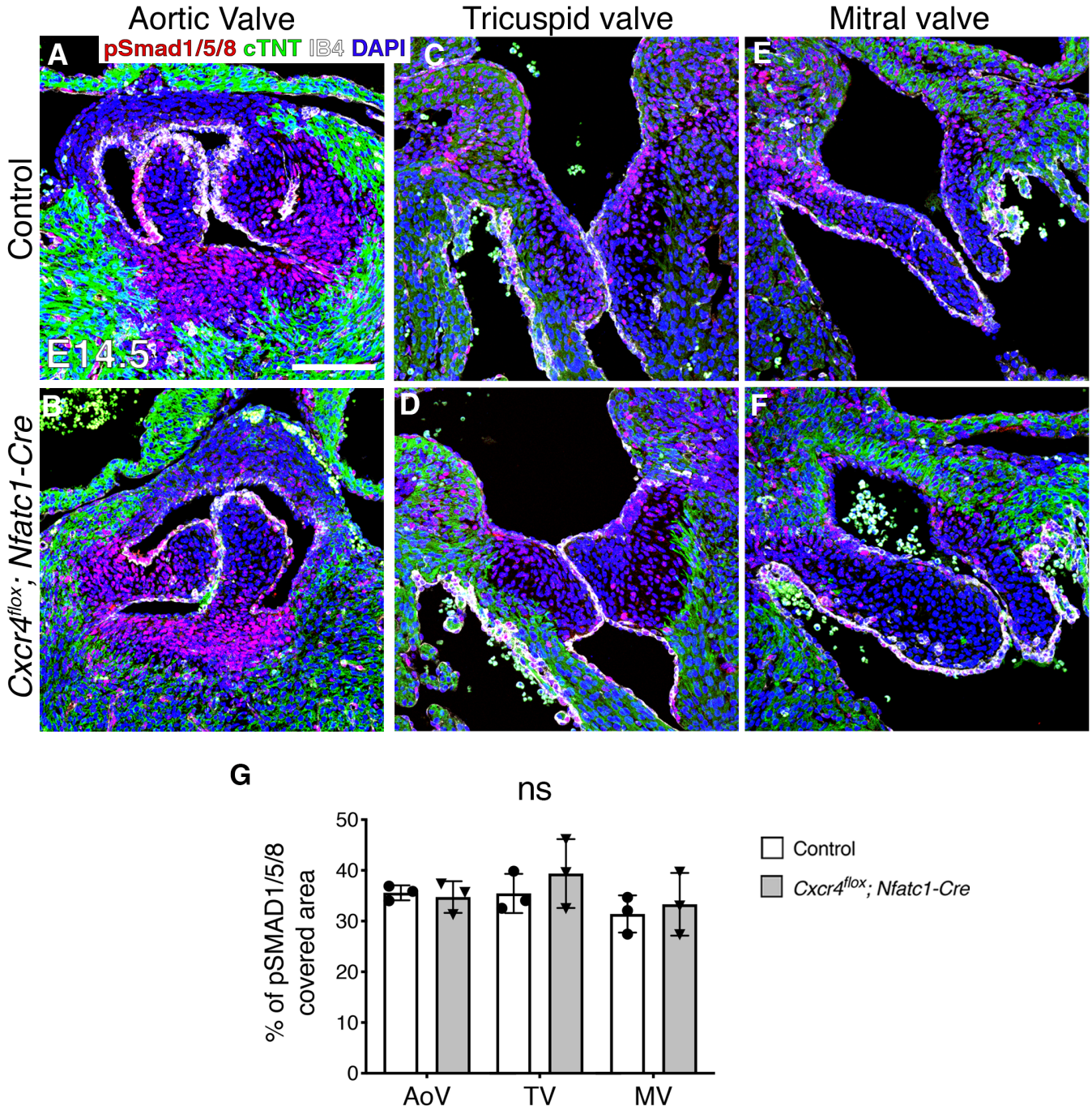

Figure 15. pSmad1/5/8 levels are unaffected in *Cxcr4^{flox}; Nfatc1-Cre* mutant mice. A, C, E: pSmad1/5/8 immunostaining of sections of control hearts at E14.5, showing the aortic (**A**) and AV valves (**C, E**). **D, F**: pSmad1/5/8 staining of sections of mutant hearts at E14.5, showing the aortic (**B**) and AV (**D, F**) valves. **G**: Quantification of pSmad1/5/8 staining at E14.5, defined as the area covered by nuclear pSmad1/5/8 overlapping with DAPI in the valve mesenchyme. Scale bar: 100µm. Data are means±SD. ns indicates non-significance by Student's *t* test (n=3 for controls, n=3 for *Cxcr4^{flox}; Nfatc1-Cre* mutants).

Pharmacological inhibition of CXCR4 results in increased mesenchymal cell proliferation in explanted OFT

To further corroborate the link between hyperplastic cardiac valves and increased valve mesenchymal cell proliferation in endocardial *Cxcr4* mutants, we performed OFT explant assays at E11.5 (Figure 16).

Explanted AVC or OFT recapitulate certain programmed morphogenetic events taking place *in vivo*, including endothelial cell proliferation and migration, and transformation into invasive mesenchyme (Camenisch et al., 2002; Runyan & Markwald, 1983). Supplementing WT OFT explants with AMD3100, a chemical compound known to specifically inhibit CXCR4 (De Clercq, 2000; Debnath et al., 2013) led to a statistically significant dose-dependent increase in proliferating mesenchymal cells (one-way ANOVA, *p*-value=0.0271). Treatment with 25μM did not produce any effect (Fig. 16F), suggesting the existence of an optimal dose-dependent response. This result indicates that supplementing the WT OFT explants with the CXCR4 antagonist mimics the *in vivo* loss-of-function phenotype resulting from loss of endocardial *Cxcr4*.

Given that the CXCL12-CXCR4 pathway regulates cellular migration in several developmental and pathological contexts (Döring et al., 2014), we examined whether AMD3100 treatment of the OFT explants led to changes of mesenchymal cell migratory behavior. However, there were no significant differences in mesenchymal cell migration or invasion of the collagen gel (measured in 2D reconstructions), after supplementing with 1, 10 or 25μM of AMD3100 (Fig. 16G, H). Thus, endocardial CXCR4 negatively regulates valve mesenchymal cell proliferation, seemingly without affecting mesenchymal cell migration or invasion.

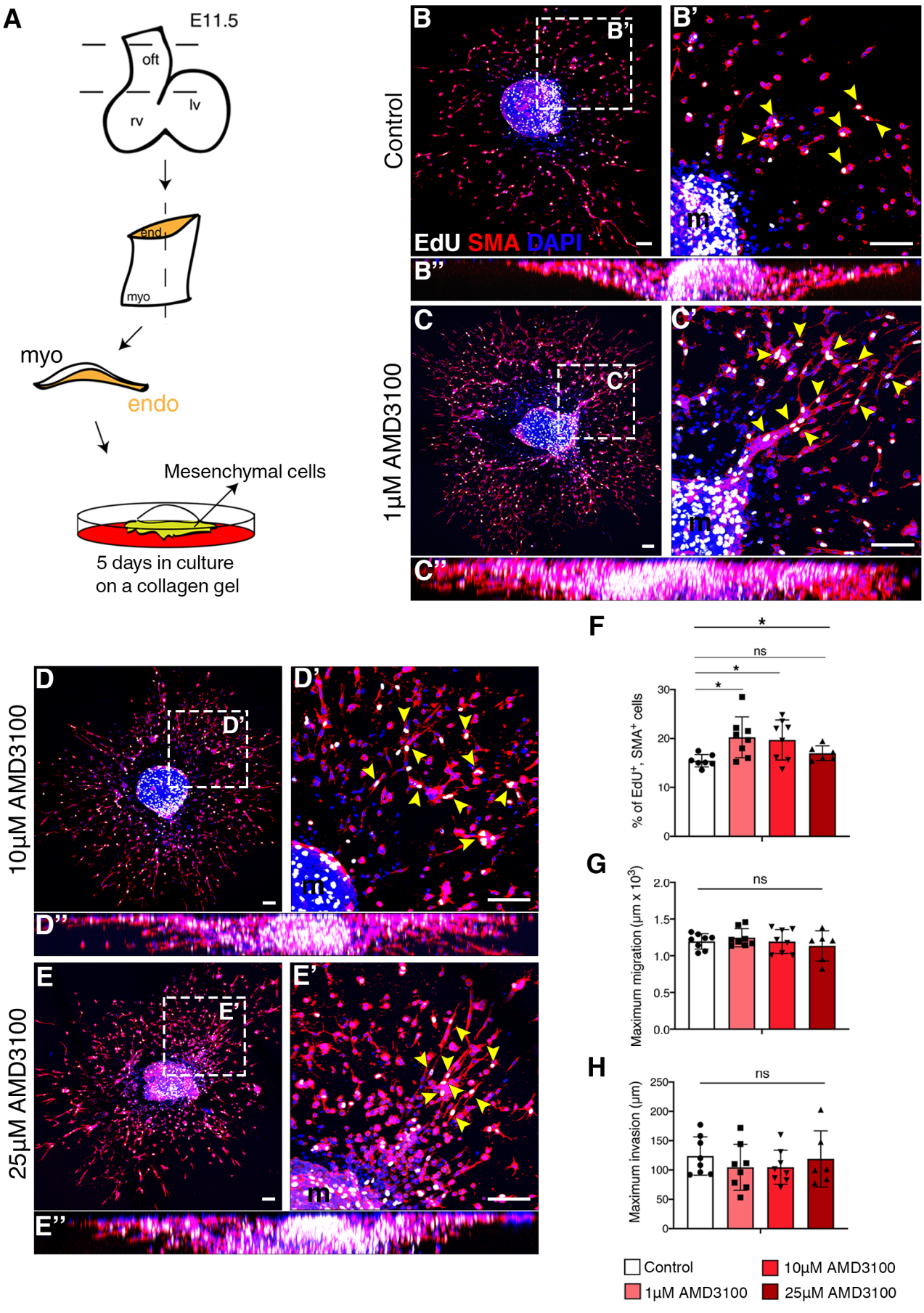
A
E11.5
oft
lv
rv
end
myo
myo
endo
Mesenchymal cells
5 days in culture
on a collagen gel
Control
1µM AMD3100
10µM AMD3100
25µM AMD3100
EdU SMA DAPI
B
B'
B''
C
C'
C''
D
D'
D''
E
E'
E''
m
F
% of EdU+, SMA+ cells
G
Maximum migration (µm x 10³)
H
Maximum invasion (µm)
ns
*
Control
1µM AMD3100
10µM AMD3100
25µM AMD3100

Figure 16. Pharmacological inhibition of CXCR4 signaling increases mesenchymal cell proliferation in WT OFT explants. A: Schematic depiction of the explant assay. OFTs are dissected from E11.5 embryos, opened and the endocardial side is placed face down on the collagen gel, where mesenchymal cells are able to migrate. **B**: Representative WT OFT explant. **C, D, E**: Explants supplemented with 1μM (**C**), 10μM (**D**) and 25μM (**E**) of AMD3100. 5-ethynyl-2'-deoxyuridine (EdU) staining (yellow arrowheads) indicates proliferating cells. **B', C', D', E**': Magnified view of body of explant and outwardly migrating mesenchymal cells, stained by α smooth muscle actin (SMA). **B'', C'', D'', E''**: 2D depiction of the explants, showing mesenchymal cell invasion into the collagen gel, and the distance travelled by the cells on the gel surface. **F**: Quantification of EdU incorporation relative to αSMA-positive cells in explants supplemented with the indicated concentrations of AMD3100. **G**: Quantification of migration, defined as the maximum distance travelled by mesenchymal cells on the gel surface, in explants supplemented with the indicated concentrations of AMD3100. **H**: Quantification of cell invasion, defined as the distance travelled by mesenchymal cells inside the collagen gel, in explants supplemented with the indicated concentrations of AMD3100. Scale bars: 100μm. oft, outflow tract; rv, right ventricle; lv, left ventricle; myo, myocardium; endo, endocardium; m, myocardial body of the explant. *P≤0.05, ns indicates non-significance by ordinary one-way ANOVA and Dunnett's multiple comparisons tests (n=7-8 for controls, n=8 for 1μM and 10μM, n=6 for 25μM).

Generation of a soluble HBEGF (sHBEGF) gain-of-function transgenic mouse model

Prior studies have shown that global and endothelial-specific *Hbegf* deletion results in cardiac valve enlargement and hyperplasia (Table 1) (Iwamoto et al., 2003; Jackson et al., 2003; Nanba et al., 2006). Given that endocardial *Cxcr4* deletion results in a similar phenotype, we wondered whether CXCR4 could be a candidate GPCR implicated in sHBEGF release during valve morphogenesis. If this were the case, the hyperplastic phenotype displayed by endocardial *Cxcr4* mutants might be rescued by breeding with *sHBEGF*-overexpressing mice. Thus, to study the role of CXCR4 in ectodomain shedding of proHBEGF and transactivation of EGFR, we generated a transgenic mouse model overexpressing the soluble portion of the human *HBEGF* gene (*sHBEGF*) (Figure 17). The ROSA26 locus (Soriano, 1999) was targeted with an expression cassette composed of loxP sites flanking a PGK-neo-PGK-polyA, a transcriptional STOP and the cDNA encoding sHBEGF, followed by a myc tag and an IRES-*eGFP* (Fig. 17A).

To produce endocardial/endothelial overexpression of *sHBEGF*, we crossed the *R26-sHBEGF*$^{tg/+}$ transgenic line with the driver *Tie2-Cre* to obtain *R26-sHBEGF*$^{tg/+}$*; Tie2-Cre* mice. We could not detect any eGFP fluorescence

in transgenic embryos, even after examining three litters at E9.5 by fluorescence confocal microscopy. Therefore, we performed qPCR using primers that specifically target the sequence encoding sHBEGF. RNA was extracted from pools of control and mutant whole hearts at E10.5, E11.5 and E12.5 (Fig. 17E). At E10.5, there is a 5-fold increase in the relative *sHBEGF* expression compared to control littermates, reaching 140-fold by E12.5 (Fig. 17E). We subsequently attributed this order of magnitude increase to the fact that *Tie2-Cre* expressing cells undergo EMT in the AVC and the OFT (Kisanuki et al., 2001), resulting in ectopic *sHBEGF* expression in the valve mesenchyme.

Interestingly, qPCR analysis of the co-expressed *eGFP* transcript showed a 4-fold increase in the mutant relative to control at E10.5, but only a 10-fold increase at E12.5 (Fig. 17F). This difference in magnitude of increase between E10.5 and E12.5 is therefore not as dramatic as the one seen for *sHBEGF*, which could be due to many different factors such as PCR efficiencies, or processing/stability of the 5' versus 3' mRNA. Nevertheless, *eGFP* mRNA was readily detected in endocardium of *R26-sHBEGF*$^{tg/+}$*; Tie2-Cre* transgenics, but not in controls (Fig. 17G, H). Therefore, *sHBEGF* mRNA overexpression is induced as expected, despite the absence of detectable eGFP fluorescence.

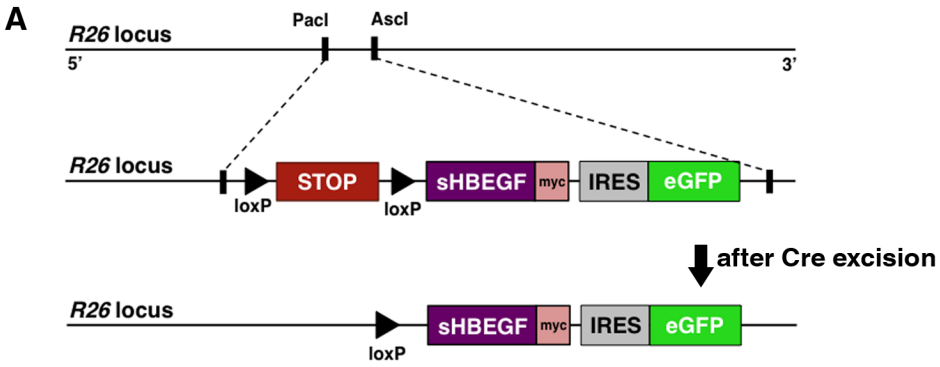
A
R26 locus
PacI
AscI
5'
3'
R26 locus
loxP
STOP
loxP
sHBEGF
myc
IRES
eGFP
after Cre excision
R26 locus
loxP
sHBEGF
myc
IRES
eGFP

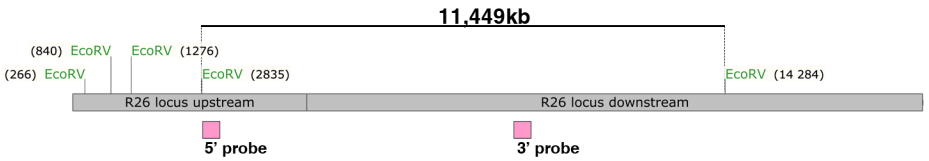
B WT locus
11,449kb
(840) EcoRV
EcoRV (1276)
(266) EcoRV
EcoRV (2835)
EcoRV (14 284)
R26 locus upstream
R26 locus downstream
5' probe
3' probe

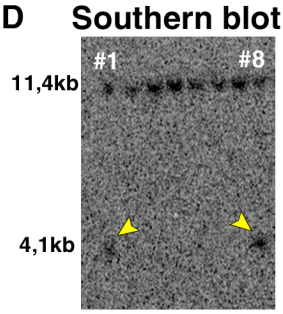
D Southern blot
11,4kb
4,1kb
#1
#8

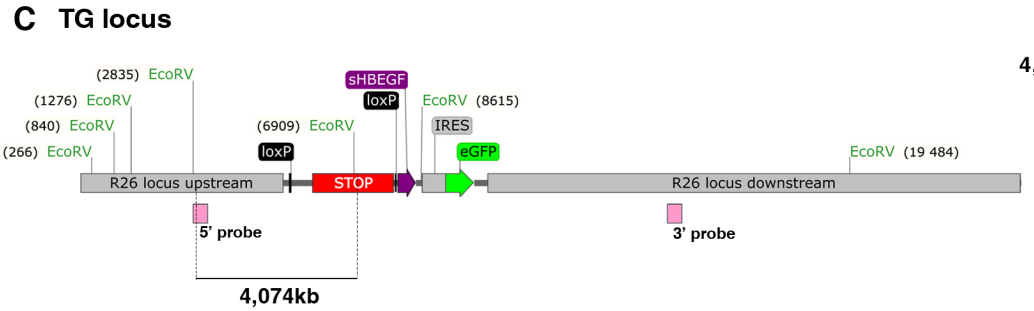
C TG locus
(2835) EcoRV
(1276) EcoRV
(840) EcoRV
(266) EcoRV
sHBEGF
loxP
(6909) EcoRV
loxP
EcoRV (8615)
IRES
eGFP
EcoRV (19 484)
R26 locus upstream
STOP
R26 locus downstream
5' probe
3' probe
4,074kb

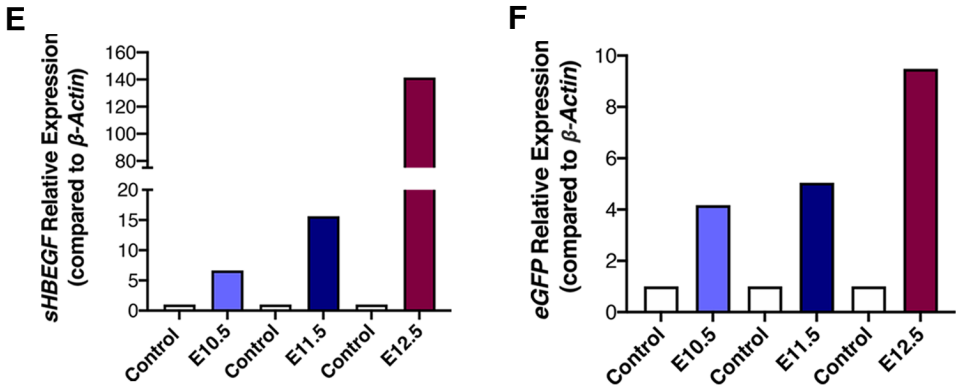
E
sHBEGF Relative Expression (compared to β-Actin)
160
140
120
100
80
20
15
10
5
0
Control
E10.5
Control
E11.5
Control
E12.5
F
eGFP Relative Expression (compared to β-Actin)
10
8
6
4
2
0
Control
E10.5
Control
E11.5
Control
E12.5

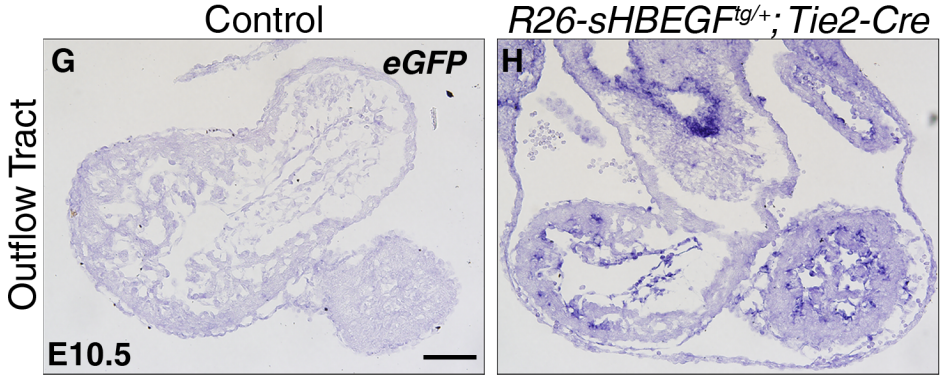
Control
R26-sHBEGFtg/+; Tie2-Cre
Outflow Tract
G
eGFP
E10.5
H

Figure 17. Generation of a conditional mouse transgenic line overexpressing *sHBEGF*. **A**: Mouse ESC targeting strategy. A fragment consisting of floxed PGK-NEO-pA, STOP cassette (three SV40 polyadenylation sequences), *sHBEGF* cDNA, myc tag and IRES-*eGFP* was inserted into the ROSA26 locus of mouse ESC by homologous recombination. **B**: Cutting sites for EcoRV in WT genomic DNA, with the respective fragment detected by 5' and 3' probes. **C**: Cutting sites for EcoRV in transgenic genomic DNA, with respective fragment detected by 5' and 3' probes. **D**: Southern blot analysis of EcoRV-digested genomic DNA, using 5' and 3' probes to identify a WT 4.1kb and a transgenic 14.2kb fragments. **E**: qPCR of *sHBEGF* and *eGFP* relative to *βActin* expression, analyzed on pools of E10.5, E11.5 and E12.5 control and *sHBEGF* overexpressing hearts. **G, H** ISH on E10.5 control and *R26-sHBEGF$^{tg/+}$; Tie2-Cre* OFT sections using an *eGFP* probe. Scale bar: 100μm.

Endocardial/endothelial overexpression of *sHBEGF* leads to valve defects that persist and worsen post-natally

Previous studies have demonstrated that global or endothelial loss of *Hbegf* leads to valve enlargement (Iwamoto et al., 2003, 2010; Jackson et al., 2003; Nanba et al., 2006; Yamazaki et al., 2003). Unexpectedly, examination of transverse sections of E14.5 *R26-sHBEGF$^{tg/+}$; Tie2-Cre* transgenic hearts revealed severely thickened and unremodeled leaflets in both SL and AV sets of valves, with an abnormally expanded mesenchymal domain, when compared to control littermates (Fig. 18A-F). These defects became more obvious and pronounced at E16.5 (Fig. 18G-L), indicating that precise regulation of endothelial sHBEGF levels during embryonic development is essential for proper cardiac valve formation and remodeling.

R26-sHBEGF$^{tg/+}$; Tie2-Cre transgenic mice survive birth and are born at normal Mendelian ratios. H&E staining of one-month-old (P30) *R26-sHBEGF$^{tg/+}$; Tie2-Cre* transgenic hearts exhibited grossly oversized valve leaflets when compared to controls (Fig. 19A-B''). Transgenic hearts at P30 (n=2) were larger and had abnormal myocardial walls, with one displaying ventricular septal defects (Fig. 19B). The same heart displayed cartilaginous metaplasia in one of the mitral valve leaflets, indicative of an ongoing endochondral ossification process (Fig. 19B''). Collectively, these results show that overexpressing *sHBEGF* in endothelium during development elicits severe valve defects in the embryo that worsen and extend to the myocardium in juvenile mice.

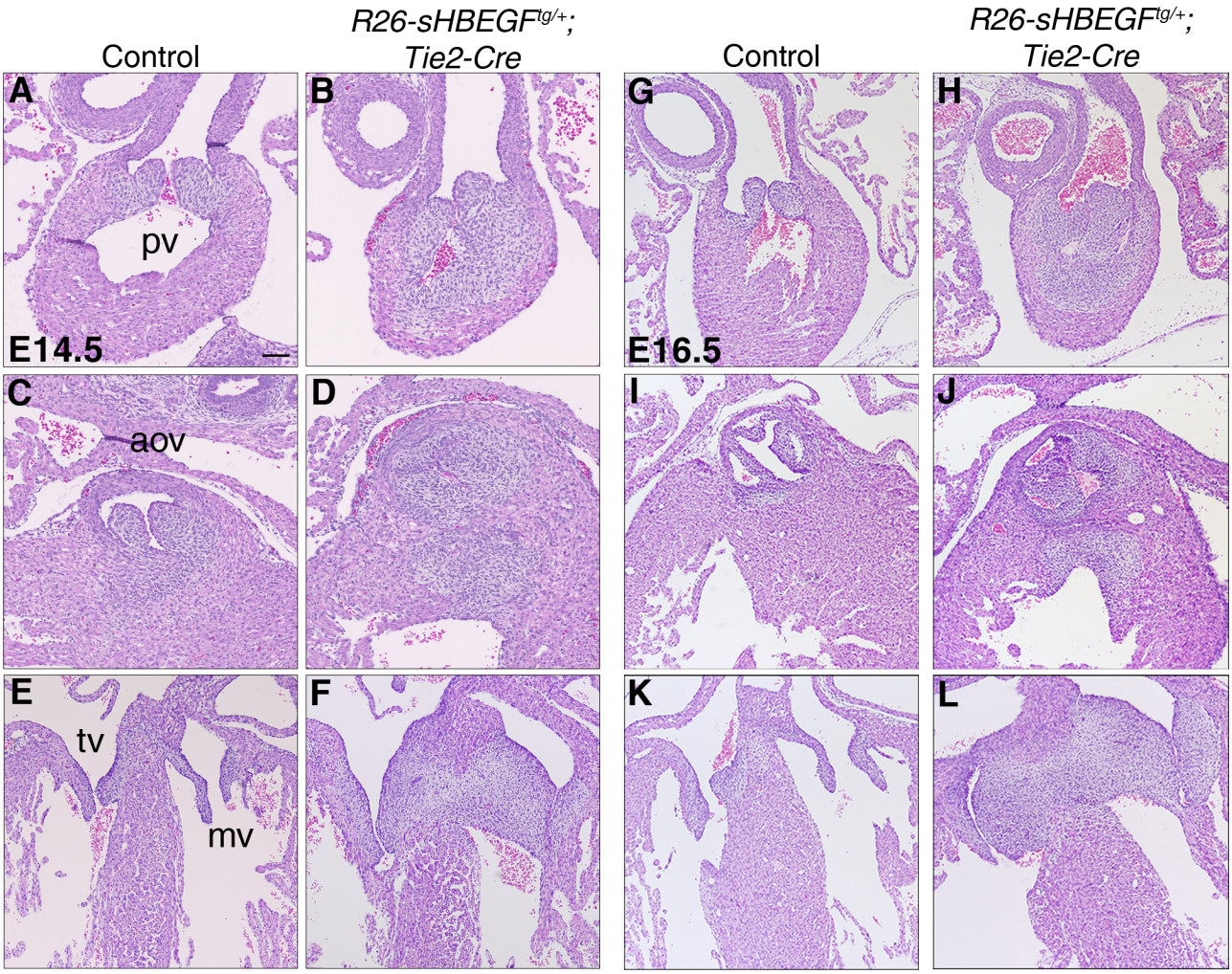

Figure 18. *R26-sHBEGF$^{tg/+}$; Tie2-Cre* valves are grossly enlarged. H&E staining of control and *R26-sHBEGF$^{tg/+}$; Tie2-Cre* heart sections at E14.5 (**A**-**F**) and 16.5 (**G**-**L**). Mutants show severe leaflet enlargement of both SL (**B, D, H, J**) and A-V valves (**F, L**), compared to control littermates Scale bar: 100µm. pv, pulmonary valve; aov, aortic valve; tv, tricuspid valve; mv, mitral valve.

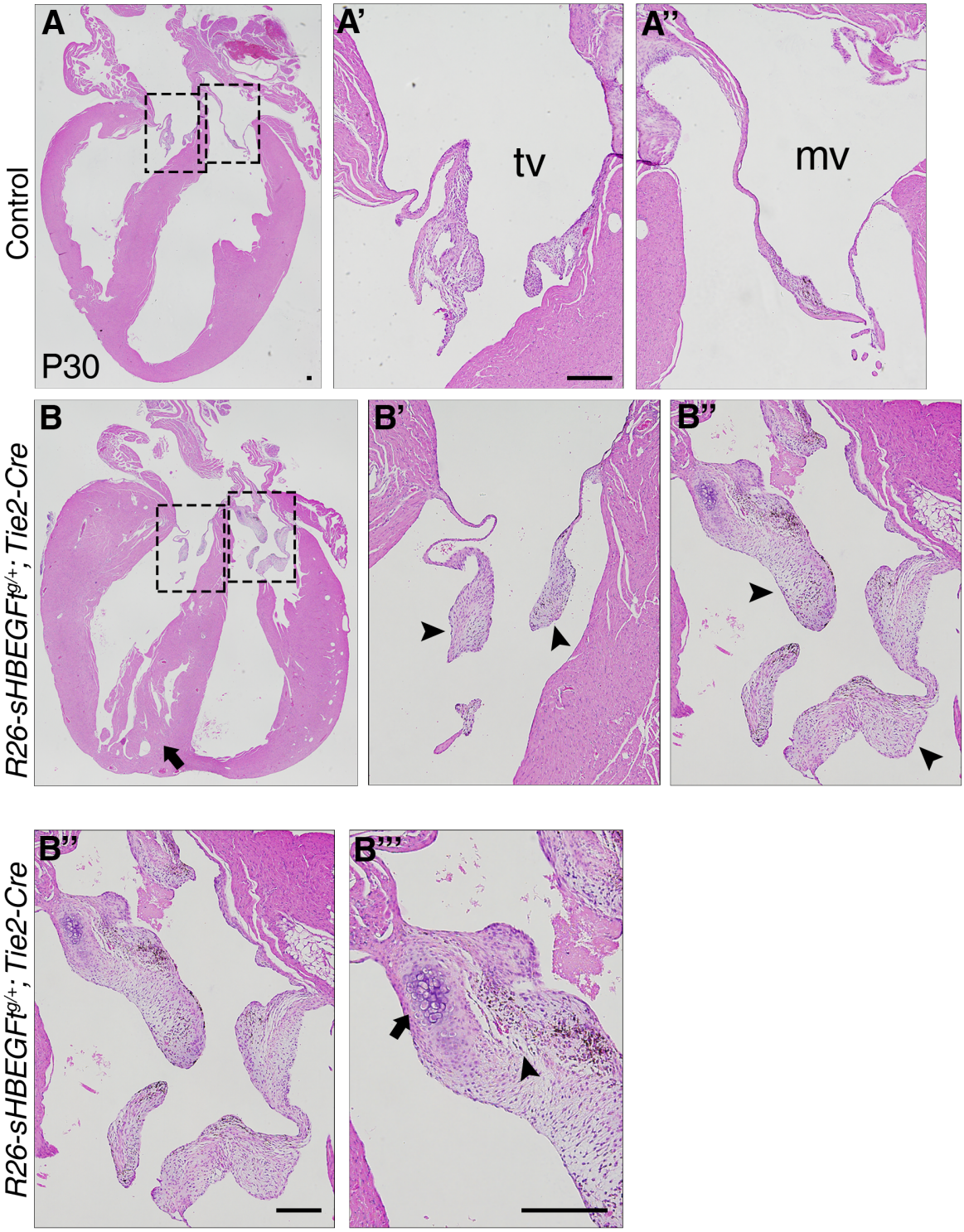

Figure 19. One-month-old *R26-sHBEGF$^{tg/+}$; Tie2-Cre* mice display severe cardiac defects. H&E staining of P30 heart sections showing normal valves in control mice (**A-A''**) and enlarged leaflets (**B-B''**) in transgenics. Arrowheads indicate the thickened cusps. Arrow in **B** indicates defects in the ventricular septum. **B''-B'''**: Aberrant cartilaginous metaplasia (arrow) in one of the cusps of the mitral valve of a mutant, with evidence of fibrosis close by (arrowhead). Scale bar: 100µm. tv, tricuspid valve; mv, mitral valve.

Excessive EMT does not contribute to the enlarged valve phenotype in *R26-sHBEGF$^{tg/+}$; Tie2-Cre* transgenic mice

HBEGF has been shown to promote EMT in different cell types, partly by activating the VE-cadherin transcriptional repressor Snail2/Slug (Smith et al., 2009; Stoll et al., 2012). We examined whether excessive EMT could be contributing to the valve enlargement seen in *R26-sHBEGF$^{tg/+}$; Tie2-Cre* transgenic mice (Figure 20). Histological examination of hearts at E10.5 revealed no excess cell invasion in the OFT or AV endocardial cushions of the *sHBEGF* transgenic embryos compared to WT controls (Fig. 20A-D), neither were there morphological differences in the post-EMT endocardial cushions at E11.5 or E12.5 (Fig. 20E-L). Moreover, we performed qPCR on pools of whole hearts collected at E10.5, E11.5 and E12.5 to detect changes in the expression of the EMT markers *Snail1*, *Snail2* and *Twist1*. EMT marker expression was unaffected in the transgenic mice relative to control (Fig. 20M).

Therefore, we conclude that the enlarged valves phenotype seen in *sHBEGF* transgenic embryos at E14.5 is not due to EMT occurring beyond its normal developmental time window.

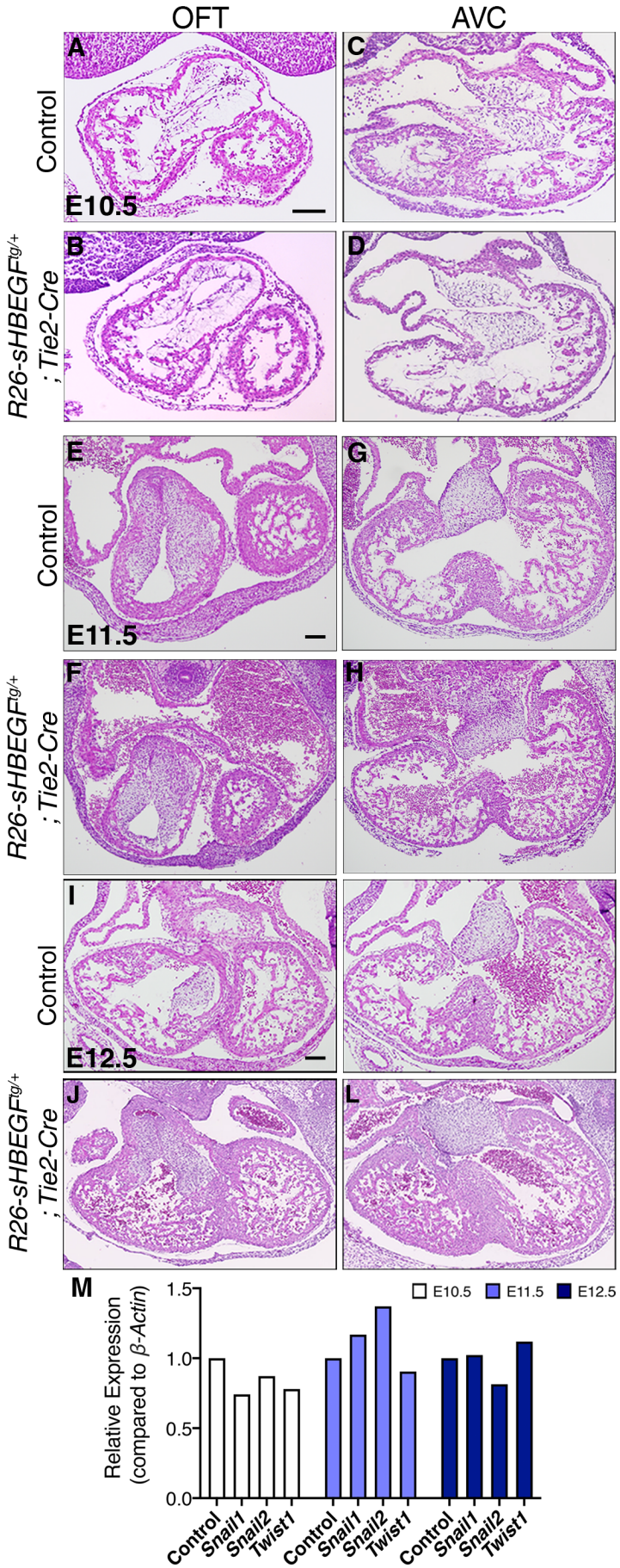
OFT
AVC
A
C
Control
E10.5
B
D
R26-sHBEGF tg/+ ; Tie2-Cre
E
G
Control
E11.5
F
H
R26-sHBEGF tg/+ ; Tie2-Cre
I
Control
E12.5
J
L
R26-sHBEGF tg/+ ; Tie2-Cre
M
E10.5
E11.5
E12.5
Relative Expression (compared to β-Actin)
1.5
1.0
0.5
0.0
Control
Snail1
Snail2
Twist1

Figure 20. EMT is unaffected in *R26-sHBEGF$^{tg/+}$; Tie2-Cre* embryos. H&E staining of heart sections at E10.5 (**A**-**D**), E11.5 (**E-H**) and E12.5 (**I-L**), indicating the absence of morphological differences between controls and *R26-sHBEGF$^{tg/+}$; Tie2-Cre* hearts. **M**: *Snail1*, *Snail2* and *Twist1* expression relative to *β-actin*, analyzed by qPCR of pools of E10.5, E11.5 and E12.5 control and *sHBEGF* transgenic hearts.

Increased post-EMT mesenchymal cell proliferation in *R26-sHBEGF$^{tg/+}$; Tie2-Cre* mice

To further investigate the cellular basis for the enlarged valve phenotype observed in endothelial *sHBEGF* transgenic mice, we measured BrdU incorporation at E12.5 and E14.5 (Figure 21). Increased BrdU incorporation was detected at E12.5 in OFT and AVC endocardial cushions of *R26-sHBEGF$^{tg/+}$; Tie2-Cre* transgenic embryos, despite the fact that there were no major morphological differences compared to controls (Fig. 21A-D, K). The increased valve mesenchymal cell proliferation persisted in the transgenic animals until at least E14.5 (Fig. 21E-H, L).

Thus, the early increase in mesenchymal cell proliferation post-EMT is the likely cause of the severely thickened and unremodeled leaflets displayed by transgenic animals overexpressing endothelial *sHBEGF*.

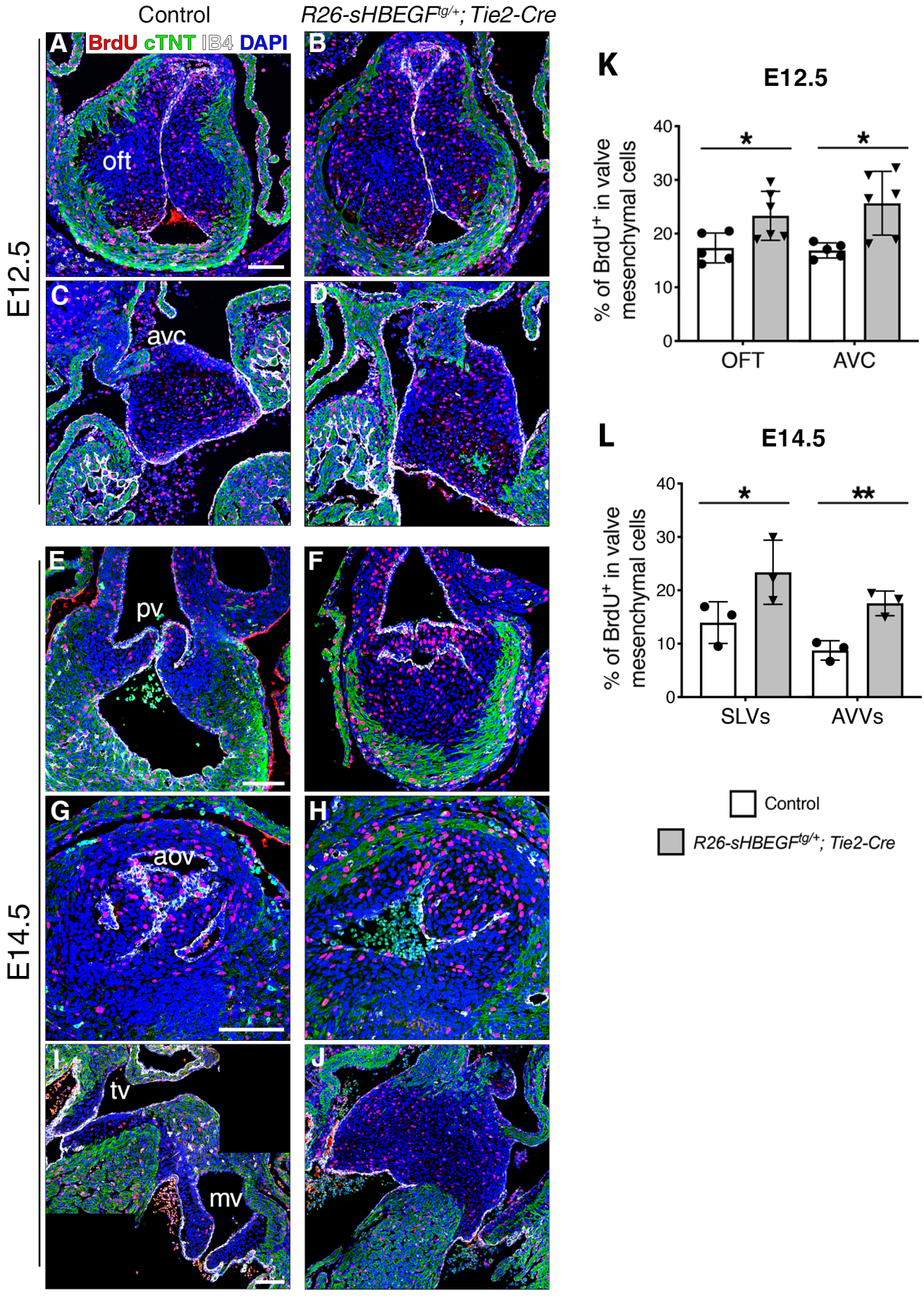
Control
R26-sHBEGF^tg/+; Tie2-Cre
A
BrdU cTNT IB4 DAPI
B
oft
C
avc
D
E12.5
E
pv
F
G
aov
H
E14.5
I
tv
mv
J
K
E12.5
% of BrdU+ in valve mesenchymal cells
40
30
20
10
0
*
*
OFT
AVC
L
E14.5
% of BrdU+ in valve mesenchymal cells
40
30
20
10
0
*
**
SLVs
AVVs
Control
R26-sHBEGF^tg/+; Tie2-Cre

Figure 21. Endothelial *sHBEGF* transgenic mice display increased valve mesenchymal cell proliferation as early as E12.5. BrdU immunostaining (in red) of heart sections of WT controls and *R26-sHBEGF$^{tg/+}$; Tie2-Cre* mutant littermates at E12.5 (**A**-**D**) and E14.5 (**E**-**J**). **A-D**: BrdU staining of *sHBEGF* transgenics and controls at E12.5, showing the precursors of the SL (**A**, **C**) and AV valves (**B, D**). **E-J**: BrdU staining of *sHBEGF* transgenics and controls at E14.5, showing the precursors of the SL (**E, G, F, H**) and AV valves (**I, J**). **K**: Quantification of proliferation at E12.5, defined as the percentage of BrdU-positive nuclei, in both control and mutant embryos. **L**: Quantification of proliferation at E14.5, defined as the percentage of BrdU-positive nuclei, in both control and mutant embryos. pv, pulmonary valve; aov, aortic valve; tv, tricuspid valve; mv, mitral valve; SLVs, semilunar valves; AVVs, atrioventricular valves. Data are means±SD. *P≤0.05, **P≤0.01 by Student's *t* test (n=3-5 for controls, n=3-6 for *R26-sHBEGF$^{tg/+}$; Tie2-Cre* mutants).

Mesenchymal cell proliferation is increased in explanted *R26-sHBEGF$^{tg/+}$; Tie2-Cre* OFT tissue

To further elucidate the role of HBEGF in the regulation of valve mesenchymal cell proliferation, we employed the OFT explant system. OFTs explanted from *R26-sHBEGF$^{tg/+}$; Tie2-Cre* mice and WT littermates were cultured in separate wells containing collagen gel to determine whether the excess sHBEGF secreted from *R26-sHBEGF$^{tg/+}$; Tie2-Cre* OFTs might affect the rate of mesenchymal proliferation (Figure 22).

Mesenchymal cells derived from transgenic OFTs incorporated significantly more EdU than the ones derived from control littermates (Student's *t* test *p*-value=0.0484) (Fig. 22C). No changes were detected in mesenchymal cell migration or invasion of the collagen gel (Fig. 22D, E).

Therefore, excessive sHBEGF secretion by explanted *R26-sHBEGF$^{tg/+}$; Tie2-Cre* OFTs results in increased proliferation of mesenchymal cells, mimicking the *in vivo* phenotype.

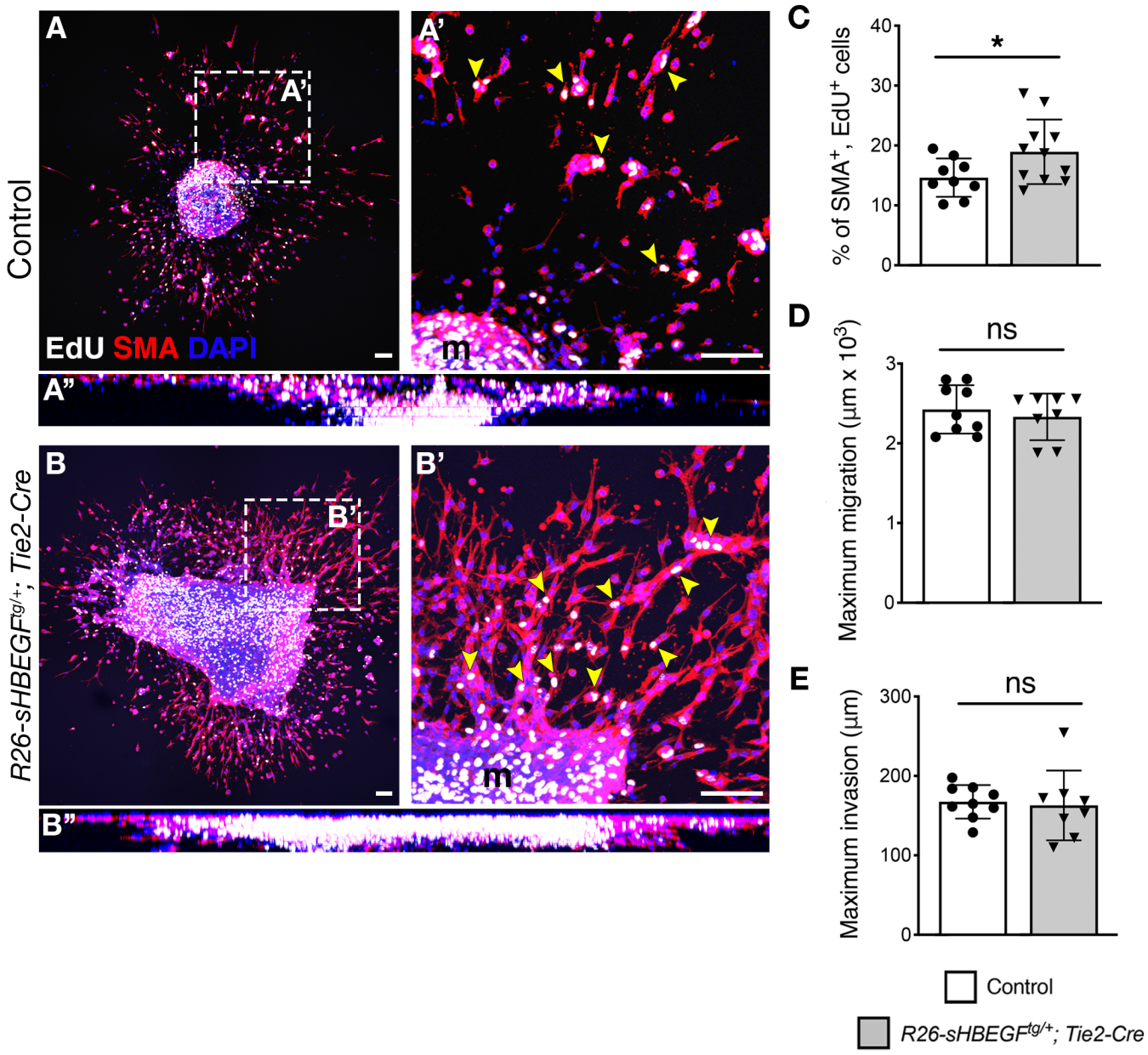

Figure 22. Increased mesenchymal cell proliferation in explanted *R26-sHBEGF$^{tg/+}$; Tie2-Cre* OFT tissue. A: Representative control WT OFT explant. **B**: OFT explant from a *R26-sHBEGF$^{tg/+}$; Tie2-Cre* embryo. Proliferating cells have incorporated EdU (yellow arrowheads). **A', B'**: Magnified view of the outwardly migrating mesenchymal cells, as stained by αSMA. **A'', B''**: 2D view of the explants. **C**: Quantification of EdU incorporation relative to αSMA-positive cells derived from control and transgenic embryos. **G**: Quantification of mesenchymal cell migration in OFT explants from control and transgenic embryos. **H**: Quantification of mesenchymal cell migration in OFT explants from control and transgenic embryos. Scale bars: 100µm. m, myocardial body of the explant. *P≤0.05, ns indicates non-significance by Student's *t* test (n=9 for control OFTs, n=8 for *R26-sHBEGF$^{tg/+}$; Tie2-Cre* transgenic OFTs).

Supplementing explanted OFT tissue with sHBEGF increases mesenchymal cell proliferation and migration

To support the pro-proliferative role of sHBEGF on valve mesenchymal cells, we supplemented explanted WT OFTs with increasing doses of recombinant mouse sHBEGF (Figure 23). This had a dramatic growth-inducing effect on the explanted OFT tissue, evidenced by increased EdU incorporation by mesenchymal cells in a treatment-dependent manner (one-way ANOVA, *p*-value=0.0027) (Fig. 23F). Moreover, mesenchymal cells migrated further away on the gel when treated with 50ng/ml sHBEGF, in comparison to controls (Fig. 23G). Likewise, the size of the explant myocardial body dramatically increased, suggesting that sHBEGF might also increase myocardial proliferation. Indeed, several reports suggest that HBEGF plays a trophic role in cardiomyocyte proliferation (Ieda et al., 2009; Lian et al., 2012). While mesenchyme and myocardium are both stained by αSMA, mesenchymal cells organize in characteristic sheets of cells that can be distinguished from the cardiomyocytes composing the body of the explant.

These data indicate that recombinant sHBEGF has a pro-proliferative effect in explanted OFT tissue that recapitulates the effect of overexpressing *sHBEGF* in the endothelium (and mesenchymal derivatives) of *R26-sHBEGF*$^{tg/+}$*; Tie2-Cre* mice.

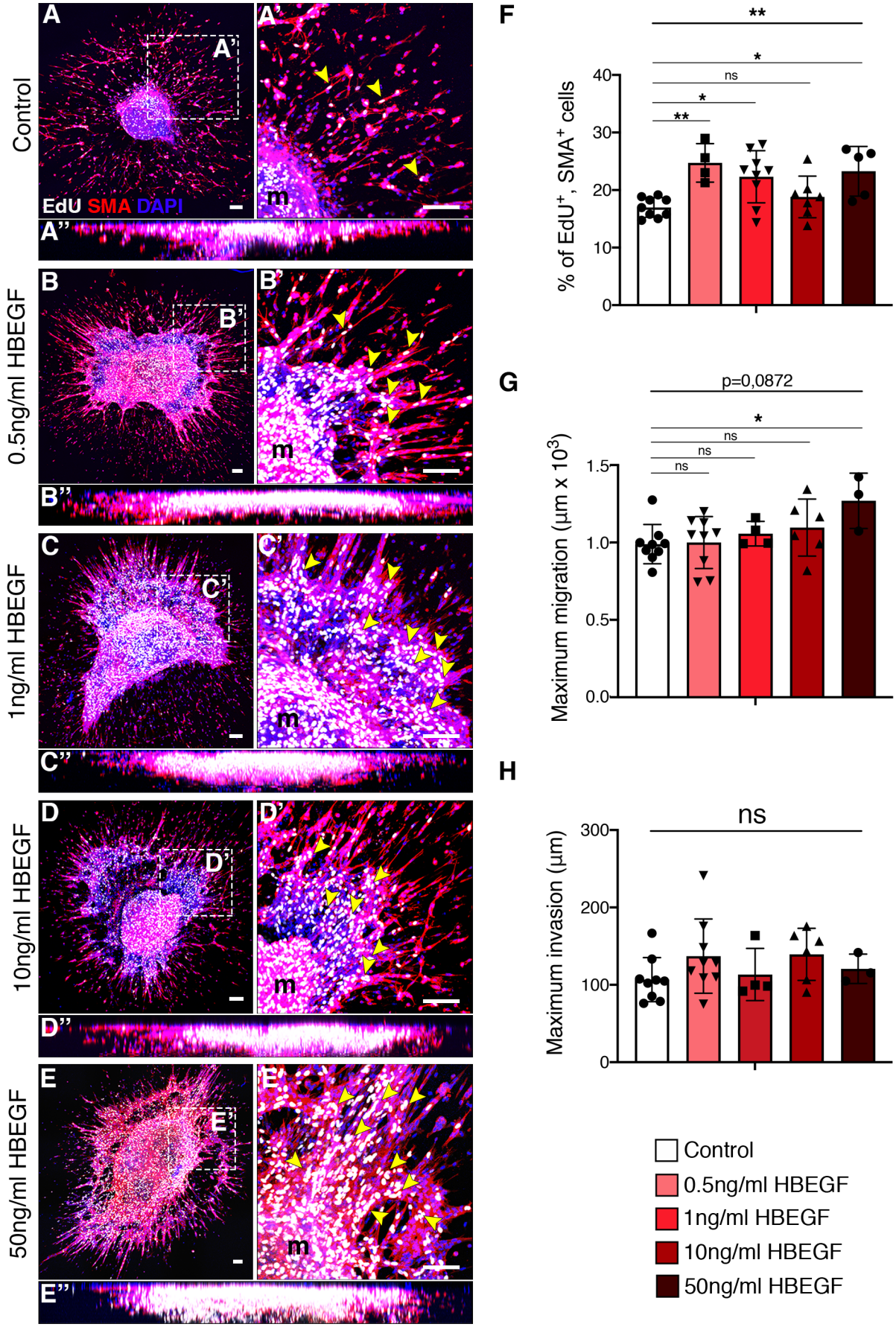
Control
0.5ng/ml HBEGF
1ng/ml HBEGF
10ng/ml HBEGF
50ng/ml HBEGF
EdU SMA DAPI
m
F
% of EdU+, SMA+ cells
G
Maximum migration (µm x 10³)
p=0,0872
H
Maximum invasion (µm)
ns
Control
0.5ng/ml HBEGF
1ng/ml HBEGF
10ng/ml HBEGF
50ng/ml HBEGF

Figure 23. Recombinant sHBEGF increases mesenchymal cell proliferation and migration in OFT explants. A: Representative control WT OFT explant. **B, C, D, E**: Explant supplemented with 0.5ng/ml **(B)**, 1ng/ml **(C)**, 10ng/ml **(D)** and 50ng/ml (**E**) of recombinant soluble HBEGF. Proliferating cells have incorporated EdU (yellow arrowheads). **A', B', C', D', E**': Magnified view of the outwardly migrating mesenchymal cells, as stained by αSMA. **A'', B'', C'', D'', E''**: 2D view of the explants. **F**: Quantification of EdU incorporation relative to αSMA-positive cells in explants supplemented with the indicated concentrations of sHBEGF. **G**: Quantification of mesenchymal cell migration in explants supplemented with the indicated concentrations of sHBEGF. **H**: Quantification of mesenchymal cell invasion in explants supplemented with the indicated concentrations of sHBEGF. Scale bars: 100µm. m, myocardial body of the explant. *P≤0.05, **P≤0.01, ns indicates non-significance by ordinary one-way ANOVA and Dunnett's multiple comparisons tests (n=9 for controls, n=4-9 for 0.5 and 1ng/ml sHBEGF, n=6-7 for 10ng/ml sHBEGF, n=3-5 for 50ng/ml sHBEGF).

Supplementing OFT explants with a pan-ErbB inhibitor decreases mesenchymal cell proliferation, migration and invasion

To investigate the identity of the receptor(s) for sHBEGF-driven proliferation, we treated OFT explants with PD158780, a chemical pan-ErbB receptor inhibitor used at micromolar concentrations in cell culture and explant assays (Ledonne et al., 2015; MacGrogan et al., 2016; Matsuoka et al., 2016). Supplementing OFT explants with PD158780 caused a significant reduction in the percentage of proliferative mesenchymal cells, in a treatment-dependent manner (one-way ANOVA, *p*-value=0,0009) (Figure 24). The most severe effect was observed at the concentration of 10µM (Dunnett's multiple comparisons test, *p*-value=0.0005) (Fig. 24E). Explants grew very poorly in presence of the inhibitor, as there were visibly less cells around the myocardial body (Fig. 24B, C, D). Likewise, outward cell migration from the body of the explant and invasion of the collagen gel measured in 2D reconstructions was decreased (Fig. 24F, G).

These results indicate that mesenchymal cell proliferation, migration and invasion are mediated by one or more receptors of the ErbB family. Whether known sHBEGF receptors such as EGFR can transduce pro-proliferative signals in OFT explants remains to be determined.

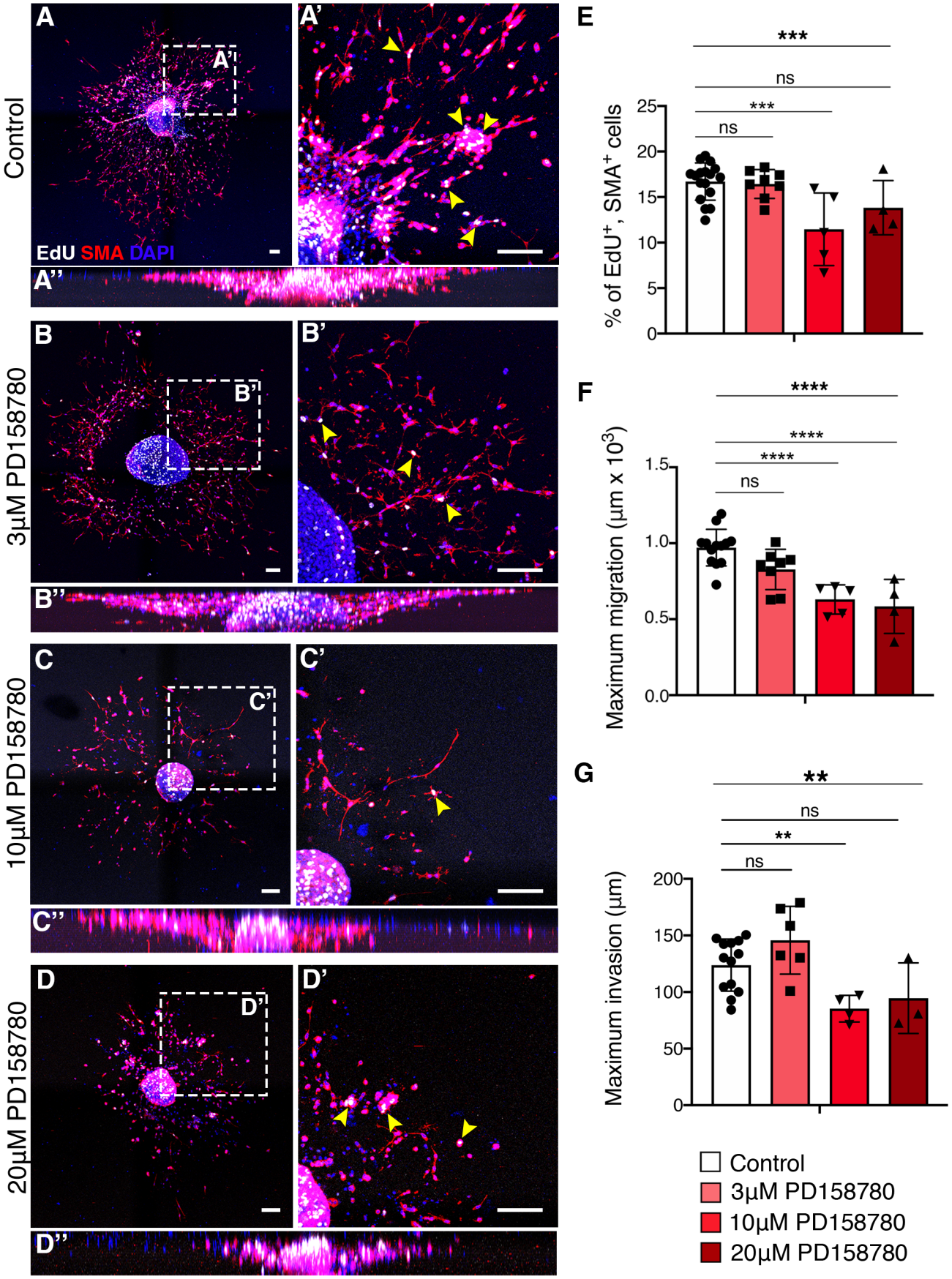
Control
3μM PD158780
10μM PD158780
20μM PD158780
A
A'
A''
B
B'
B''
C
C'
C''
D
D'
D''
EdU SMA DAPI
E
% of EdU+, SMA+ cells
***
ns
***
ns
F
Maximum migration (μm x 10^3)
****
****
****
ns
G
Maximum invasion (μm)
**
ns
**
ns
Control
3μM PD158780
10μM PD158780
20μM PD158780

Figure 24. PD158780 inhibits mesenchymal cell proliferation, migration and invasion in WT OFT explants. A: Representative control OFT explant. **B-D**: Explant supplemented with of PD158780 at 3µM (B), 10µM (C) and 20µM (D). EdU incorporation (yellow arrowheads) marks proliferating cells. **A', B', C', D**': Magnified view of the migrating mesenchymal cells, stained by alpha smooth muscle actin (αSMA). **A'', B'', C'', D''**: 2D view of the explants. **E**: Quantification of EdU relative to αSMA-positive cells in OFT explants supplemented with the indicated concentrations of PD158780. **F**: Quantification of mesenchymal cell migration in OFT explants supplemented with the indicated concentrations of PD158780. **G**: Quantification of mesenchymal cell invasion in OFT explants supplemented with the indicated concentrations of PD158780. Scale bars: 100µm. m, myocardial body of the explant. **P≤0.01, ***P≤0.001, ****P≤0.0001, ns indicates non-significance by ordinary one-way ANOVA and Dunnett's multiple comparisons tests (n=13-17 for controls, n=7-8 for 3µM PD158780, n=3-5 for 10µM PD158780, n=3-4 for 20µM PD158780).

sHBEGF overexpression using the *Nfatc1-valveCre* driver does not recapitulate the *Tie2-Cre* driver phenotype

In the AVC and OFT, *Tie2-Cre*-expressing valve endocardial cells undergo EMT and become mesenchyme (Kisanuki et al., 2001). Since the transgene is not silenced during EMT, *R26-sHBEGF$^{tg/+}$; Tie2-Cre* mice express transgenic *sHBEGF* not only in endocardial cells, but also ectopically in mesenchymal derivatives.

Therefore, to restrict *sHBEGF* expression to the valve endocardium, we crossed *R26-sHBEGF$^{tg/+}$* mice with the *Nfatc1-valveCre* driver line (Wu et al., 2011) (Figure 25). *Cre* expression in this line is associated to an enhancer that is restricted to a subpopulation of valve endocardial cells that do not undergo EMT (Wu et al., 2011; MacGrogan et al., 2016). Accordingly, X-gal staining of post-EMT *R26-LacZ; Nfatc1-valveCre* heart sections show that Cre activity is indeed restricted to valve endocardium (Fig. 25A-B'). However, examination of H&E staining of *R26-sHBEGF$^{tg/+}$; Nfatc1-Valve-Cre* heart sections at E16.5 did not reveal any obvious morphological changes between control and transgenics (Fig. 25C-H).

This indicates that overexpression of *sHBEGF* by the population of cells that express the valve-specific *Nfatc1* enhancer is not sufficient to mimic the enlarged valve phenotype obtained with the *Tie2-Cre* driver, at least until E16.5. Possibly, the level of *sHBEGF* expression achieved using the valve endocardial-specific driver line is insufficient to affect mesenchyme proliferation. Alternatively, the release of sHBEGF from the endocardium and diffusion into the ECM may delay its effects on mesenchyme cell proliferation.

Therefore, any morphological changes would only be detected at later developmental timepoints.

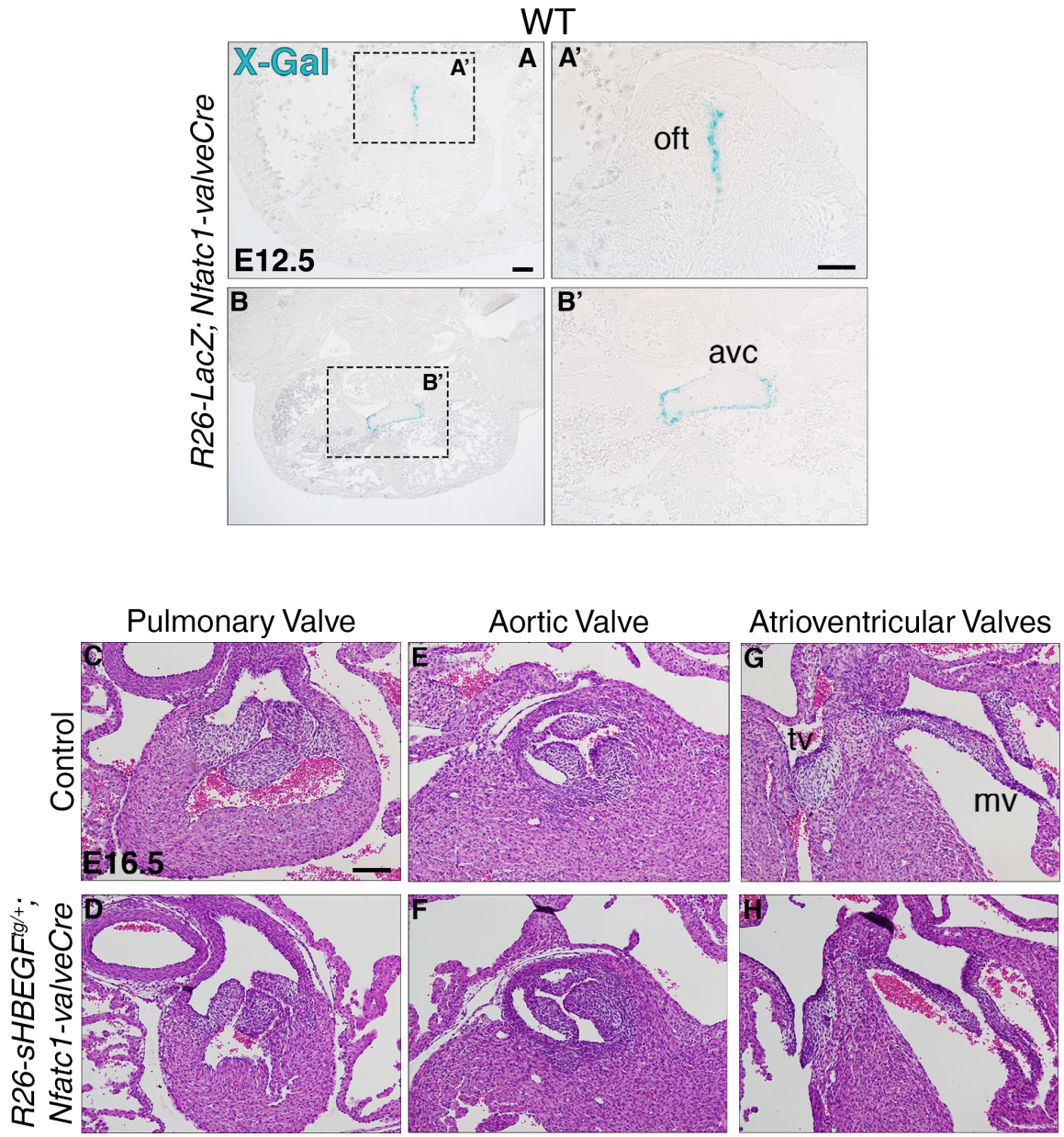

Figure 25. *sHBEGF* overexpression in valve endocardium does not affect cardiac valve development. X-gal stained sections of E12.5 *R26-LacZ; Nfatc1-valveCre* OFT (**A, A'**) and AVC (**B, B'**), showing expression restricted to the valve endocardium. H&E staining of control and *R26-sHBEGF$^{tg/+}$; Nfatc1-Valve-Cre* valve sections at E14.5, revealing normal morphology (**C-H**). Scale bar: 100µm. oft, outflow tract; avc, atrioventricular canal; pv, pulmonary valve; aov, aortic valve; tv, tricuspid valve; tv, mitral valve.

DISCUSSION

Abundant evidence implicates abnormal valve formation as an underlying cause of valve pathogenesis. Cardiac valve defects account for about a third of all congenital cardiovascular malformations (Pierpont et al., 2007). In adults, valve disease remains a major source of chronic illness and mortality (Brickner et al., 2000; Rostagno, 2019). A wide range of genetic studies using mouse models, as well as *ex vivo* studies on explanted endocardial cushions, have identified key pathways and essential players during valve development. However, despite decades of research, the precise mechanisms underlying valve morphogenesis and remodeling remain elusive. Here, we study the chemokine receptor CXCR4, the growth factor HBEGF and their respective pathways, in an effort to shed light into their function in the control of mesenchymal cell proliferation during cardiac valve remodeling.

Insights from previous *Cxcl12*, *Cxcr4* and *Cxcr7* knockout models

In this study, we show that endocardial expression of *Cxcr4* is required for limiting the proliferation of mesenchymal cells during valve morphogenesis. Loss of *Cxcr4* in endocardial/endothelial lineages led to obvious SL and AV valve enlargement at E16.5, often accompanied by BAV. This phenotype was related to increased mesenchymal cell proliferation at E14.5, supporting a critical role for CXCR4 in the reduction of proliferation that occurs during valve remodeling. Consistent with these findings, treatment of WT OFT explants with the CXCR4 inhibitor AMD3100 led to increased mesenchymal cell proliferation. The endocardial *Cxcr4* mutant developmental defects persisted post-natally and resulted in cardiac hypertrophy, fibrosis and chondrogenic metaplasia at P30. The valve enlargement phenotype observed in endocardial *Cxcr4* mutants is likely due to the excessive mesenchymal proliferation detected at E14.5. Given the severe abnormalities observed in juvenile mutant mice, we speculate that morphological changes brought about by upregulated or uncontrolled proliferation continue well beyond E14.5. Part of the ventricular defects could be due to adaptive processes taking place in late fetal and early post-natal development.

While *Cxcr4* is expressed as early as E11.5 in the AVC and the OFT (Ivins et al., 2015), H&E examination did not reveal any discernible morphologic changes in loss-of-function mutant mice up until E14.5-15.5. This suggests that loss of *Cxcr4* does not affect EMT in the AVC and OFT, given that endocardial cushion formation and cellularization occur normally. These results suggest an important role for CXCR4 in the post-EMT remodeling phase of valvulogenesis.

Previous studies have demonstrated that genetic alterations of the CXCL12-CXCR4/CXCR7 signaling axis affect valve morphogenesis. To facilitate comparison, a summary of the defects reported in the different knockout models of *Cxcr4*, *Cxcl12* and *Cxcr7* can be found in Table 6.

Genotype	SLV thickening	AVV thickening	BAV	Other phenotypes	Reference
Previous studies					
Cxcl12-/-				perinatal lethality hematopoiesis defects myelopoiesis defects VSD	Nagasawa et al., 1996
Cxcr4-/-				*in utero* or perinatal lethality hematopoiesis defects myelopoiesis defects abnormal neuron migration	Ma et al., 1998
Cxcr4-/-				defective fetal cerebellar development hematopoiesis defects myelopoiesis defects VSD	Zou et al., 1998
Cxcr7-/-	yes		yes	perinatal lethality reduction in B cell population dilatation of the RV overriding aorta bicuspid pulmonary valve VSD AoV chondrification and calcification (in adult mice)	Sierro et al., 2007
Cxcr7-/-, Tie2-Cre	yes		yes		Sierro et al., 2007
Cxcr7-/-	yes			*in utero* or perinatal lethality overriding aorta VSD	Yu et al., 2011
Cxcr7-/-, Tie2-Cre	yes			cardiac hypertrophy (in adult mice)	Yu et al., 2011
Cxcl12-/-	yes			defective coronary artery development	Ivins et al., 2015
Cxcr4-/-	yes			defective coronary artery development	Ivins et al., 2015
Cxcr4flox/-; Tie2-Cre	yes			defective coronary artery development	Ivins et al., 2015
Our findings					
Cxcr4flox; Nfatc1-Cre	yes	yes	yes	chondrification (in juvenile mice)	
				VSD (in juvenile mice)	
				cardiac hypertrophy (in juvenile mice)	
Cxcr4flox; Tie2-Cre	yes	yes	yes		

Table 6. Summary of the major valvuloseptal phenotypes in *Cxcl12*, *Cxcr4* and *Cxcr7* standard and conditional knockout mouse models. SLV, semilunar valves; AVV, atrioventricular valves; BAV, bicuspid aortic valve; VSD, ventricular septal defects.

Both *Cxcr4*- and *Cxcl12*-null mice die *in utero* or perinatally, and present hematopoietic and nervous system defects, as well as VSD (Table 6) (Nagasawa et al., 1996; Zou et al., 1998). More recently, Ivins et al. further assessed the role of CXCL12 and CXCR4 in cardiac development.

Examination of *Cxcl12*- and *Cxcr4*-null hearts late in development revealed a complete absence of intra-ventricular coronary arteries and abnormalities in the number and position of coronary ostia (Table 6) (Ivins et al., 2015). In contrast, the coronary arteries appeared to develop normally in our *Cxcr4*^{flox}; *Nfatc1-Cre* mice, given the normal location and caliber of the vessels, visible in the histological sections of the ventricles.

Moreover, the *Cxcl12*- and *Cxcr4*-null mutants described by Ivins et al. displayed enlarged SL leaflets (Table 6) (Ivins et al 2015). Deletion of *Cxcr4* in the endothelial lineage by crossing a floxed *Cxcr4* allele (Nie et al., 2004) with the *Tie2-Cre* driver recapitulated the phenotype found in *Cxcl12*- and *Cxcr4*-null embryos (Table 6) (Ivins et al., 2015). Given that we used both *Tie2-Cre* and *Nfatc1-Cre* driver lines to delete *Cxcr4*, our results are consistent with the finding of abnormally enlarged SL valves in the *Cxcr4* mutants. However, Ivins et al. did not describe the effect of endothelial *Cxcr4* deletion on the AV valves, but rather focused on the extensive coronary artery defects. In contrast, we extended our examination of *Cxcr4*^{flox}*; Nfatc1-Cre* and *Cxcr4*^{flox}*; Tie2-Cre* mutant embryos to the AV valves and found a hyperplastic phenotype similar, albeit less prominent, to the one seen in the SL valves. One possible explanation for this discrepancy is that development of the endocardial cushions of the OFT involves multiple cellular sources, including the NCCs, which migrate from the hindbrain and invade the distal components of the cushions. In contrast, the mesenchyme of AV valve primordia derives from the endocardium and from a small contribution of epicardial cells (Snarr et al., 2008). CXCL12-CXCR4 signaling may play a role in NCC migration, which would make the SL valves more sensitive to variations in dosage in the endocardium/endothelium than AV valves. In fact, disruption of several genes involved in valve development seem to affect the SL valves more than the AV valves, as is the case for *Cxcr7*-null mice (Table 1) (Sierro et al., 2007; Yu et al., 2011)

CXCR7 is an alternate chemokine receptor for CXCL12. CXCR7 regulates CXCL12-CXCR4 signaling by forming heterodimers with CXCR4 and positively modulating its binding to CXCL12 (Hartmann et al., 2008; Kalatskaya et al., 2009a; Levoye et al., 2009; Sierro et al., 2007). In the heart, expression of both receptors significantly overlaps in the valve region and the microvasculature (Sierro et al., 2007; Yu et al., 2011). Ubiquitous knockout of *Cxcr7* leads to perinatal lethality, often accompanied by thickened SL valves, overriding aortas and VSD (Table 6) (Sierro et al., 2007; Yu et al., 2011). Similar to the ectopic cartilage we observed in P30 *Cxcr4*^{flox}*; Nfatc1-Cre* animals, adult *Cxcr7*-null survivors show evidence of chondrogenesis (Table 6) (Sierro et al., 2007). Furthermore, SL valve enlargement was associated with increased valve mesenchymal cell proliferation and enhanced BMP signaling at E14.5-E15.5 (Sierro et al., 2007; Yu et al., 2011).

Given that it has not been reported for other *Cxcr4*, *Cxcr7* or *Cxcl12* knockout mice, AV valve enlargement appears to be an exclusive phenotype of endocardial/endothelial *Cxcr4* loss-of-function mutants. Nonetheless, the similarities between *Cxcr4* and *Cxcr7* mutants suggest that both receptors play non-redundant roles during valve remodeling. Whether receptor heterodimerization is a relevant aspect of the regulation of CXCR4/CXCR7 function during valvulogenesis remains to be investigated.

BMP-Smad1/5/8 is not a CXCR4 effector pathway

Activation of BMP signaling is known to promote proliferation of valve mesenchymal cells (Combs & Yutzey, 2009). Expression and functional studies in the developing heart, have implicated Bmp2 and Bmp4 in endocardial cushion development (Abdelwahid et al., 2001; Délot et al., 2003; Liu et al., 2004; L. Ma et al., 2005; Yamagishi et al., 1999), and Bmp6 and Bmp7 in OFT cushion formation and septation (Kim et al., 2001). Loss of *Bmp4* using a SHF-specific driver results in severe defects in OFT septation and impaired cushion formation and expansion (McCulley et al., 2008). Conversely, deletion of *Smad6*, the BMP inhibitory Smad, results in AVC and OFT valve hyperplasia (Table 1) (Galvin et al., 2000). EGFR is thought to exert a tight negative control of BMP signaling, via differential phosphorylation of Smad1/5/8, the intracellular mediator of Bmp2/4/6/10 signals to the nucleus (Kretzschmar et al., 1997; Lo et al., 2001).

Cardiac valve enlargement due to increased proliferation has often been associated with enhanced BMP signaling, as measured by upregulated pSmad1/5/8 in multiple models of valve hyperplasia (Iwamoto et al., 2003; Jackson et al., 2003; MacGrogan et al., 2016; Tadano et al., 2005; Yu et al., 2011). Furthermore, BMPs play important roles in endochondral bone formation (Kugimiya et al., 2005). Bmp2, 4, 6, 7 and 9 are commonly referred to as the osteogenic BMPs, based on their potent bone-inducing activity (Luu et al., 2007). Accordingly, cartilaginous metaplasia was observed in the OFT of *Smad6*-null juvenile mice (Galvin et al., 2000), and expression of Bmp2/4 was detected in ossified areas in the cardiac valves of patients undergoing valve replacement (Mohler et al., 2001). However, despite the ectopic chondrogenesis detected in the aortic valve of P30 *Cxcr4^{flox}; Nfatc1-Cre* mice, immunofluorescent analysis of Smad1/5/8 phosphorylation with an antibody specific for the C-terminus phosphorylated form did not reveal any change that might implicate dysregulated BMP signaling in these mutants. This suggests that the control of valve mesenchymal cell proliferation by endocardial CXCR4 is independent of BMP/Smad activity.

Nuanced effects of AMD3100 on CXCR4 and CXCR7

To investigate CXCR4-mediated regulation of mesenchymal cell proliferation, we employed AMD3100 to inhibit CXCR4 in the OFT explant system. This molecule is a highly specific antagonist of CXCL12 binding to CXCR4, resulting in downstream signaling inhibition (Fricker et al., 2006; Gerlach et al., 2001). However, AMD3100 has also been shown to positively modulate CXCR7, acting both as a ligand and an allosteric agonist (Kalatskaya et al., 2009b). The presence of an allosteric modulator may increase or decrease binding of the orthosteric ligand. Kalatskaya et al. found that, in contrast to its antagonist effect on CXCR4, AMD3100 increases CXCL12 binding to CXCR7 by a positive allosteric mechanism. Moreover, AMD3100 alone can recruit β-arrestin to CXCR7, albeit at relatively high concentrations (≥10μM), identifying it as a ligand for this receptor (Kalatskaya et al., 2009b). Furthermore, the binding site of AMD3100 on CXCR4 might be different from that of CXCL12, because mutations that substantially change AMD3100 binding have little effect on CXCL12 binding (Gerlach et al., 2001). Thus, the mechanism by which AMD3100 interferes with CXCL12-CXCR4 binding and CXCR4 activity could be more complex than originally thought, given that AMD3100 might act as an allosteric inhibitor of CXCR4 rather than as an antagonist.

Regardless of the precise mechanism, treatment of OFT explants with increasing doses of AMD3100 resulted in an overall significant increase of mesenchymal cell proliferation that was consistent with our *in vivo* deletion of endocardial/endothelial *Cxcr4*. Nonetheless, it is possible that AMD3100 impact on proliferation occurs via a combination of negative modulation of CXCR4 in parallel with positive modulation of CXCR7. Additional experiments using OFTs from *Cxcr4*^{flox}; *Nfatc1-Cre* mice and their control littermates, or supplementing WT OFTs with a CXCR7-specfic inhibitor might clarify this point.

Insights from *Hbegf* knockout models

In this study, we show that *in vivo sHBEGF* overexpression under the control of the *Tie2-Cre* driver leads to severe SL and AV valve hyperplasia as early as E12.5. The increased proliferation of valve mesenchymal cells persisted at least until E14.5 and were aggravated in P30 animals, which displayed cartilaginous metaplasia and septal defects, consistent with ongoing endochondral ossification. Moreover, the defects extended to the ventricular chambers, which displayed increased myocardial wall thickness, suggestive of a hypertrophic adaptive process due to reduced valve function. We saw a similar effect using the explant assay, where mesenchymal cells derived from OFTs from endothelial *sHBEGF* transgenic embryos proliferated more compared to the ones derived from their WT counterparts. Similarly, explanted WT OFTs supplemented with mouse recombinant soluble HBEGF presented increased mesenchymal cell proliferation compared to controls, while pan-pharmacological inhibition of the ErbB family of receptors decreased it.

The hyperplastic valve defects seen in our *R26-sHBEGF$^{tg/+}$; Tie2-Cre* transgenic mice suggest that sHBEGF does not regulate earlier stages of valvulogenesis, given that cushion formation and EMT-led cellularization occur normally. Instead, the valve phenotype in our *sHBEGF* gain-of-function mice was likely caused by excessive proliferation and/or failure to arrest cell proliferation, prior to differentiation into valve interstitial cells. We speculate that the hyperproliferation continues beyond E14.5, taking in account that the valves of young adults appear to be even larger and un-remodeled.

Several lines of evidence have demonstrated the essential function carried out by HBEGF during valve remodeling. Different strategies have been employed by independent groups to manipulate HBEGF function *in vivo* (Iwamoto et al., 2003; Jackson et al., 2003; Nanba et al., 2006; Yamazaki et al., 2003). Thus, to globally inactivate *Hbegf*, Jackson et al. replaced exons 1 and 2 with PGK-Neo, whereas Iwamoto et al. removed exon 1, with both strategies resulting in *Hbegf*-null mice with grossly enlarged SL and AV valves. Moreover, conditional deletion of *Hbegf* under the control of *Tie2-Cre* also results in SL and AV valve enlargement, indicating that endothelial/endocardial HBEGF is essential for proper cardiac valve development (Nanba et al., 2006).

To determine whether ectodomain shedding was required for HBEGF function, Yamazaki et al. replaced the WT *Hbegf* gene with an uncleavable version of the protein, bearing mutations in the juxtamembrane domain. Mice expressing uncleavable *Hbegf* developed enlarged SL and AV valves, confirming that ectodomain shedding is necessary for HBEGF function *in vivo* (Yamazaki et al., 2003). Interestingly, the same group also generated a

mouse model that expresses solely the soluble form of HBEGF (Yamazaki et al., 2003), similar to our *R26-sHBEGF* gain-of-function line. Mice overexpressing *sHBEGF* displayed severe epidermal hyperplasia but the heart defects were sparsely described (Yamazaki et al., 2003). While Yamazaki et al. reported that these mice presented ventricular hypertrophy, the effects on valve development, if any, were not mentioned.

Our results are unexpectedly at odds with the current accepted model behind HBEGF regulation of valve remodeling, which proposes that sHBEGF negatively regulates mesenchymal proliferation (Iwamoto et al., 2010). It states that endocardial sHBEGF is released via ectodomain shedding and diffuses into the cardiac jelly, where it binds to the EGFR expressed on the surface of mesenchymal cells (Iwamoto et al., 2010). However, our *in vivo* and *ex vivo* data indicate that sHBEGF has a mitogenic effect on valve mesenchymal cells, raising the question of how is the signal transduced.

Parallels between *sHBEGF* overexpression and *Shp2* overactivation models

GTP-binding proteins such as Ras play critical roles in many signaling pathways. Activation of Ras usually occurs via ligand binding and consequent activation of receptor tyrosine kinases (RTKs) of the ErbB family. Ras signaling ultimately activates the MAP kinase cascade, which affects a wide variety of cellular outcomes such as cell growth, proliferation, and migration (Yutzey et al., 2005).

In humans, mutations in several genes impacting the Ras/MAP kinase pathway, such as *PTPN11*, which encodes the protein tyrosine phosphatase SHP2, cause Noonan syndrome (Araki et al., 2009; Krenz et al., 2005). This syndrome is associated with several congenital defects, including cardiac abnormalities in tissues derived from AVC and OFT endocardial cushions, such as pulmonary valve stenosis (Fragale et al., 2004). During normal valve morphogenesis, activation of SHP2 triggers Ras, with concomitant stimulation of MAP kinase signaling through ERK1/2 (Araki et al., 2004). Mice that express a mutant version of *Shp2* with increased phosphatase activity, under the control of *Tie2-Cre*, display hyperproliferation of endothelial and mesenchymal cells in AVC and OFT valve primordia, associated with increased Erk1/2 activation (Krenz et al., 2008).

The similarities between the phenotypes caused by Shp2 hyperactivity and HBEGF overexpression could mean that HBEGF binding to RTK(s) is upstream of Shp2/MAP kinase signaling during valve remodeling. Hence, the upstream regulators of Shp2 signaling in heart valvulogenesis are likely

sHBEGF acting through one or more ErbBs. This signaling pathway would thus couple sHBEGF stimulation to gene transcription and mitogenesis. Additional experiments concerning the role of Erk1/2 activation should be performed in our *sHBEGF* gain-of-function model.

The complex relationship between HBEGF and the ErbB family of receptors

The ErbB family of receptor tyrosine kinases represents a complex and robust signaling system that mediates a wide range of cellular behaviours and outcomes. The repertoire of ErbB ligands is extensive and ligands often bind multiple receptors, with different degrees of preference. Furthermore, the receptors themselves form an array of homo- and heterodimers in various combinations (Graus-Porta et al., 1997; Riese and Stern, 1998; Yarden, 2001). Depending on the composition of the dimer, different downstream signaling cascades are activated (Olayioye et al., 2000).

EGFR deletion leads to several defects and gestational or perinatal death, depending on genetic background (Miettinen et al., 1995; Sibilia et al., 2003; Sibilia & Wagner, 1995; Threadgill et al., 1995). Surviving *EGFR* mutant mice have been reported by independent studies to display SL valve enlargement only (Chen et al., 2000) or thickening of both SL and AV valves (Jackson et al., 2003). Mice deficient for ErbB2 and ErbB4 die at around E10.5, due to defects in myocardial trabeculation and the peripheral nervous system (Gassmann et al., 1995; K. F. Lee et al., 1995). *Erbb3*-null mice present normal trabeculae but defective valve cushion formation, and survive only until about E13.5 (Erickson et al., 1997). Taken together, these studies suggest that ErbB2 and ErbB4 are required for cardiac trabeculation, while EGFR and ErbB3 play a role in valvulogenesis. Further strengthening this point, embryonic lethality in *ErbB2* and *ErbB4* knockouts can be circumvented by expressing these receptors under the control of cardiac-specific promoters (Morris et al., 1999; Tidcombe et al., 2003).

Whether EGFR is the only physiologic transducer of HBEGF in valve mesenchyme during development remains to be determined. EGFR is thought to be the receptor for sHBEGF during valve remodeling, because both *Egfr* and *Hbegf* mutant mice develop cardiac valve enlargement. However, HBEGF may bind additional receptors in the context of valvulogenesis. Activation of different ErbB receptor dimers, with different downstream cascades, could explain how the same ligand could transduce opposing signals. Rescue of lethality by myocardial expression strongly suggests that ErbB2 and ErbB4 function is essential for heart development, but restricted to the myocardium

(Morris et al., 1999; Tidcombe et al., 2003). Moreover, they are expressed in the myocardium but absent or in low levels in the valve region (Gassmann et al., 1995; Jackson et al., 2003; K. F. Lee et al., 1995). ErbB3, on the other hand, is an attractive candidate receptor for heterodimer formation, given its expression in the valve mesenchyme during development (Jackson et al., 2003; Meyer & Birchmeier, 1995). Furthermore, *ErbB3* loss-of-function mutants fail to develop valve primordia, displaying undeveloped and hypoplastic endocardial cushions at their time of death around E13.5 (Erickson et al., 1997), which directly implicates this receptor in valve morphogenesis.

Insights from the perturbation of the HBEGF-ErbB signaling axis *ex vivo*

The pro-proliferative effect of HBEGF on mesenchymal cells observed in our *in vivo* study was further corroborated by OFT explant data. *Ex vivo* experiments on endocardial cushion tissue were originally designed to study the EMT process taking place in the AVC during formation of the AV valves (Camenisch et al., 2002). A modified version of this experiment has been used to examine the proliferation of mesenchymal cells derived in OFT explants post-EMT (Iwamoto et al., 2010, 2017; MacGrogan et al., 2016).

Using this system, Iwamoto et al. reported that mesenchymal cells derived from *Hbegf*-null cushions had a significantly greater proliferative capacity than those from WT controls (Iwamoto et al., 2010). Supplementing WT explants with ZD1839, an inhibitor for EGFR, also led to the increased proliferation of mesenchymal cells (Iwamoto et al., 2010). A second, independent study showed that supplementing WT OFT explants with 10ng/ml HBEGF resulted in mesenchymal cell proliferation upregulation, while addition of the EGFR inhibitor CP380736 decreased it (MacGrogan et al., 2016). More recently, Iwamoto et al. found that ZD1839 not only increased WT mesenchymal cell proliferation, but also decreased the hyperproliferation of *Hbegf*-null cells (Iwamoto et al., 2017). Furthermore, they reported that the *ErbB4*-null mutant mouse valves rescued from embryonic lethality through reintroduction of human ErbB4 in cardiomyocytes (described in Tidcombe et al., 2003) were actually enlarged, albeit less so than *Hbegf*-null mice (Iwamoto et al., 2017). They proposed a model whereby HBEGF activation of an EGFR-ErbB4 heterodimer results in decreased mesenchymal cell proliferation, whereas an EGFR homodimer activation by other EGFR-binding ligand(s) results in the opposite effect (Iwamoto et al., 2017).

In striking contrast, our data show that mesenchymal cells derived from explanted OFTs of *R26-sHBEGF$^{tg/+}$; Tie2-Cre* transgenics proliferated significantly more than those derived from control littermates. Likewise, supplementing WT explants with increasing concentrations of recombinant sHBEGF resulted in greatly increased mesenchymal cell proliferation, even at the lowest supplemented concentration of 0.5ng/ml. In addition, adding the pan-ErbB receptor inhibitor, PD158780, decreased mesenchymal cell proliferation.

Overall, our data challenge previous reports (Iwamoto et al., 2010, 2017; MacGrogan et al., 2016) and indicate sHBEGF has a pro-proliferative effect on mesenchymal proliferation, while ErbB receptor inhibition has the opposite effect. Furthermore, our data suggest that, in addition to EGFR, at least another ErbB receptor is involved in regulating mesenchymal cell proliferation.

Limitations of the *sHBEGF* gain-of-function model

During cardiac valve development, the expression pattern of HBEGF is restricted to the endocardium (Iwamoto et al., 2003; MacGrogan et al., 2016). The use of the *Tie2-Cre* driver line with our *sHBEGF* overexpressing mice suggests that the *sHBEGF* transgene is overexpressed not only in endocardial cells, but also in the mesenchymal derivatives resulting from EMT in the AVC and OFT. Therefore, we think that the excessive mesenchymal growth in both SL and AV valves is likely due to abnormally high levels of the soluble ligand expressed and secreted by mesenchymal cells, rather than to limited diffusion from the endocardium.

Furthermore, ectopic overexpression of *sHBEGF* in the valve mesenchyme could lead to non-physiological binding of the ligand to alternate receptors in these cells. One possibility is that the increased availability of sHBEGF could induce the activation and/or dimerization of ErbB receptors that usually do not signal in valve mesenchymal cells during the remodeling phase of valvulogenesis. This non-physiological binding could perhaps account for the extreme hyperplastic phenotype we observed in mesenchymal cells both *in vivo*. To obtain an endocardial *sHBEGF* gain-of-function model better resembling the physiological situation, we employed the *Nfatc1-valveCre* driver line, whose Cre expression is restricted to a valve endocardial cell sub-population that does not undergo EMT (Wu et al., 2011). However, examination of *R26-sHBEGF$^{tg/+}$; Nfatc1-valveCre* embryos did not reveal any changes in the endocardial cushions or valves at E16.5, while *R26-sHBEGF$^{tg/+}$; Tie-Cre* valves are hyperplastic as early as E12.5. We attribute

this lack of effect to the comparatively low number of cells expressing *sHBEGF* in *Nfatc1-valveCre* mutants. Hence, the level of *sHBEGF* expressed by endocardium in *Nfatc1-valveCre* mutants may be well below that required to stimulate mesenchymal cell proliferation and observe morphological defects at E16.5. Work in progress is seeking to determine whether the hyperplastic phenotype expected in *R26-sHBEGF$^{tg/+}$; Nfatc1-valveCre* valves might become obvious at later developmental time-points, post-natally and/or in adults.

Final considerations

Our interest in the roles of CXCR4 and HBEGF in valve development stemmed from the findings that they displayed similar valve phenotypes upon genetic deletion, and that both pathways are altered in *Jag1^{flox}; Nkx2.5-Cre* mutant valves (MacGrogan et al., 2016). *Cxcr4* endothelial/endocardial mutants, *Hbegf*-null and endothelial *Hbegf* mutants all display overgrown valve mesenchyme similar to endothelial/endocardial *Jag1* mutants, suggesting they might function in the same biochemical/developmental pathway with Notch. Our hypothesis put forward CXCR4 as one of the GPCRs upstream of EGFR transactivation during valve remodeling. The proposed mechanism was that CXCR4 would activate ADAM metalloproteases in the endocardium, resulting in ectodomain shedding of proHBEGF and release sHBEGF into the valve mesenchyme. There, sHBEGF would bind and activate EGFR, triggering the inhibition of proliferation, possibly by antagonizing the BMP/Smad1/5/8 pathway.

Ultimately, the hypothesis put forward and forming the basis of this thesis could not be tested. The primary purpose of generating the *sHBEGF* gain-of-function transgenic was to rescue the phenotype of *Cxcr4* loss-of-function mice by crossbreeding *Cxcr4^{flox}; Nfatc1-Cre* mutant animals with *sHBEGF$^{tg/+}$; Tie2-Cre* transgenics. Thus, we failed to establish a functional connection between CXCR4 and HBEGF and it remains unclear whether or how CXCR4 might regulate sHBEGF release.

Nevertheless, we demonstrated that endocardial *Cxcr4* expression is required in a non-cell autonomous manner in order to regulate valve mesenchyme proliferation, likely via a diffusible factor (Figure 26). Moreover, 40% of endocardial CXCR4 mutants display a BAV phenotype, suggesting that CXCR4 regulates the number of valve endocardial cushions and/or valve cusp fusion events taking place once the endocardial cushions are formed. How CXCR4 regulates these processes remains to be elucidated. CXCR4 might function alone and/or heterodimerize with CXCR7 during these

processes, adding another layer of complexity, as the downstream effectors of CXCR4 in the endocardium might differ in the presence or absence of CXCR7. Detailed biochemical experiments will be required to answer these questions.

Our results also support the notion that strict regulation of sHBEGF shedding is necessary for correct valve formation (Figure 26). It has been firmly established that endothelial loss of *Hbegf* and expression of uncleavable *Hbegf* results in valve hyperplasia. Here, we show for the first time that intense sHBEGF availability results in upregulated mesenchymal proliferation and enlarged valves *in vivo*. Our findings, together with previous functional studies, strongly suggest that both decreased and increased signaling through sHBEGF can promote mesenchymal cell proliferation (Figure 26) and can result in lack of valve remodeling *in vivo*. Further study of ErbB receptor(s) activation by sHBEGF and its downstream effectors will be necessary to clarify the physiological outcomes of this pathway during valvulogenesis.

Cardiac valve hyperplasia has been observed in a wide range of mouse knock-out and knock-in models. In this study, we have focused on the CXCR4/CXCL12 and the HBEGF/EGFR axis, as there is extensive evidence that these pathways carry out essential functions during valve remodeling. Nonetheless, disturbances in many other pathways and processes lead to valve enlargement, such as the Notch pathway (Fischer et al., 2007; MacGrogan et al., 2016), Wnt pathway (Hulin et al., 2017), Slit-Robo pathway (Gould et al., 2019; Mommersteeg et al., 2015), O-glycosylation (Tian et al., 2015), among others (Table 1). The extensive network of signals regulating valvulogenesis gives a glimpse into the complexity of this process. To unravel the molecular mechanisms governing cell proliferation during cardiac valve development, it will be necessary to understand how these signaling pathways are integrated *in vivo*.

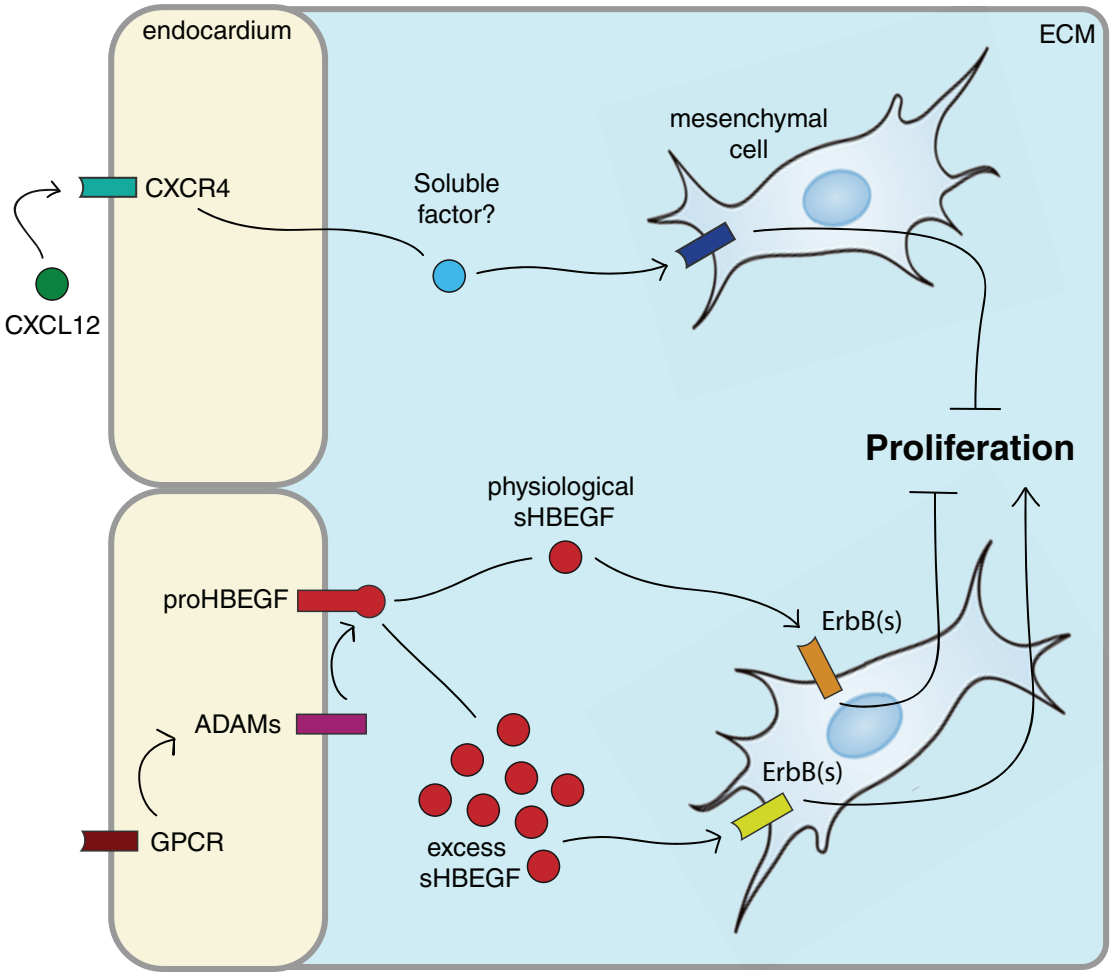

Figure 26. Proposed model for the regulation of valve mesenchymal cell proliferation by endocardial CXCR4 and sHBEGF. CXCR4 is a receptor expressed on endocardial cells. Upon binding of its ligand, the chemokine CXCL12, it activates a signaling cascade that likely culminates in the release of a diffusible factor. This molecule then diffuses into the valve mesenchyme, where it binds an unknown receptor on the surface of mesenchymal cells, triggering the inhibition of proliferation. HBEGF is first produced in the endocardium as proHBEGF, a membrane-bound protein that requires ectodomain shedding by ADAM metalloproteases (activated by GPCR(s)) in order to release the soluble form of the growth factor, sHBEGF. In physiological conditions, sHBEGF diffuses into the nearby mesenchyme, where it binds EGFR (and possibly other ErbBs such as ErbB3) on the surface of mesenchymal cells. This triggers a signaling cascade that ultimately results in the inhibition of mesenchymal cell proliferation. When there is overexpression of *sHBEGF*, it is possible that the increased availability of sHBEGF induces the activation and/or dimerization of ErbB receptors that usually do not signal in mesenchymal cells in the physiological context, leading to uncontrolled proliferation. GPCR, G-protein coupled receptor; ECM, extracellular matrix.

CONCLUSIONES/CONCLUSIONS

1. La deleción *in vivo* del gen endocardial/endothelial *Cxcr4* provoca el engrandecimiento de las válvulas cardiacas, la ocurrencia frecuente de válvulas aorticas bicúspides y el aumento de la proliferación de las células mesenquimales a E14.5.

2. La inhibición de CXCR4 resulta en un aumento en la proliferación de las células mesenquimales en el sistema *ex vivo* de explantes de tracto de salida del corazón.

3. La señalización de CXCR4 es indispensable para el control de la proliferación de las células mesenquimales durante la fase de remodelado de las válvulas cardíacas.

4. La sobreexpresión *in vivo* del HBEGF soluble (sHBEGF) en células endocardiales/endoteliales y sus derivados resulta en el engrosamiento de las válvulas cardiacas, con un aumento asociado en la proliferación de las células mesenquimales valvulares a E12.5 y E14.5

5. Las células mesenquimales derivadas de explantes de embriones transgénicos *sHBEGF* proliferan más que las que provienen de explantes control, y la adición de sHBEGF a explantes control también resulta en un aumento en la proliferación de las células mesenquimales *ex vivo.*

6. La inhibición farmacológica de los receptores ErbB reduce la proliferación de las células mesenquimales en el sistema *ex vivo* de explantes de tracto de salida del corazón.

7. El sHBEGF y la via ErbB son esenciales para el control de la proliferación de las células mesenquimales durante la fase de remodelado de las válvulas cardíacas.

1. *In vivo* deletion of *Cxcr4* from the endocardium/endothelium causes enlargement of the cardiac valves, frequent BAV and increased mesenchymal cell proliferation at E14.5.

2. Pharmacological inhibition of CXCR4 leads to increased mesenchymal cell proliferation in *ex vivo* OFT explants.

3. CXCR4 signaling is required for the regulation of mesenchymal cell proliferation during cardiac valve remodeling.

4. *In vivo* overexpression of soluble *HBEGF* (*sHBEGF*) in endothelial/endocardial cells and mesenchymal derivatives results in grossly enlarged cardiac valves and increased mesenchymal cell proliferation at E12.5 and E14.5.

5. Mesenchymal cells derived from *sHBEGF* transgenic OFT explants proliferate more than cells derived from WT controls, and addition of recombinant sHBEGF to WT explants leads to increased mesenchymal cell proliferation *ex vivo.*

6. Pharmacological inhibition of the ErbB receptor family inhibits mesenchymal cell proliferation in *ex vivo* OFT explants.

7. sHBEGF and the ErbB pathway are required for the regulation of mesenchymal cell proliferation during cardiac valve remodeling.

BIBLIOGRAPHY

Abdelwahid, E., Rice, D., Pelliniemi, L. J., & Jokinen, E. (2001). Overlapping and differential localization of Bmp-2, Bmp-4, Msx-2 and apoptosis in the endocardial cushion and adjacent tissues of the developing mouse heart. *Cell and Tissue Research*. https://doi.org/10.1007/s004410100399

Abramovitch, R., Neeman, M., Reich, R., Stein, I., Keshet, E., Abraham, J., Solomon, A., & Marikovsky, M. (1998). Intercellular communication between vascular smooth muscle and endothelial cells mediated by heparin-binding epidermal growth factor-like growth factor and vascular endothelial growth factor. *FEBS Letters*. https://doi.org/10.1016/S0014-5793(98)00283-X

Abu-Issa, R., & Kirby, M. L. (2007). Heart field: From mesoderm to heart tube. In *Annual Review of Cell and Developmental Biology*. https://doi.org/10.1146/annurev.cellbio.23.090506.123331

Aikawa, E., Whittaker, P., Farber, M., Mendelson, K., Padera, R. F., Aikawa, M., & Schoen, F. J. (2006). Human semilunar cardiac valve remodeling by activated cells from fetus to adult: Implications for postnatal adaptation, pathology, and tissue engineering. *Circulation*. https://doi.org/10.1161/CIRCULATIONAHA.105.591768

Aleksandrova, A., Czirók, A., Szabó, A., Filla, M. B., Hossain, M. J., Whelan, P. F., Lansford, R., & Rongish, B. J. (2012). Convective tissue movements play a major role in avian endocardial morphogenesis. *Developmental Biology*. https://doi.org/10.1016/j.ydbio.2011.12.036

Allen, J. A., & Roth, B. L. (2011). Strategies to discover unexpected targets for drugs active at G protein-coupled receptors. *Annual Review of Pharmacology and Toxicology*. https://doi.org/10.1146/annurev-pharmtox-010510-100553

Araki, T., Chan, G., Newbigging, S., Morikawa, L., Bronson, R., & Neel, B. G. (2009). Noonan syndrome cardiac defects are caused by PTPN11 acting in endocardium to enhance endocardial-mesenchymal transformation. *Proceedings of the National Academy of Sciences of the United States of America*. https://doi.org/10.1073/pnas.0810053106

Araki, T., Mohi, M. G., Ismat, F. A., Bronson, R. T., Williams, I. R., Kutok, J. L., Yang, W., Pao, L. I., Gilliland, D. G., Epstein, J. A., & Neel, B. G. (2004). Mouse model of Noonan syndrome reveals cell type- and gene dosage-dependent effects of Ptpn11 mutation. *Nature Medicine*. https://doi.org/10.1038/nm1084

Armstrong, E. J., & Bischoff, J. (2004). Heart valve development: Endothelial cell signaling and differentiation. In *Circulation Research*. https://doi.org/10.1161/01.RES.0000141146.95728.da

Asakura, M., Kitakaze, M., Takashima, S., Liao, Y., Ishikura, F., Yoshinaka, T., Ohmoto, H., Node, K., Yoshino, K., Ishiguro, H., Asanuma, H., Sanada, S., Matsumura, Y., Takeda, H., Beppu, S., Tada, M., Hori, M., & Higashiyama, S. (2002). Cardiac hypertrophy is inhibited by antagonism of ADAM12 processing of HB-EGF: Metalloproteinase inhibitors as a new therapy. *Nature Medicine*. https://doi.org/10.1038/nm0102-35

Bachelerie, F., Graham, G. J., Locati, M., Mantovani, A., Murphy, P. M., Nibbs, R., Rot, A., Sozzani, S., & Thelen, M. (2015). An atypical addition to the chemokine receptor nomenclature: IUPHAR Review 15. In *British Journal of Pharmacology*. https://doi.org/10.1111/bph.13182

Baggiolini, M. (1998). Chemokines and leukocyte traffic. In *Nature*. https://doi.org/10.1038/33340

Belsches, A. P., Haskell, M. D., & Parsons, S. J. (1997). Role of c-Src tyrosine kinase in EGF-induced mitogenesis. In *Frontiers in bioscience : a journal and virtual library*. https://doi.org/10.2741/a208

Blanchet, X., Langer, M., Weber, C., Koenen, R., & von Hundelshausen, P. (2012).

Touch of chemokines. *Frontiers in Immunology*. https://doi.org/10.3389/fimmu.2012.00175
Bleul, C. C., Farzan, M., Choe, H., Parolin, C., Clark-Lewis, I., Sodroski, J., & Springer, T. A. (1996). The lymphocyte chemoattractant SDF-1 is a ligand for LESTR/fusin and blocks HIV-1 entry. *Nature*. https://doi.org/10.1038/382829a0
Blobel, C. P. (2005). ADAMs: Key components in egfr signalling and development. In *Nature Reviews Molecular Cell Biology*. https://doi.org/10.1038/nrm1548
Blotnick, S., Peoples, G. E., Freeman, M. R., Eberlein, T. J., & Klagsbrun, M. (1994). T lymphocytes synthesize and export heparin-binding epidermal growth factor-like growth factor and basic fibroblast growth factor, mitogens for vascular cells and fibroblasts: Differential production and release by CD4+ and CD8+ T cells. *Proceedings of the National Academy of Sciences of the United States of America*. https://doi.org/10.1073/pnas.91.8.2890
Boldajipour, B., Mahabaleshwar, H., Kardash, E., Reichman-Fried, M., Blaser, H., Minina, S., Wilson, D., Xu, Q., & Raz, E. (2008). Control of Chemokine-Guided Cell Migration by Ligand Sequestration. *Cell*. https://doi.org/10.1016/j.cell.2007.12.034
Bonachea, E. M., Chang, S. W., Zender, G., Lahaye, S., Fitzgerald-Butt, S., Mcbride, K. L., & Garg, V. (2014). Rare GATA5 sequence variants identified in individuals with bicuspid aortic valve. *Pediatric Research*. https://doi.org/10.1038/pr.2014.67
Bondue, A., & Blanpain, C. (2010). Mesp1: A key regulator of cardiovascular lineage commitment. In *Circulation Research*. https://doi.org/10.1161/CIRCRESAHA.110.227058
Brickner, M. E., Hillis, L. D., & Lange, R. A. (2000). Congenital heart disease in adults: First of two parts. In *New England Journal of Medicine*. https://doi.org/10.1056/NEJM200001273420407
Brown, C. B., Feiner, L., Lu, M. M., Li, J., Ma, X., Webber, A. L., Jia, L., Raper, J. A., & Epstein, J. A. (2001). PlexinA2 and semaphorin signaling during cardiac neural crest development. *Development*.
Buckingham, M., Meilhac, S., & Zaffran, S. (2005). Building the mammalian heart from two sources of myocardial cells. In *Nature Reviews Genetics*. https://doi.org/10.1038/nrg1710
Butcher, J. T., & Markwald, R. R. (2007). Valvulogenesis: The moving target. In *Philosophical Transactions of the Royal Society B: Biological Sciences*. https://doi.org/10.1098/rstb.2007.2130
Cai, C. L., Liang, X., Shi, Y., Chu, P. H., Pfaff, S. L., Chen, J., & Evans, S. (2003). Isl1 identifies a cardiac progenitor population that proliferates prior to differentiation and contributes a majority of cells to the heart. *Developmental Cell*. https://doi.org/10.1016/S1534-5807(03)00363-0
Camenisch, T. D., Molin, D. G. M., Person, A., Runyan, R. B., Gittenberger-de Groot, A. C., McDonald, J. A., & Klewer, S. E. (2002). Temporal and distinct TGFβ ligand requirements during mouse and avian endocardial cushion morphogenesis. *Developmental Biology*. https://doi.org/10.1006/dbio.2002.0731
Camenisch, T. D., Runyan, R. B., & Markwald, R. R. (2010). Molecular Regulation of Cushion Morphogenesis. In *Heart Development and Regeneration: Vol. I*. Elsevier Inc. https://doi.org/10.1016/B978-0-12-381332-9.00018-9
Camenisch, T. D., Spicer, A. P., Brehm-Gibson, T., Biesterfeldt, J., Augustine, M. Lou, Calabro, A., Kubalak, S., Klewer, S. E., & McDonald, J. A. (2000). Disruption of hyaluronan synthase-2 abrogates normal cardiac morphogenesis and hyaluronan-mediated transformation of epithelium to mesenchyme. *Journal of Clinical Investigation*, *106*(3), 349–360. https://doi.org/10.1172/JCI10272

Chang, C. P., Neilson, J. R., Bayle, J. H., Gestwicki, J. E., Kuo, A., Stankunas, K., Graef, I. A., & Crabtree, G. R. (2004). A field of myocardial-endocardial NFAT signaling underlies heart valve morphogenesis. *Cell*, *118*(5), 649–663. https://doi.org/10.1016/j.cell.2004.08.010

Chen, B., Bronson, R. T., Klaman, L. D., Hampton, T. G., Wang, J. F., Green, P. J., Magnuson, T., Douglas, P. S., Morgan, J. P., & Neel, B. G. (2000). Mice mutant for Egfr and Shp2 have defective cardiac semilunar valvulogenesis. *Nature Genetics*, *24*(3), 296–299. https://doi.org/10.1038/73528

Combs, M. D., & Yutzey, K. E. (2009). Heart valve development: Regulatory networks in development and disease. In *Circulation Research*. https://doi.org/10.1161/CIRCRESAHA.109.201566

D'Amato, G., Luxán, G., Del Monte-Nieto, G., Martínez-Poveda, B., Torroja, C., Walter, W., Bochter, M. S. M. S., Benedito, R., Cole, S., Martinez, F., Hadjantonakis, A.-K. A.-K., Uemura, A., Jiménez-Borreguero, L. J. L. J., & de la Pompa, J. L. J. L. (2015). Sequential Notch activation regulates ventricular chamber development. *Nature Cell Biology*, *18*(1), 7–20. https://doi.org/10.1038/ncb3280

Dambly-Chaudière, C., Cubedo, N., & Ghysen, A. (2007). Control of cell migration in the development of the posterior lateral line: Antagonistic interactions between the chemokine receptors CXCR4 and CXCR7/RDC1. *BMC Developmental Biology*. https://doi.org/10.1186/1471-213X-7-23

de Boer, B. A., van den Berg, G., de Boer, P. A. J., Moorman, A. F. M., & Ruijter, J. M. (2012). Growth of the developing mouse heart: An interactive qualitative and quantitative 3D atlas. *Developmental Biology*. https://doi.org/10.1016/j.ydbio.2012.05.001

De Clercq, E. (2000). Inhibition of HIV infection by bicyclams, highly potent and specific CXCR4 antagonists. In *Molecular Pharmacology*.

de la Cruz, M. V., & Markwald, R. R. (1998). Embryological Development of the Ventricular Inlets. Septation and Atrioventricular Valve Apparatus. In *Living Morphogenesis of the Heart*. https://doi.org/10.1007/978-1-4612-1788-6_6

de la Pompa, J L, Timmerman, L. A., Takimoto, H., Yoshida, H., Elia, A. J., Samper, E., Potter, J., Wakeham, A., Marengere, L., Langille, B. L., Crabtree, G. R., & Mak, T. W. (1998). Role of the NF-ATc transcription factor in morphogenesis of cardiac valves and septum. *Nature*, *392*(6672), 182–186. https://doi.org/10.1038/32419

de la Pompa, José Luis, & Epstein, J. A. (2012). Coordinating tissue interactions: Notch signaling in cardiac development and disease. *Developmental Cell*, *22*(2), 244–254. https://doi.org/10.1016/j.devcel.2012.01.014

Debnath, B., Xu, S., Grande, F., Garofalo, A., & Neamati, N. (2013). Small molecule inhibitors of CXCR4. In *Theranostics*. https://doi.org/10.7150/thno.5376

Délot, E. C., Bahamonde, M. E., Zhao, M., & Lyons, K. M. (2003). BMP signaling is required for septation of the outflow tract of the mammalian heart. In *Development*. https://doi.org/10.1242/dev.00181

Döring, Y., Pawig, L., Weber, C., & Noels, H. (2014). The CXCL12/CXCR4 chemokine ligand/receptor axis in cardiovascular disease. *Frontiers in Physiology*. https://doi.org/10.3389/fphys.2014.00212

Dyer, L. A., & Kirby, M. L. (2009). The role of secondary heart field in cardiac development. In *Developmental Biology*. https://doi.org/10.1016/j.ydbio.2009.10.009

Eguchi, S., Numaguchi, K., Iwasaki, H., Matsumoto, T., Yamakawa, T., Utsunomiya, H., Motley, E. D., Kawakatsu, H., Owada, K. M., Hirata, Y., Marumo, F., & Inagami, T. (1998). Calcium-dependent epidermal growth factor receptor

transactivation mediates the angiotensin II-induced mitogen-activated protein/kinase activation in vascular smooth muscle cells. *Journal of Biological Chemistry*. https://doi.org/10.1074/jbc.273.15.8890

Eisenberg, L. M., & Markwald, R. R. (1995). Molecular regulation of atrioventricular valvuloseptal morphogenesis. In *Circulation Research*. https://doi.org/10.1161/01.RES.77.1.1

Elenius, K., Corfas, G., Paul, S., Choi, C. J., Rio, C., Plowman, G. D., & Klagsbrun, M. (1997). A novel juxtamembrane domain isoform of HER4/ErbB4. Isoform-specific tissue distribution and differential processing in response to phorbol ester. *Journal of Biological Chemistry*. https://doi.org/10.1074/jbc.272.42.26761

Eley, L., Alqahtani, A. M. S., Macgrogan, D., Richardson, R. V., Murphy, L., Salguero-Jimenez, A., Sintes Rodriguez San Pedro, M., Tiurma, S., McCutcheon, L., Gilmore, A., de La Pompa, J. L., Chaudhry, B., & Henderson, D. J. (2018). A novel source of arterial valve cells linked to bicuspid aortic valve without raphe in mice. *ELife*, *7*, 1–27. https://doi.org/10.7554/eLife.34110

Erickson, S. L., O'Shea, K. S., Ghaboosi, N., Loverro, L., Frantz, G., Bauer, M., Lu, L. H., & Moore, M. W. (1997). ErbB3 is required for normal cerebellar and cardiac development: A comparison with ErbB2- and heregulin-deficient mice. *Development*.

Fedak, P. W. M., Verma, S., David, T. E., Leask, R. L., Weisel, R. D., & Butany, J. (2002). Clinical and pathophysiological implications of a bicuspid aortic valve. In *Circulation*. https://doi.org/10.1161/01.CIR.0000027905.26586.E8

Federsppiel, B., Melhado, I. G., Duncan, A. M. V., Delaney, A., Schappert, K., Clark-Lewis, I., & Jirik, F. R. (1993). Molecular cloning of the cDNA and chromosomal localization of the gene for a putative seven-transmembrane segment (7-TMS) receptor isolated from human spleen. *Genomics*. https://doi.org/10.1006/geno.1993.1251

Feng, Y., Broder, C. C., Kennedy, P. E., & Berger, E. A. (1996). HIV-1 entry cofactor: Functional cDNA cloning of a seven-transmembrane, G protein-coupled receptor. *Science*. https://doi.org/10.1126/science.272.5263.872

Fernändez Gonzalez, A. L., Montera, J. A., Monzonis, A. M., Gil, O., & Alemany, P. (1997). Osseous metaplasia and hematopoietic bone marrow in a calcified aortic valve. *Texas Heart Institute Journal*.

Fischer, A., Steidl, C., Wagner, T. U., Lang, E., Jakob, P. M., Friedl, P., Knobeloch, K. P., & Gessler, M. (2007). Combined loss of Hey1 and HeyL causes congenital heart defects because of impaired epithelial to mesenchymal transition. *Circulation Research*. https://doi.org/10.1161/01.RES.0000260913.95642.3b

Fishman, M. C., & Chien, K. R. (1997). Fashioning the vertebrate heart: Earliest embryonic decisions. *Development*.

Fragale, A., Tartaglia, M., Wu, J., & Gelb, B. D. (2004). Noonan Syndrome-Associated SHP2/PTPN11 Mutants Cause EGF-Dependent Prolonged GAB1 Binding and Sustained ERK2/MAPK1 Activation. *Human Mutation*, *23*(3), 267–277. https://doi.org/10.1002/humu.20005

Fricker, S. P., Anastassov, V., Cox, J., Darkes, M. C., Grujic, O., Idzan, S. R., Labrecque, J., Lau, G., Mosi, R. M., Nelson, K. L., Qin, L., Santucci, Z., & Wong, R. S. Y. (2006). Characterization of the molecular pharmacology of AMD3100: A specific antagonist of the G-protein coupled chemokine receptor, CXCR4. *Biochemical Pharmacology*, *72*(5), 588–596. https://doi.org/10.1016/j.bcp.2006.05.010

Friedman, T., Mani, A., & Elefteriades, J. A. (2008). Bicuspid aortic valve: Clinical approach and scientific review of a common clinical entity. In *Expert Review of*

Cardiovascular Therapy. https://doi.org/10.1586/14779072.6.2.235
Galvin, K. M., Donovan, M. J., Lynch, C. a, Meyer, R. I., Paul, R. J., Lorenz, J. N., Fairchild-Huntress, V., Dixon, K. L., Dunmore, J. H., Gimbrone, M. a, Falb, D., & Huszar, D. (2000). A role for smad6 in development and homeostasis of the cardiovascular system. *Nature Genetics*, *24*(february), 171–174. https://doi.org/10.1038/72835
Ganju, R. K., Brubaker, S. A., Meyer, J., Dutt, P., Yang, Y., Qin, S., Newman, W., & Groopman, J. E. (1998). The α-chemokine, stromal cell-derived factor-1α, binds to the transmembrane G-protein-coupled CXCR-4 receptor and activates multiple signal transduction pathways. *Journal of Biological Chemistry*. https://doi.org/10.1074/jbc.273.36.23169
Garg, V. (2006). Molecular genetics of aortic valve disease. In *Current Opinion in Cardiology*. https://doi.org/10.1097/01.hco.0000221578.18254.70
Garg, V., Muth, A. N., Ransom, J. F., Schluterman, M. K., Barnes, R., King, I. N., Grossfeld, P. D., & Srivastava, D. (2005). Mutations in NOTCH1 cause aortic valve disease. *Nature*. https://doi.org/10.1038/nature03940
Gassmann, M., Casagranda, F., Orloli, D., Simon, H., Lai, C., Kleint, R., & Lemke, G. (1995). Aberrant neural and cardiac development in mice lacking the ErbB4 neuregulin receptor. *Nature*. https://doi.org/10.1038/378390a0
George, A. J., Hannan, R. D., & Thomas, W. G. (2013). Unravelling the molecular complexity of GPCR-mediated EGFR transactivation using functional genomics approaches. *FEBS Journal*. https://doi.org/10.1111/febs.12509
Gerlach, L. O., Skerlj, R. T., Bridger, G. J., & Schwartz, T. W. (2001). Molecular Interactions of Cyclam and Bicyclam Non-peptide Antagonists with the CXCR4 Chemokine Receptor. *Journal of Biological Chemistry*. https://doi.org/10.1074/jbc.M010429200
Gharibeh, L., Komati, H., Bossé, Y., Boodhwani, M., Heydarpour, M., Fortier, M., Hassanzadeh, R., Ngu, J., Mathieu, P., Body, S., & Nemer, M. (2018). GATA6 regulates aortic valve remodeling, and its haploinsuffciency leads to right-left type bicuspid aortic valve. *Circulation*, *138*(10), 1025–1038. https://doi.org/10.1161/CIRCULATIONAHA.117.029506
Gittenberger-de Groot, A. C., Vrancken Peeters, M. P. F. M., Mentink, M. M. T., Gourdie, R. G., & Poelmann, R. E. (1998). Epicardium-derived cells contribute a novel population to the myocardial wall and the atrioventricular cushions. *Circulation Research*. https://doi.org/10.1161/01.RES.82.10.1043
Goddeeris, M. M., Rho, S., Petiet, A., Davenport, C. L., Johnson, G. A., Meyers, E. N., Klingensmith, J., & Goddeeris, M. M. (2008). Intracardiac septation requires hedgehog-dependent cellular contributions from outside the heart. *Development*. https://doi.org/10.1242/dev.016147
Goishi, K., Higashiyama, S., Klagsbrun, M., Nakano, N., Umata, T., Ishikawa, M., Mekada, E., & Taniguchi, N. (1995). Phorbol ester induces the rapid processing of cell surface heparin-binding EGF-like growth factor: Conversion from juxtacrine to paracrine growth factor activity. *Molecular Biology of the Cell*. https://doi.org/10.1091/mbc.6.8.967
Gould, R. A., Aziz, H., Woods, C. E., Seman-Senderos, M. A., Sparks, E., Preuss, C., Wünnemann, F., Bedja, D., Moats, C. R., McClymont, S. A., Rose, R., Sobreira, N., Ling, H., MacCarrick, G., Kumar, A. A., Luyckx, I., Cannaerts, E., Verstraeten, A., Björk, H. M., … Dietz, H. C. (2019). ROBO4 variants predispose individuals to bicuspid aortic valve and thoracic aortic aneurysm. In *Nature Genetics*. https://doi.org/10.1038/s41588-018-0265-y
Harrelson, Z., Kelly, R. G., Goldin, S. N., Gibson-Brown, J. J., Bollag, R. J., Silver, L. M., & Papaioannou, V. E. (2004). Tbx2 is essential for patterning the

atrioventricular canal and for morphogenensis of the outflow tract during heart development. *Development*. https://doi.org/10.1242/dev.01378
Hartmann, T. N., Grabovsky, V., Pasvolsky, R., Shulman, Z., Buss, E. C., Spiegel, A., Nagler, A., Lapidot, T., Thelen, M., & Alon, R. (2008). A crosstalk between intracellular CXCR7 and CXCR4 involved in rapid CXCL12-triggered integrin activation but not in chemokine-triggered motility of human T lymphocytes and CD34 + cells . *Journal of Leukocyte Biology*. https://doi.org/10.1189/jlb.0208088
Hashimoto, K., Higashiyama, S., Asada, H., Hashimura, E., Kobayashi, T., Sudo, K., Nakagawa, T., Damm, D., Yoshikawa, K., & Taniguchi, N. (1994). Heparin-binding epidermal growth factor-like growth factor is an autocrine growth factor for human keratinocytes. *Journal of Biological Chemistry*.
Henderson, D. J., & Copp, A. J. (1998). Versican expression is associated with chamber specification, septation, and valvulogenesis in the developing mouse heart. *Circulation Research*. https://doi.org/10.1161/01.RES.83.5.523
Higashiyama, S., Lau, K., Besner, G. E., Abraham, J. A., & Klagsbrun, M. (1992). Structure of heparin-binding EGF-like growth factor. Multiple forms, primary structure, and glycosylation of the mature protein. *Journal of Biological Chemistry*.
Higashiyama, Shigeki, Abraham, J. A., & Klagsbrun, M. (1993). Heparin-binding EGF-like growth factor stimulation of smooth muscle cell migration: Dependence on interactions with cell surface heparan sulfate. *Journal of Cell Biology*. https://doi.org/10.1083/jcb.122.4.933
Higashiyama, Shigeki, Abraham, J. A., Miller, J., Fiddes, J. C., & Klagsbrun, M. (1991). A heparin-binding growth factor secreted by macrophage-like cells that is related to EGF. *Science*. https://doi.org/10.1126/science.1840698
Hinton, R. B., Lincoln, J., Deutsch, G. H., Osinska, H., Manning, P. B., Benson, D. W., & Yutzey, K. E. (2006). Extracellular matrix remodeling and organization in developing and diseased aortic valves. *Circulation Research*. https://doi.org/10.1161/01.RES.0000224114.65109.4e
Hinton, R. B., & Yutzey, K. E. (2011). Heart valve structure and function in development and disease. *Annual Review of Physiology*. https://doi.org/10.1146/annurev-physiol-012110-142145
Hoffman, J. I. E., & Kaplan, S. (2002). The incidence of congenital heart disease. In *Journal of the American College of Cardiology*. https://doi.org/10.1016/S0735-1097(02)01886-7
Hulin, A., Moore, V., James, J. M., & Yutzey, K. E. (2017). Loss of Axin2 results in impaired heart valve maturation and subsequentmyxomatous valve disease. *Cardiovascular Research*. https://doi.org/10.1093/cvr/cvw229
Hurle, J. M., Colveé, E., & Blanco, A. M. (1980). Development of mouse semilunar valves. *Anatomy and Embryology*. https://doi.org/10.1007/BF00315651
Icardo, J. M., & Colvee, E. (1995). Atrioventricular valves of the mouse: III. Collagenous skeleton and myotendinous junction. *The Anatomical Record*. https://doi.org/10.1002/ar.1092430311
Ieda, M., Tsuchihashi, T., Ivey, K. N., Ross, R. S., Hong, T. T., Shaw, R. M., & Srivastava, D. (2009). Cardiac Fibroblasts Regulate Myocardial Proliferation through β1 Integrin Signaling. *Developmental Cell*. https://doi.org/10.1016/j.devcel.2008.12.007
Ivins, S., Chappell, J., Vernay, B., Suntharalingham, J., Martineau, A., Mohun, T. J., & Scambler, P. J. (2015). The CXCL12/CXCR4 Axis Plays a Critical Role in Coronary Artery Development. *Developmental Cell*, *33*(4), 455–468. https://doi.org/10.1016/j.devcel.2015.03.026
Iwamoto, R., & Mekada, E. (2006). ErbB and HB-EGF signaling in heart development

and function. *Cell Structure and Function*, *31*(1), 1–14. https://doi.org/10.1247/csf.31.1

Iwamoto, R., Mine, N., Kawaguchi, T., Minami, S., Saeki, K., & Mekada, E. (2010). HB-EGF function in cardiac valve development requires interaction with heparan sulfate proteoglycans. *Development (Cambridge, England)*, *137*(13), 2205–2214. https://doi.org/10.1242/dev.048926

Iwamoto, R., Mine, N., Mizushima, H., & Mekada, E. (2017). ErbB1 and ErbB4 generate opposing signals regulating mesenchymal cell proliferation during valvulogenesis. *Journal of Cell Science*, jcs.196618. https://doi.org/10.1242/jcs.196618

Iwamoto, R., Yamazaki, S., Asakura, M., Takashima, S., Hasuwa, H., Miyado, K., Adachi, S., Kitakaze, M., Hashimoto, K., Raab, G., Nanba, D., Higashiyama, S., Hori, M., Klagsbrun, M., & Mekada, E. (2003). Heparin-binding EGF-like growth factor and ErbB signaling is essential for heart function. *Proceedings of the National Academy of Sciences of the United States of America*, *100*(6), 3221–3226. https://doi.org/10.1073/pnas.0537588100

Izumi, Y., Hirata, M., Hasuwa, H., Iwamoto, R., Umata, T., Miyado, K., Tamai, Y., Kurisaki, T., Sehara-Fujisawa, A., Ohno, S., & Mekada, E. (1998). A metalloprotease-disintegrin, MDC9/meltrin-γ/ADAM9 and PKCδ are involved in TPA-induced ectodomain shedding of membrane-anchored heparin-binding EGF-like growth factor. *EMBO Journal*. https://doi.org/10.1093/emboj/17.24.7260

Jackson, L. F., Qiu, T. H., Sunnarborg, S. W., Chang, A., Zhang, C., Patterson, C., & Lee, D. C. (2003). Defective valvulogenesis in HB-EGF and TACE-null mice is associated with aberrant BMP signaling. *EMBO Journal*, *22*(11), 2704–2716. https://doi.org/10.1093/emboj/cdg264

Jänicke, R. U., Sprengart, M. L., Wati, M. R., & Porter, A. G. (1998). Caspase-3 is required for DNA fragmentation and morphological changes associated with apoptosis. *Journal of Biological Chemistry*. https://doi.org/10.1074/jbc.273.16.9357

Jiang, X., Rowitch, D. H., Soriano, P., McMahon, A. P., & Sucov, H. M. (2000). Fate of the mammalian cardiac neural crest. *Development*.

Jiao, K., Kulessa, H., Tompkins, K., Zhou, Y., Batts, L., Baldwin, H. S., & Hogan, B. L. M. (2003). An essential role of Bmp4 in the atrioventricular septation of the mouse heart. *Genes and Development*. https://doi.org/10.1101/gad.1124803

Jiménez, C., Portela, R. A., Mellado, M., Rodríguez-Frade, J. M., Collard, J., Serrano, A., Martínez-A, C., Avila, J., & Carrera, A. C. (2000). Role of the PI3K regulatory subunit in the control of actin organization and cell migration. *Journal of Cell Biology*. https://doi.org/10.1083/jcb.151.2.249

Kalatskaya, I., Berchiche, Y. A., Gravel, S., Limberg, B. J., Rosenbaum, J. S., & Heveker, N. (2009a). AMD3100 is a CXCR7 ligand with allosteric agonist properties. *Molecular Pharmacology*. https://doi.org/10.1124/mol.108.053389

Kalatskaya, I., Berchiche, Y. a, Gravel, S., Limberg, B. J., Rosenbaum, J. S., & Heveker, N. (2009b). AMD3100 is a CXCR7 ligand with allosteric agonist properties. *Molecular Pharmacology*, *75*(5), 1240–1247. https://doi.org/10.1124/mol.108.053389.luciferase

Kanzler, B., Kuschert, S. J., Liu, Y. H., & Mallo, M. (1998). Hoxa-2 restricts the chondrogenic domain and inhibits bone formation during development of the branchial area. *Development*.

Kelly, R. G., Brown, N. A., & Buckingham, M. E. (2001). The Arterial Pole of the Mouse Heart Forms from Fgf10-Expressing Cells in Pharyngeal Mesoderm. *Developmental Cell*. https://doi.org/10.1016/S1534-5807(01)00040-5

Kim, R. Y., Robertson, E. J., & Solloway, M. J. (2001). Bmp6 and Bmp7 are required for cushion formation and septation in the developing mouse heart. *Developmental Biology*. https://doi.org/10.1006/dbio.2001.0284

Kirby, M. L. (1999). Contribution of Neural Crest to Heart and Vessel Morphology. In *Heart Development*. https://doi.org/10.1016/b978-012329860-7/50013-1

Kirby, M. L., Gale, T. F., & Stewart, D. E. (1983). Neural crest cells contribute to normal aorticopulmonary septation. *Science*. https://doi.org/10.1126/science.6844926

Kisanuki, Y. Y., Hammer, R. E., Miyazaki, J. ichi, Williams, S. C., Richardson, J. A., & Yanagisawa, M. (2001). Tie2-Cre transgenic mice: A new model for endothelial cell-lineage analysis in vivo. *Developmental Biology*. https://doi.org/10.1006/dbio.2000.0106

Koenraadt, W. M. C., Bartelings, M. M., Bökenkamp, R., Gittenberger-De Groot, A. C., DeRuiter, M. C., Schalij, M. J., & Jongbloed, M. R. M. (2018). Coronary anatomy in children with bicuspid aortic valves and associated congenital heart disease. *Heart*, *104*(5), 385–393. https://doi.org/10.1136/heartjnl-2017-311178

Krenz, M., Gulick, J., Osinska, H. E., Colbert, M. C., Molkentin, J. D., & Robbins, J. (2008). Role of ERK1/2 signaling in congenital valve malformations in Noonan syndrome. *Proceedings of the National Academy of Sciences of the United States of America*, *105*(48), 18930–18935. https://doi.org/10.1073/pnas.0806556105

Krenz, M., Yutzey, K. E., & Robbins, J. (2005). Noonan syndrome mutation Q79R in Shp2 increases proliferation of valve primordia mesenchymal cells via extracellular signal-regulated kinase 1/2 signaling. *Circulation Research*. https://doi.org/10.1161/01.RES.0000186194.06514.b0

Kretzschmar, M., Liu, F., Hata, A., Doody, J., & Massagué, J. (1997). The TGF-β family mediator Smad1 is phosphorylated directly and activated functionally by the BMP receptor kinase. *Genes and Development*. https://doi.org/10.1101/gad.11.8.984

Kugimiya, F., Kawaguchi, H., Kamekura, S., Chikuda, H., Ohba, S., Yano, F., Ogata, N., Katagiri, T., Harada, Y., Azuma, Y., Nakamura, K., & Chung, U. Il. (2005). Involvement of endogenous bone morphogenetic protein (BMP) 2 and BMP6 in bone formation. *Journal of Biological Chemistry*. https://doi.org/10.1074/jbc.M505166200

Ladich, E., Butany, J., & Virmani, R. (2016). Aneurysms of the Aorta: Ascending, Thoracic and Abdominal and Their Management. In *Cardiovascular Pathology: Fourth Edition*. https://doi.org/10.1016/B978-0-12-420219-1.00005-7

Lawson, K. A., Meneses, J. J., & Pedersen, R. A. (1991). Clonal analysis of epiblast fate during germ layer formation in the mouse embryo. *Development*.

Ledonne, A., Nobili, A., Latagliata, E. C., Cavallucci, V., Guatteo, E., Puglisi-Allegra, S., D'Amelio, M., & Mercuri, N. B. (2015). Neuregulin 1 signalling modulates mGluR1 function in mesencephalic dopaminergic neurons. *Molecular Psychiatry*. https://doi.org/10.1038/mp.2014.109

Lee, K. F., Simon, H., Chen, H., Bates, B., Hung, M. C., & Hauser, C. (1995). Requirement for neuregulin receptor erbB2 in neural and cardiac development. *Nature*. https://doi.org/10.1038/378394a0

Lee, T. C., Zhao, Y. D., Courtman, D. W., & Stewart, D. J. (2000). Abnormal aortic valve development in mice lacking endothelial nitric oxide synthase. *Circulation*. https://doi.org/10.1161/01.CIR.101.20.2345

Lemjabbar, H., & Basbaum, C. (2002). Platelet-activating factor receptor and ADAM10 mediate responses to Staphylococcus aureus in epithelial cells. *Nature Medicine*. https://doi.org/10.1038/nm0102-41

Levoye, A., Balabanian, K., Baleux, F., Bachelerie, F., & Lagane, B. (2009). CXCR7 heterodimerizes with CXCR4 and regulates CXCL12-mediated G protein signaling. *Blood*. https://doi.org/10.1182/blood-2008-12-196618

Lian, H., Ma, Y., Feng, J., Dong, W., Yang, Q., Lu, D., & Zhang, L. (2012). Heparin-Binding EGF-Like Growth Factor Induces Heart Interstitial Fibrosis via an Akt/mTor/p70s6k Pathway. *PLoS ONE*, *7*(9). https://doi.org/10.1371/journal.pone.0044946

Lin, C. J., Lin, C. Y., Chen, C. H., Zhou, B., & Chang, C. P. (2012). Partitioning the heart: Mechanisms of cardiac septation and valve development. *Development (Cambridge)*, *139*(18), 3277–3299. https://doi.org/10.1242/dev.063495

Lincoln, J., Alfieri, C. M., & Yutzey, K. E. (2004). Development of heart valve leaflets and supporting apparatus in chicken and mouse embryos. *Developmental Dynamics*. https://doi.org/10.1002/dvdy.20051

Lincoln, J., & Yutzey, K. E. (2011). Molecular and developmental mechanisms of congenital heart valve disease. In *Birth Defects Research Part A - Clinical and Molecular Teratology*. https://doi.org/10.1002/bdra.20799

Liu, W., Selever, J., Wang, D., Lu, M. F., Mosest, K. A., Schwartz, R. J., & Martin, J. F. (2004). Bmp4 signaling is required for outflow-tract septation and branchial-arch artery remodeling. *Proceedings of the National Academy of Sciences of the United States of America*. https://doi.org/10.1073/pnas.0308466101

Lo, R. S., Wotton, D., & Massagué, J. (2001). Epidermal growth factor signaling via Ras controls the Smad transcriptional co-repressor TGIF. *EMBO Journal*. https://doi.org/10.1093/emboj/20.1.128

Luetteke, N. C., Phillips, H. K., Qiu, T. H., Copeland, N. G., Shelton Earp, H., Jenkins, N. A., & Lee, D. C. (1994). The mouse waved-2 phenotype results from a point mutation in the EGF receptor tyrosine kinase. *Genes and Development*. https://doi.org/10.1101/gad.8.4.399

Luker, K. E., Steele, J. M., Mihalko, L. A., Ray, P., & Luker, G. D. (2010). Constitutive and chemokine-dependent internalization and recycling of CXCR7 in breast cancer cells to degrade chemokine ligands. *Oncogene*. https://doi.org/10.1038/onc.2010.212

Luna-Zurita, L., Prados, B., Grego-Bessa, J., Luxán, G., Del Monte, G., Benguría, A., Adams, R. H., Pérez-Pomares, J. M., & De La Pompa, J. L. (2010). Integration of a Notch-dependent mesenchymal gene program and Bmp2-driven cell invasiveness regulates murine cardiac valve formation. *Journal of Clinical Investigation*, *120*(10), 3493–3507. https://doi.org/10.1172/JCI42666

Luu, H. H., Song, W. X., Luo, X., Manning, D., Luo, J., Deng, Z. L., Sharff, K. A., Montag, A. G., Haydon, R. C., & He, T. C. (2007). Distinct roles of bone morphogenetic proteins in osteogenic differentiation of mesenchymal stem cells. *Journal of Orthopaedic Research*. https://doi.org/10.1002/jor.20359

Luxán, G., Casanova, J. C., Martínez-Poveda, B., Prados, B., D'Amato, G., MacGrogan, D., Gonzalez-Rajal, A., Dobarro, D., Torroja, C., Martinez, F., Izquierdo-García, J. L., Fernández-Friera, L., Sabater-Molina, M., Kong, Y. Y., Pizarro, G., Ibañez, B., Medrano, C., García-Pavía, P., Gimeno, J. R., … De La Pompa, J. L. (2013). Mutations in the NOTCH pathway regulator MIB1 cause left ventricular noncompaction cardiomyopathy. *Nature Medicine*. https://doi.org/10.1038/nm.3046

Luxán, G., D'Amato, G., MacGrogan, D., & De La Pompa, J. L. (2016). Endocardial Notch Signaling in Cardiac Development and Disease. In *Circulation Research*. https://doi.org/10.1161/CIRCRESAHA.115.305350

Ma, L., Lu, M. F., Schwartz, R. J., & Martin, J. F. (2005). Bmp2 is essential for cardiac cushion epithelial-mesenchymal transition and myocardial patterning.

Development. https://doi.org/10.1242/dev.02156
Ma, Q., Jones, D., Borghesani, P. R., Segal, R. A., Nagasawa, T., Kismimoto, T., Bronson, R. T., & Springer, T. A. (1998). Impaired B-lymphopoiesis, myelopoiesis, and derailed cerebellar neuron migration in CXCR4- and SDF-1-deficient mice. *Proceedings of the National Academy of Sciences of the United States of America*. https://doi.org/10.1073/pnas.95.16.9448
MacGrogan, D., D'Amato, G., Travisano, S., Martinez-Poveda, B., Luxán, G., Del Monte-Nieto, G., Papoutsi, T., Sbroggio, M., Bou, V., Gomez-Del Arco, P., Gómez, M. J., Zhou, B., Redondo, J. M., Jiménez-Borreguero, L. J., & De La Pompa, J. L. (2016). Sequential Ligand-Dependent Notch Signaling Activation Regulates Valve Primordium Formation and Morphogenesis. *Circulation Research*, *118*(10), 1480–1497. https://doi.org/10.1161/CIRCRESAHA.115.308077
MacGrogan, D., Münch, J., & de la Pompa, J. L. (2018). Notch and interacting signalling pathways in cardiac development, disease, and regeneration. In *Nature Reviews Cardiology*. https://doi.org/10.1038/s41569-018-0100-2
Markwald, R. R., Fitzharris, T. P., & Manasek, F. J. (1977). Structural development of endocardial cushions. *American Journal of Anatomy*. https://doi.org/10.1002/aja.1001480108
Martinsen, B. J. (2005). Reference guide to the stages of chick heart embryology. In *Developmental Dynamics*. https://doi.org/10.1002/dvdy.20468
Massagué, J., Seoane, J., & Wotton, D. (2005). Smad transcription factors. In *Genes and Development*. https://doi.org/10.1101/gad.1350705
Matsuoka, R. L., Marass, M., Avdesh, A., Helker, C. S. M., Maischein, H. M., Grosse, A. S., Kaur, H., Lawson, N. D., Herzog, W., & Stainier, D. Y. R. (2016). Radial glia regulate vascular patterning around the developing spinal cord. *ELife*. https://doi.org/10.7554/eLife.20253
Mazo, I. B., Massberg, S., & von Andrian, U. H. (2011). Hematopoietic stem and progenitor cell trafficking. In *Trends in Immunology*. https://doi.org/10.1016/j.it.2011.06.011
McCulley, D. J., Kang, J. O., Martin, J. F., & Black, B. L. (2008). BMP4 is required in the anterior heart field and its derivatives for endocardial cushion remodeling, outflow tract septation, and semilunar valve development. *Developmental Dynamics*. https://doi.org/10.1002/dvdy.21743
McGuire, P. G., & Orkin, R. W. (1992). Urokinase activity in the developing avian heart: A spatial and temporal analysis. *Developmental Dynamics*. https://doi.org/10.1002/aja.1001930105
Mekada, E., & Iwamoto, R. (2008). Hb-Egf. *AfCS-Nature Molecule Pages*, 1–14. https://doi.org/10.1038/mp.a002932.01
Meyer, D., & Birchmeier, C. (1995). Multiple essential functions of neuregulin in development. *Nature*. https://doi.org/10.1038/378386a0
Miettinen, P. J., Berger, J. E., Meneses, J., Phung, Y., Pedersen, R. A., Werb, Z., & Derynck, R. (1995). Epithelial immaturity and multiorgan failure in mice lacking epidermal growth factor receptor. *Nature*. https://doi.org/10.1038/376337a0
Mine, N., Iwamoto, R., & Mekada, E. (2005). HB-EGF promotes epithelial cell migration in eyelid development. *Development*. https://doi.org/10.1242/dev.02030
Mjaatvedt, C. H., Nakaoka, T., Moreno-Rodriguez, R., Norris, R. A., Kern, M. J., Eisenberg, C. A., Turner, D., & Markwald, R. R. (2001). The outflow tract of the heart is recruited from a novel heart-forming field. *Developmental Biology*. https://doi.org/10.1006/dbio.2001.0409
Mohler, E. R., Gannon, F., Reynolds, C., Zimmerman, R., Keane, M. G., & Kaplan, F.

S. (2001). Bone formation and inflammation in cardiac valves. *Circulation*. https://doi.org/10.1161/01.CIR.103.11.1522

Mommersteeg, M. T. M., Soufan, A. T., De Lange, F. J., Van Den Hoff, M. J. B., Anderson, R. H., Christoffels, V. M., & Moorman, A. F. M. (2006). Two distinct pools of mesenchyme contribute to the development of the atrial septum. *Circulation Research*. https://doi.org/10.1161/01.RES.0000238360.33284.a0

Mommersteeg, M. T. M., Yeh, M. L., Parnavelas, J. G., & Andrews, W. D. (2015). Disrupted Slit-Robo signalling results in membranous ventricular septum defects and bicuspid aortic valves. *Cardiovascular Research*. https://doi.org/10.1093/cvr/cvv040

Moorman, A. F. M., & Christoffels, V. M. (2003). Cardiac chamber formation: Development, genes, and evolution. In *Physiological Reviews*. https://doi.org/10.1152/physrev.00006.2003

Moorman, A., Webb, S., Brown, N. A., Lamers, W., & Anderson, R. H. (2003). Development of the heart: (1) Formation of the cardiac chambers and arterial trunks. In *Heart*. https://doi.org/10.1136/heart.89.7.806

Morris, J. K., Weichun, L., Hauser, C., Marchuk, Y., Getman, D., & Kuo-Fen, L. (1999). Rescue of the cardiac defect in erbB2 mutant mice reveals essential roles of erbB2 in peripheral nervous system development. *Neuron*. https://doi.org/10.1016/S0896-6273(00)80779-5

Mulholland, D. L., & Gotlieb, A. I. (1996). Cell biology of valvular interstitial cells. In *Canadian Journal of Cardiology*.

Nagasawa, T., Hirota, S., Tachibana, K., Takakura, N., Nishikawa, S. I., Kitamura, Y., Yoshida, N., Kikutani, H., & Kishimoto, T. (1996). Defects of B-cell lymphopoiesis and bone-marrow myelopoiesis in mice lacking the CXC chemokine PBSF/SDF-1. *Nature*. https://doi.org/10.1038/382635a0

Nanba, D., Kinugasa, Y., Morimoto, C., Koizumi, M., Yamamura, H., Takahashi, K., Takakura, N., Mekada, E., Hashimoto, K., & Higashiyama, S. (2006). Loss of HB-EGF in smooth muscle or endothelial cell lineages causes heart malformation. *Biochemical and Biophysical Research Communications*, *350*(2), 315–321. https://doi.org/10.1016/j.bbrc.2006.09.060

Naumann, U., Cameroni, E., Pruenster, M., Mahabaleshwar, H., Raz, E., Zerwes, H. G., Rot, A., & Thelen, M. (2010). CXCR7 functions as a scavenger for CXCL12 and CXCL11. *PLoS ONE*. https://doi.org/10.1371/journal.pone.0009175

Neeb, Z., Lajiness, J. D., Bolanis, E., & Conway, S. J. (2013). Cardiac outflow tract anomalies. In *Wiley Interdisciplinary Reviews: Developmental Biology*. https://doi.org/10.1002/wdev.98

Nie, Y., Waite, J., Brewer, F., Sunshine, M. J., Littman, D. R., & Zou, Y. R. (2004). The role of CXCR4 in maintaining peripheral B cell compartments and humoral immunity. *Journal of Experimental Medicine*. https://doi.org/10.1084/jem.20041185

Oberlin, E., Amara, A., Bachelerie, F., Bessia, C., Virelizier, J. L., Arenzana-Seisdedos, F., Schwartz, O., Heard, J. M., Clark-Lewis, I., Legler, D. F., Loetscher, M., Baggiolini, M., & Moser, B. (1996). The CXC chemokine SDF-1 is the ligand for LESTR/fusin and prevents infection by T-cell-line-adapted HIV-1. *Nature*. https://doi.org/10.1038/382833a0

Orsini, M. J., Parent, J.-L., Mundell, S. J., & Benovic, J. L. (1999). Trafficking of the HIV Coreceptor CXCR4. *Journal of Biological Chemistry*. https://doi.org/10.1074/jbc.274.43.31076

Otto, C. M. (2002). Calcification of bicuspid aortic valves. In *Heart*. https://doi.org/10.1136/heart.88.4.321

Peacock, J. D., Lu, Y., Koch, M., Kadler, K. E., & Lincoln, J. (2008). Temporal and

spatial expression of collagens during murine atrioventricular heart valve development and maintenance. *Developmental Dynamics*. https://doi.org/10.1002/dvdy.21719

Pérez-Pomares, J. M., & Muñoz-Chápuli, R. (2002). Epithelial-mesenchymal transitions: A mesodermal cell strategy for evolutive innovation in metazoans. *Anatomical Record*. https://doi.org/10.1002/ar.10165

Pérez-Pomares, J. M., Phelps, A., Sedmerova, M., & Wessels, A. (2003). Epicardial-like cells on the distal arterial end of the cardiac outflow tract do not derive from the proepicardium but are derivatives of the cephalic pericardium. *Developmental Dynamics*. https://doi.org/10.1002/dvdy.10284

Person, A. D., Klewer, S. E., & Runyan, R. B. (2005). Cell biology of cardiac cushion development. *International Review of Cytology*. https://doi.org/10.1016/S0074-7696(05)43005-3

Pierpont, M. E., Basson, C. T., Benson, D. W., Gelb, B. D., Giglia, T. M., Goldmuntz, E., McGee, G., Sable, C. A., Srivastava, D., & Webb, C. L. (2007). Genetic basis for congenital heart defects: Current knowledge - A scientific statement from the American Heart Association Congenital Cardiac Defects Committee, Council on Cardiovascular Disease in the Young. In *Circulation*. https://doi.org/10.1161/CIRCULATIONAHA.106.183056

Plageman, T. F., & Yutzey, K. E. (2005). T-box genes and heart development: Putting the “T” in hearT. In *Developmental Dynamics*. https://doi.org/10.1002/dvdy.20201

Poelmann, R. E., Lie-Venema, H., & Gittenberger-De Groot, A. C. (2002). The role of the epicardium and neural crest: As extracardiac contributors to coronary vascular development. In *Texas Heart Institute Journal*.

Prenzel, N., Zwick, E., Daub, H., Leserer, M., Abraham, R., Wallasch, C., & Ullrich, A. (1999). EGF receptor transactivation by G-protein-coupled receptors requires metalloproteinase cleavage of proHB-EGF. *Nature*. https://doi.org/10.1038/47260

Raab, G., & Klagsbrun, M. (1997). Heparin-binding EGF-like growth factor. In *Biochimica et Biophysica Acta - Reviews on Cancer*. https://doi.org/10.1016/S0304-419X(97)00024-3

Rabkin-Aikawa, E., Farber, M., Aikawa, M., & Schoen, F. J. (2004). Dynamic and reversible changes of interstitial cell phenotype during remodeling of cardiac valves. *Journal of Heart Valve Disease*.

Rajagopal, S., & Shenoy, S. K. (2018). GPCR desensitization: Acute and prolonged phases. In *Cellular Signalling*. https://doi.org/10.1016/j.cellsig.2017.01.024

Riese, D. J., & Stern, D. F. (1998). Specificity within the EGF family/ErbB receptor family signaling network. In *BioEssays*. https://doi.org/10.1002/(SICI)1521-1878(199801)20:1<41::AID-BIES7>3.0.CO;2-V

Rivera-Feliciano, J., & Tabin, C. J. (2006). Bmp2 instructs cardiac progenitors to form the heart-valve-inducing field. *Developmental Biology*. https://doi.org/10.1016/j.ydbio.2006.03.043

Romano, L. A., & Runyan, R. B. (1999). Slug is a mediator of epithelial-mesenchymal cell transformation in the developing chicken heart. *Developmental Biology*. https://doi.org/10.1006/dbio.1999.9339

Romano, L. A., & Runyan, R. B. (2000). Slug is an essential target of TGFβ2 signaling in the developing chicken heart. *Developmental Biology*. https://doi.org/10.1006/dbio.2000.9750

Rostagno, C. (2019). Heart valve disease in elderly. *World Journal of Cardiology*. https://doi.org/10.4330/wjc.v11.i2.71

Runyan, R. B., & Markwald, R. R. (1983). Invasion of mesenchyme into three-

dimensional collagen gels: A regional and temporal analysis of interaction in embryonic heart tissue. *Developmental Biology*. https://doi.org/10.1016/0012-1606(83)90010-6

Saga, Y., Kitajima, S., & Miyagawa-Tomita, S. (2000). Mesp1 expression is the earliest sign of cardiovascular development. In *Trends in Cardiovascular Medicine*. https://doi.org/10.1016/S1050-1738(01)00069-X

Schaefer, B. M., Lewin, M. B., Stout, K. K., Gill, E., Prueitt, A., Byers, P. H., & Otto, C. M. (2008). The bicuspid aortic valve: An integrated phenotypic classification of leaflet morphology and aortic root shape. *Heart*. https://doi.org/10.1136/hrt.2007.132092

Schroeder, J. A., Jackson, L. F., Lee, D. C., & Camenisch, T. D. (2003). Form and function of developing heart valves: Coordination by extracellular matrix and growth factor signaling. In *Journal of Molecular Medicine*. https://doi.org/10.1007/s00109-003-0456-5

Shah, B. H., & Catt, K. J. (2003). A central role of EGF receptor transactivation in angiotensin II-induced cardiac hypertrophy. In *Trends in Pharmacological Sciences*. https://doi.org/10.1016/S0165-6147(03)00079-8

Shigeta, A., Huang, V., Zuo, J., Besada, R., Nakashima, Y., Lu, Y., Ding, Y., Pellegrini, M., Kulkarni, R. P., Hsiai, T., Deb, A., Zhou, B., Nakano, H., & Nakano, A. (2019). Endocardially Derived Macrophages Are Essential for Valvular Remodeling. *Developmental Cell*. https://doi.org/10.1016/j.devcel.2019.01.021

Shirakata, Y., Kimura, R., Nanba, D., Iwamoto, R., Tokumaru, S., Morimoto, C., Yokota, K., Nakamura, M., Sayama, K., Mekada, E., Higashiyama, S., & Hashimoto, K. (2005). Heparin-binding EGF-like growth factor accelerates keratinocyte migration and skin wound healing. *Journal of Cell Science*. https://doi.org/10.1242/jcs.02346

Shirozu, M., Nakano, T., Inazawa, J., Tashiro, K., Tada, H., Shinohara, T., & Honjo, T. (1995). Structure and chromosomal localization of the human stromal cell-derived factor 1 (SDF1) gene. *Genomics*. https://doi.org/10.1006/geno.1995.1180

Sibilia, M., Steinbach, J. P., Stingl, L., Aguzzi, A., & Wagner, E. F. (1998). A strain-independent postnatal neurodegeneration in mice lacking the EGF receptor. *EMBO Journal*. https://doi.org/10.1093/emboj/17.3.719

Sibilia, M., Wagner, B., Hoebertz, A., Elliott, C., Marino, S., Jochum, W., & Wagner, E. F. (2003). Mice humanised for the EGF receptor display hypomorphic phenotypes in skin, bone and heart. *Development (Cambridge, England)*, *130*(19), 4515–4525. https://doi.org/10.1242/dev.00664

Sibilia, M., & Wagner, E. F. (1995). Strain-dependent epithelial defects in mice lacking the EGF receptor. *Science*. https://doi.org/10.1126/science.7618085

Sierro, F., Biben, C., Martı, L., Woehl, B., Leung, H., Groom, J., Batten, M., Harvey, R. P., Martı, C., Mackay, C. R., Mackay, F., Martínez-Muñoz, L., Mellado, M., Ransohoff, R. M., Li, M., Woehl, B., Leung, H., Groom, J., Batten, M., … Mackay, F. (2007). Disrupted cardiac development but normal hematopoiesis in mice deficient in the second CXCL12/SDF-1 receptor, CXCR7. *Proceedings of the National Academy of Sciences of the United States of America*, *104*(37), 14759–14764. https://doi.org/10.1073/pnas.0702229104

Sievers, H. H., & Schmidtke, C. (2007). A classification system for the bicuspid aortic valve from 304 surgical specimens. *Journal of Thoracic and Cardiovascular Surgery*. https://doi.org/10.1016/j.jtcvs.2007.01.039

Sillesen, H., Sartori, S., Sandholt, B., Baber, U., Mehran, R., & Fuster, V. (2018). Carotid plaque thickness and carotid plaque burden predict future

cardiovascular events in asymptomatic adult Americans. *European Heart Journal Cardiovascular Imaging*. https://doi.org/10.1093/ehjci/jex239
Smith, A. P., Verrecchia, A., Fagà, G., Doni, M., Perna, D., Martinato, F., Guccione, E., & Amati, B. (2009). A positive role for Myc in TGFβ-induced Snail transcription and epithelial-to-mesenchymal transition. *Oncogene*. https://doi.org/10.1038/onc.2008.395
Snarr, B. S., Kern, C. B., & Wessels, A. (2008). Origin and fate of cardiac mesenchyme. *Developmental Dynamics*, *237*(10), 2804–2819. https://doi.org/10.1002/dvdy.21725
Soriano, P. (1999). Generalized lacZ expression with the ROSA26 Cre reporter strain [1]. In *Nature Genetics*. https://doi.org/10.1038/5007
Srivastava, D. (2006). Making or Breaking the Heart: From Lineage Determination to Morphogenesis. In *Cell*. https://doi.org/10.1016/j.cell.2006.09.003
Srivastava, D., & Olson, E. N. (2000). A genetic blueprint for cardiac development. In *Nature*. https://doi.org/10.1038/35025190
Stoll, S. W., Rittié, L., Johnson, J. L., & Elder, J. T. (2012). Heparin-binding EGF-like growth factor promotes epithelial-mesenchymal transition in human keratinocytes. *Journal of Investigative Dermatology*. https://doi.org/10.1038/jid.2012.78
Sugi, Y., Yamamura, H., Okagawa, H., & Markwald, R. R. (2004). Bone morphogenetic protein-2 can mediate myocardial regulation of atrioventricular cushion mesenchymal cell formation in mice. *Developmental Biology*. https://doi.org/10.1016/j.ydbio.2004.01.045
Sunnarborg, S. W., Leann Hinkle, C., Stevenson, M., Russell, W. E., Raska, C. S., Peschon, J. J., Castner, B. J., Gerhart, M. J., Paxton, R. J., Black, R. A., & Lee, D. C. (2002). Tumor necrosis factor-α converting enzyme (TACE) regulates epidermal growth factor receptor ligand availability. *Journal of Biological Chemistry*. https://doi.org/10.1074/jbc.M112050200
Suzuki, H. R., Solursh, M., & Baldwin, H. S. (1995). Relationship between fibronectin expression during gastrulation and heart formation in the rat embryo. *Developmental Dynamics*. https://doi.org/10.1002/aja.1002040305
Tadano, M., Edamatsu, H., Minamisawa, S., Yokoyama, U., Ishikawa, Y., Suzuki, N., Saito, H., Wu, D., Masago-Toda, M., Yamawaki-Kataoka, Y., Setsu, T., Terashima, T., Maeda, S., Satoh, T., & Kataoka, T. (2005). Congenital semilunar valvulogenesis defect in mice deficient in phospholipase C epsilon. *Molecular and Cellular Biology*, *25*(6), 2191–2199. https://doi.org/10.1128/MCB.25.6.2191-2199.2005
Tam, P. P. L., & Behringer, R. R. (1997). Mouse gastrulation: The formation of a mammalian body plan. *Mechanisms of Development*. https://doi.org/10.1016/S0925-4773(97)00123-8
Teicher, B. A., & Fricker, S. P. (2010). CXCL12 (SDF-1)/CXCR4 pathway in cancer. In *Clinical Cancer Research*. https://doi.org/10.1158/1078-0432.CCR-09-2329
Theis, J. L., Hrstka, S. C. L., Evans, J. M., O'Byrne, M. M., de Andrade, M., O'Leary, P. W., Nelson, T. J., & Olson, T. M. (2015). Compound heterozygous NOTCH1 mutations underlie impaired cardiogenesis in a patient with hypoplastic left heart syndrome. *Human Genetics*. https://doi.org/10.1007/s00439-015-1582-1
Threadgill, D. W., Dlugosz, A. A., Hansen, L. A., Tennenbaum, T., Lichti, U., Yee, D., LaMantia, C., Mourton, T., Herrup, K., Harris, R. C., Barnard, J. A., Yuspa, S. H., Coffey, R. J., & Magnuson, T. (1995). Targeted disruption of mouse EGF receptor: Effect of genetic background on mutant phenotype. *Science*. https://doi.org/10.1126/science.7618084
Tian, E., Stevens, S. R., Guan, Y., Springer, D. A., Anderson, S. A., Starost, M. F.,

Patel, V., Hagen, K. G. T., & Tabak, L. A. (2015). Galnt1 is required for normal heart valve development and cardiac function. *PLoS ONE*, *10*(1), 1–19. https://doi.org/10.1371/journal.pone.0115861

Tidcombe, H., Jackson-Fishert, A., Mathers, K., Stern, D. F., Gassmann, M., & Golding, J. P. (2003). Neural and mammary gland defects in Erbb4 knockout mice genetically rescued from embryonic lethality. *Proceedings of the National Academy of Sciences of the United States of America*. https://doi.org/10.1073/pnas.1436402100

Timmerman, L. A., Grego-Bessa, J., Raya, A., Bertrán, E., Pérez-Pomares, J. M., Díez, J., Aranda, S., Palomo, S., McCormick, F., Izpisúa-Belmonte, J. C., & De La Pompa, J. L. (2004). Notch promotes epithelial-mesenchymal transition during cardiac development and oncogenic transformation. *Genes and Development*, *18*(1), 99–115. https://doi.org/10.1101/gad.276304

Tokumaru, S., Higashiyama, S., Endo, T., Nakagawa, T., Miyagawa, J. I., Yamamoru, K., Hanakawa, Y., Ohmoto, H., Yoshino, K., Shirakata, Y., Matsuzawa, Y., Hashimoto, K., & Taniguchi, N. (2000). Ectodomain shedding of epidermal growth factor receptor ligands is required for keratinocyte migration in cutaneous wound healing. *Journal of Cell Biology*. https://doi.org/10.1083/jcb.151.2.209

Torre, M., Hwang, D. H., Padera, R. F., Mitchell, R. N., & Vanderlaan, P. A. (2016). Osseous and chondromatous metaplasia in calcific aortic valve stenosis. *Cardiovascular Pathology*. https://doi.org/10.1016/j.carpath.2015.08.008

Toyofuku, T., Yoshida, J., Sugimoto, T., Yamamoto, M., Makino, N., Takamatsu, H., Takegahara, N., Suto, F., Hori, M., Fujisawa, H., Kumanogoh, A., & Kikutani, H. (2008). Repulsive and attractive semaphorins cooperate to direct the navigation of cardiac neural crest cells. *Developmental Biology*. https://doi.org/10.1016/j.ydbio.2008.06.028

Van Den Berg, G., & Moorman, A. F. M. (2009). Concepts of Cardiac Development in Retrospect. *Pediatric Cardiology*. https://doi.org/10.1007/s00246-008-9369-y

Van Den Hoff, M. J. B., Moorman, A. F. M., Ruijter, J. M., Lamers, W. H., Bennington, R. W., Markwald, R. R., & Wessels, A. (1999). Myocardialization of the cardiac outflow tract. *Developmental Biology*. https://doi.org/10.1006/dbio.1999.9366

Vinante, F., & Rigo, A. (2013). Heparin-binding epidermal growth factor-like growth factor/diphtheria toxin receptor in normal and neoplastic hematopoiesis. In *Toxins*. https://doi.org/10.3390/toxins5061180

Vincent, S. D., & Buckingham, M. E. (2010). How to make a heart. The origin and regulation of cardiac progenitor cells. In *Current Topics in Developmental Biology*. https://doi.org/10.1016/S0070-2153(10)90001-X

von Gise, A., Zhou, B., Honor, L. B., Ma, Q., Petryk, A., & Pu, W. T. (2011). WT1 regulates epicardial epithelial to mesenchymal transition through β-catenin and retinoic acid signaling pathways. *Developmental Biology*. https://doi.org/10.1016/j.ydbio.2011.05.668

Walenkamp, A. M. E., Lapa, C., Herrmann, K., & Wester, H. J. (2017). CXCR4 ligands: The next big hit? *Journal of Nuclear Medicine*, *58*, 77S-82S. https://doi.org/10.2967/jnumed.116.186874

Watanabe, M., Jafri, A., & Fisher, S. A. (2001). Apoptosis is required for the proper formation of the ventriculo-arterial connections. *Developmental Biology*. https://doi.org/10.1006/dbio.2001.0466

Weismann, C. G., & Gelb, B. D. (2007). The genetics of congenital heart disease: A review of recent developments. In *Current Opinion in Cardiology*. https://doi.org/10.1097/HCO.0b013e3280f629c7

Wessels, A., Markman, M. W. M., Vermeulen, J. L. M., Anderson, R. H., Moorman, A. F. M., & Lamers, W. H. (1996). The development of the atrioventricular junction in the human heart. *Circulation Research*. https://doi.org/10.1161/01.RES.78.1.110

Wessels, Andy, & Sedmera, D. (2004). Developmental anatomy of the heart: A tale of mice and man. *Physiological Genomics*. https://doi.org/10.1152/physiolgenomics.00033.2003

Wessels, Andy, van den Hoff, M. J. B., Adamo, R. F., Phelps, A. L., Lockhart, M. M., Sauls, K., Briggs, L. E., Norris, R. A., van Wijk, B., Perez-Pomares, J. M., Dettman, R. W., & Burch, J. B. E. (2012). Epicardially derived fibroblasts preferentially contribute to the parietal leaflets of the atrioventricular valves in the murine heart. *Developmental Biology*. https://doi.org/10.1016/j.ydbio.2012.04.020

Wilson, C. L., Gough, P. J., Chang, C. A., Chan, C. K., Frey, J. M., Liu, Y., Braun, K. R., Chin, M. T., Wight, T. N., & Raines, E. W. (2013). Endothelial deletion of ADAM17 in mice results in defective remodeling of the semilunar valves and cardiac dysfunction in adults. *Mechanisms of Development*, *130*(4–5), 272–289. https://doi.org/10.1016/j.mod.2013.01.001

Wu, B., Wang, Y., Lui, W., Langworthy, M., Tompkins, K. L., Hatzopoulos, A. K., Baldwin, H. S., & Zhou, B. (2011). Nfatc1 coordinates valve endocardial cell lineage development required for heart valve formation. *Circulation Research*. https://doi.org/10.1161/CIRCRESAHA.111.245035

Wu, B., Zhang, Z., Lui, W., Chen, X., Wang, Y., Chamberlain, A. A., Moreno-Rodriguez, R. A., Markwald, R. R., O'Rourke, B. P., Sharp, D. J., Zheng, D., Lenz, J., Baldwin, H. S., Chang, C. P., & Zhou, B. (2012). Endocardial cells form the coronary arteries by angiogenesis through myocardial-endocardial VEGF signaling. *Cell*. https://doi.org/10.1016/j.cell.2012.10.023

Ya, J., Van den Hoff, M. J. B., De Boer, P. A. J., Tesink-Taekema, S., Franco, D., Moorman, A. F. M., & Lamers, W. H. (1998). Normal development of the outflow tract in the rat. *Circulation Research*. https://doi.org/10.1161/01.RES.82.4.464

Yacoub, M. H., Kilner, P. J., Birks, E. J., & Misfeld, M. (1999). The aortic outflow and root: A tale of dynamism and crosstalk. *Annals of Thoracic Surgery*. https://doi.org/10.1016/s0003-4975(99)00745-6

Yamagishi, T., Nakajima, Y., Miyazono, K., & Nakamura, H. (1999). Bone morphogenetic protein-2 acts synergistically with transforming growth factor-β3 during endothelial-mesenchymal transformation in the developing chick heart. *Journal of Cellular Physiology*. https://doi.org/10.1002/(SICI)1097-4652(199907)180:1<35::AID-JCP4>3.0.CO;2-R

Yamazaki, S., Iwamoto, R., Saeki, K., Asakura, M., Takashima, S., Yamazaki, A., Kimura, R., Mizushima, H., Moribe, H., Higashiyama, S., Endoh, M., Kaneda, Y., Takagi, S., Itami, S., Takeda, N., Yamada, G., & Mekada, E. (2003). Mice with defects in HB-EGF ectodomain shedding show severe developmental abnormalities. *Journal of Cell Biology*, *163*(3), 469–475. https://doi.org/10.1083/jcb.200307035

Yan, Y., Shirakabe, K., & Werb, Z. (2002). The metalloprotease Kuzbanian (ADAM10) mediates the transactivation of EGF receptor by G protein-coupled receptors. *Journal of Cell Biology*. https://doi.org/10.1083/jcb.200112026

Yu, S., Crawford, D., Tsuchihashi, T., Behrens, T. W., & Srivastava, D. (2011). The chemokine receptor CXCR7 functions to regulate cardiac valve remodeling. *Developmental Dynamics*. https://doi.org/10.1002/dvdy.22549

Yutzey, K. E., Colbert, M., & Robbins, J. (2005). Ras-related signaling pathways in valve development: Ebb and flow. *Physiology*, *20*(6), 390–397.

https://doi.org/10.1152/physiol.00035.2005
Zaffran, S., Kelly, R. G., Meilhac, S. M., Buckingham, M. E., & Brown, N. A. (2004). Right ventricular myocardium derives from the anterior heart field. *Circulation Research*. https://doi.org/10.1161/01.RES.0000136815.73623.BE
Zhou, B., Cron, R. Q., Wu, B., Genin, A., Wang, Z., Liu, S., Robson, P., & Scott Baldwin, H. (2002). Regulation of the murine Nfatc1 gene by NFATc2. *Journal of Biological Chemistry*. https://doi.org/10.1074/jbc.M107068200
Zhou, B., von Gise, A., Ma, Q., Hu, Y. W., & Pu, W. T. (2010). Genetic fate mapping demonstrates contribution of epicardium-derived cells to the annulus fibrosis of the mammalian heart. *Developmental Biology*. https://doi.org/10.1016/j.ydbio.2009.12.007
Zhou, B., Wu, B., Tompkins, K. L., Boyer, K. L., Grindley, J. C., & Baldwin, H. S. (2005). Characterization of Nfatc1 regulation identifies an enhancer required for gene expression that is specific to pro-valve endocardial cells in the developing heart. *Development (Cambridge, England)*, *132*(5), 1137–1146. https://doi.org/10.1242/dev.01640
Zou, Y. R., Kottman, A. H., Kuroda, M., Taniuchi, I., & Littman, D. R. (1998). Function of the chemokine receptor CXCR4 in heaematopolesis and in cerebellar development. *Nature*. https://doi.org/10.1038/31269


GOBIERNO
DE ESPAÑA
MINISTERIO
DE CIENCIA, INNOVACIÓN
Y UNIVERSIDADES